



UNIVERSITAT DE  
BARCELONA

# The role of the RPL5/RPL11/5S rRNA complex in mediating p53 levels in response to c-Myc depletion in colorectal carcinoma

Carmen Morcelle Magaña



Aquesta tesi doctoral està subjecta a la llicència **Reconeixement- NoComercial – SenseObraDerivada 3.0. Espanya de Creative Commons.**

Esta tesis doctoral está sujeta a la licencia **Reconocimiento - NoComercial – SinObraDerivada 3.0. España de Creative Commons.**

This doctoral thesis is licensed under the **Creative Commons Attribution-NonCommercial-NoDerivs 3.0. Spain License.**



UNIVERSITAT DE  
BARCELONA



UNIVERSITAT DE BARCELONA  
FACULTAT DE FARMÀCIA I CIÈNCIES DE L'ALIMENTACIÓ

---

PROGRAMA DE DOCTORAT EN BIOMEDICINA

# **The role of the RPL5/RPL11/5S rRNA complex in mediating p53 levels in response to c-Myc depletion in colorectal carcinoma**

A thesis submitted by Carmen Morcelle Magaña  
for the fulfillment of the degree of *Doctor of Philosophy* at the  
Universitat de Barcelona

The work presented in this thesis was performed  
at the Laboratory of Cancer Metabolism located in the Institut  
d'Investigació Biomèdica de Bellvitge (IDIBELL)

Candidate:	Supervisor:	Tutor:
<b>Carmen Morcelle Magaña</b>	<b>Dr George Thomas</b>	<b>Dr Albert Tauler i Girona</b>

Carmen Morcelle Magaña, June 2017



*A mis padres,*

*Por haberme apoyado durante todo este  
camino incondicionalmente.*



## Contents

<b>List of figures</b> .....	<b>V</b>
<b>Abstract</b> .....	<b>IX</b>
<b>Abbreviations</b> .....	<b>XI</b>
<b>1 Introduction</b> .....	<b>1</b>
<b>1.1 The c-Myc transcription factor</b> .....	<b>1</b>
1.1.1 c-Myc structure .....	2
1.1.2 Transcriptional properties of c-Myc .....	4
1.1.3 The control of c-Myc expression.....	5
1.1.4 Major cellular functions induced by c-Myc.....	11
1.1.5 c-Myc in cancer .....	15
<b>1.2 Ribosome biogenesis</b> .....	<b>18</b>
1.2.1 The process of ribosome biogenesis.....	19
1.2.2 Lesion in ribosome biogenesis and the IRBC.....	24
<b>1.3 c-Myc, ribosome biogenesis and cancer</b> .....	<b>33</b>
1.3.1 Ribosome biogenesis in c-Myc-driven tumorigenesis .	33
1.3.2 Ribosome biogenesis in colorectal cancer .....	36
1.3.3 p53 response in c-Myc-driven tumors .....	37
<b>2 Objectives</b> .....	<b>43</b>
<b>3 Results</b> .....	<b>47</b>
<b>3.1 Global effects of c-Myc depletion in colon cancer cells</b>	<b>47</b>
3.1.1 c-Myc depletion results in decreased proliferation .....	47
and accumulation of cells in G <sub>0</sub> /G <sub>1</sub> phase of the cell cycle .....	47

## CONTENTS

---

3.1.2	Reduction of c-Myc levels modifies cellular size and shape and causes a decrease in the rate of global protein synthesis.....	53
<b>3.2</b>	<b>Function of c-Myc in production of ribosomal components.....</b>	<b>55</b>
3.2.1	c-Myc depletion decreases the synthesis of RPs .....	55
3.2.2	c-Myc depletion decreases the synthesis of rRNA .....	60
<b>3.3</b>	<b>Effect of c-Myc depletion on p53 levels .....</b>	<b>63</b>
3.3.1	Reduction of c-Myc levels causes a drop in p53 protein .....	63
<b>3.4</b>	<b>Role of the RPL5/RPL11/5S rRNA complex in mediating p53 levels in response to c-Myc depletion .....</b>	<b>71</b>
3.4.1	c-Myc depletion decreases the availability of the IRBC complex .....	71
<b>4</b>	<b>Discussion .....</b>	<b>79</b>
<b>5</b>	<b>Conclusions .....</b>	<b>97</b>
<b>6</b>	<b>Materials and Methods.....</b>	<b>101</b>
6.1	Cell culture and drug treatment.....	101
6.2	Transfection procedures .....	101
6.3	Total cellular proteins extraction .....	102
6.4	Western blot analysis .....	102
6.5	Quantitative real-time PCR.....	103
6.6	Immunoprecipitation .....	105
6.6	Cell cycle analysis .....	107
6.7	De novo protein analysis .....	107
6.8	Labelling of cells with <sup>3</sup> H-leucine .....	108
6.9	Autoradiographic analysis of rRNA synthesis.....	109

## CONTENTS

---

<b>6.10 Crystal violet staining.....</b>	<b>111</b>
<b>6.11 Statistics.....</b>	<b>111</b>
<b>7 Acknowledgements.....</b>	<b>115</b>
<b>8 Bibliography.....</b>	<b>121</b>

## CONTENTS

---

## List of figures

<b>Figure 1.1:</b> Architecture of the MYC family.....	3
<b>Figure 1.2:</b> Levels of regulation of c-Myc .....	7
<b>Figure 1.3:</b> pS62/pT58 c-Myc degradation pathway.....	10
<b>Figure 1.4:</b> Regulation of ARF and the three RNA polymerases by c-Myc. ....	13
<b>Figure 1.5:</b> Composition of the eukaryotic 80S ribosome.....	19
<b>Figure 1.6:</b> Eukaryotic cap-dependent translation.....	21
<b>Figure 1.7:</b> Schematic representation of ribosome biogenesis. ....	23
<b>Figure 1.8:</b> p53 structure. ....	25
<b>Figure 1.9:</b> Schematic representation of MDM2 structure.....	27
<b>Figure 1.10:</b> The p53 signaling pathway.. ....	28
<b>Figure 1.11:</b> The RPL5/RPL11/5S rRNA complex. ....	32
<b>Figure 1.12:</b> Model for RP-MDM2-p53 signaling in response to oncogenic c-Myc.....	35
<b>Figure 3.1:</b> Effects of c-Myc depletion on c-Myc protein levels in HCT116 cells. ....	48
<b>Figure 3.2:</b> Effects of c-Myc depletion on c-Myc protein levels in HCT116 cells at different time points.....	49
<b>Figure 3.3:</b> Effects of c-Myc depletion on c-Myc mRNA levels in CRC cells.....	50
<b>Figure 3.4:</b> c-Myc depletion decreases proliferation in CRC cells. .....	51
<b>Figure 3.5:</b> Cell cycle analyses of CRC cells.....	52

## LIST OF FIGURES

---

<b>Figure 3.6:</b> c-Myc depletion induces changes in cell size and cell shape in CRC cells.....	54
<b>Figure 3.7:</b> c-Myc depletion decreases the global protein synthesis rate in RKO cells.....	55
<b>Figure 3.8:</b> Effect of c-Myc depletion on RP mRNAs in CRC cells..	56
<b>Figure 3.9:</b> Effect of c-Myc depletion on RPs in CRC cells. ....	57
<b>Figure 3.10:</b> Effect of c-Myc depletion on newly synthesized proteins.....	59
<b>Figure 3.11:</b> “Non-ribosomal” RPs decrease upon c-Myc depletion in CRC cells.....	60
<b>Figure 3.12:</b> Effect of c-Myc depletion on newly synthesized rRNAs. ....	61
<b>Figure 3.13:</b> Effect of c-Myc depletion on p53 and MDM2 protein levels in CRC cells.....	64
<b>Figure 3.14:</b> Effect of c-Myc depletion on p53 and MDM2 protein levels in HepG2 cells. ....	65
<b>Figure 3.15:</b> Effect of c-Myc depletion on p53 mRNA levels.. ....	66
<b>Figure 3.16:</b> Decreased half-life of p53 and MDM2 proteins under c-Myc depleted conditions. ....	68
<b>Figure 3.17:</b> Effect of c-Myc depletion on MDM2 mRNA levels. ..	69
<b>Figure 3.18:</b> Increased degradation of the p53 protein under c-Myc-depleted conditions.....	70
<b>Figure 3.19:</b> Effects of depleting c-Myc on the IRBC complex under impaired ribosomal stress conditions. ....	72
<b>Figure 3.20:</b> Effects of depleting c-Myc on the IRBC complex under non-stressed conditions.....	73

LIST OF FIGURES

---

**Figure 3.21:** Effects of depleting c-Myc on the levels of the 5S rRNA-  
component of the IRBC complex.....74

## LIST OF FIGURES

---

## Abstract

In most human cancers, the c-Myc transcription factor is deregulated and/or its levels are elevated, particularly in colorectal cancer (CRC). Earlier studies suggested a direct relationship between ribosome biogenesis and c-Myc-induced tumorigenesis, with recent reports arguing that ribosomal proteins L5 (RPL5) and RPL11 act against c-Myc-driven tumorigenesis as tumor suppressors by inhibiting MDM2 and inducing p53 stabilization. Our laboratory recently showed that upon inhibition of ribosome biogenesis, a nascent pre-ribosomal complex containing RPL5, RPL11 and 5S rRNA is redirected from 60S ribosome biogenesis to the inhibition of MDM2 and p53 stabilization. We have termed this response the impaired ribosome biogenesis checkpoint (IRBC). Here, we demonstrate that c-Myc silencing causes a drop in p53 protein levels through increased proteasome degradation. Moreover, c-Myc depletion significantly reduces the levels of the RPL5/RPL11/5S rRNA complex, even following impaired ribosome biogenesis by treatment with Actinomycin D, a RNA polymerase I inhibitor. Thus, diminished p53 stability appears to be mediated by a reduction of the RPL5/RPL11/5S rRNA complex and a decrease of the inhibition of MDM2. This thesis examines the relationship between c-Myc, p53 and components of the IRBC complex, including the 5S rRNA, defining a mechanism by which cells respond to c-Myc levels.

ABSTRACT

---

## Abbreviations

<b>3'UTR</b>	3'untranslated region
<b>5-FU</b>	5-fluorouracil
<b>5'TOP</b>	5' terminal oligopyrimidine
<b>5'UTR</b>	5'untranslated region
<b>ActD</b>	Actinomycin D
<b>AHA</b>	Azidohomoalanine
<b>APS</b>	Ammonium persulfate
<b>B-HLH-LZ</b>	Basic helix-loop-helix-leucine zipper
<b>CHX</b>	Cycloheximide
<b>CRC</b>	Colorectal cancer
<b>DBD</b>	DNA-binding domain
<b>DDR</b>	DNA damage response
<b>DNMT3<math>\alpha</math></b>	DNA (cytosine-5)-methyltransferase 3 $\alpha$
<b>EB</b>	Ethidium bromide
<b>E-box</b>	Enhancer box
<b>ER</b>	Endoplasmic reticulum
<b>FSC</b>	Forward scatter
<b>GSK-3<math>\beta</math></b>	Glycogen synthase kinase 3 $\beta$
<b>HAT</b>	Histone acetyltransferase
<b>HDAC</b>	Histone deacetylase
<b>IgG</b>	Immunoglobulin G

## ABBREVIATIONS

---

- IP** Immunoprecipitation
- IRBC** Impaired ribosome biogenesis checkpoint
- IRES** Internal ribosome entry site
- m<sup>7</sup>G** 7-methylguanosine
- Mb** Myc box
- Met-tRNA** Methionyl tRNA
- MK5** MAP kinase-activated protein kinase 5
- mRNA** Messenger RNA
- mTORC1** mTOR complex 1
- NES** Nuclear export signal
- NLS** Nucleolar localization signal
- NS** Non-silencing
- PABP** Poly A binding protein
- PBS** Phosphate-buffered saline
- PI** Propidium iodide
- PIC** Pre-initiation complex
- PoI I** RNA polymerase I
- PoI II** RNA polymerase II
- PoI III** RNA polymerase III
- PP2A** Protein phosphatase 2A
- PRD** Proline-rich domain
- pS62** Phospho-serine 62
- pT58** Phospho-threonine 58

## ABBREVIATIONS

---

<b>RP</b>	Ribosomal protein
<b>rRNA</b>	Ribosomal RNA
<b>RT</b>	Room temperature
<b>S62</b>	Serine 62
<b>S6K1</b>	S6 kinase 1
<b>siMyc</b>	c-Myc siRNA
<b>siNS</b>	Non-silencing siRNA
<b>siRNA</b>	Small interfering RNA
<b>snoRNA</b>	Small nucleolar RNA
<b>snoRNP</b>	Small ribonucleoprotein particle
<b>SSC</b>	Side scatter
<b>T58</b>	Threonine 58
<b>TAD</b>	Transcriptional activation domain
<b>TBS</b>	Tris-buffered saline
<b>TBS-T</b>	TBS-Tween
<b>TCA</b>	Trichloroacetic acid
<b>TET</b>	Tetramerization domain
<b>TFIIIA</b>	Transcription factor IIIA
<b>TFIIIB</b>	Transcription factor IIIB
<b>tRNA</b>	Transfer RNA

## ABBREVIATIONS

---

# **INTRODUCTION**



# 1 Introduction

## 1.1 The c-Myc transcription factor

c-Myc is a transcription factor that regulates the expression of numerous genes involved in proliferation, cell growth, differentiation, apoptosis, metabolism and neoplastic transformation (Dai et al., 2007).

c-Myc belongs to the MYC proto-oncogenic transcription factor family, that also comprises N-Myc and L-Myc, which have similar functions, but show differences in patterns of expression and potency in driving gene targets. The c-Myc gene, located on human chromosome 8q24, consists of three exons. There are two major species of the oncoprotein: a 67-kDa protein referred as to “p67” or “c-Myc1” (453 amino acids) and a 64-kDa species “p64” or “c-Myc2” (439 amino acids), arising from an CTG initiation codon at the 3' end of exon I, and ATG codon at the 5' end of exon II, respectively (Wierstra and Alves, 2008). The relative abundance of p67 and p64 varies among tissues and cell lines, but p64 is the predominant isoform in most cases. Both isoforms are competent to drive cellular transformation in vitro (Blackwood et al., 1994), however the vast majority of recent studies have focused on the predominant p64 isoform. Two other variants have been described: a third isoform of c-Myc, termed c-MycS, initiating from an internal translation initiation start site 300 base pairs down-stream of the amino-terminus, and a truncated c-Myc version, termed c-Myc-nick, generated in the cytoplasm by proteolytic cleavage of full-length c-Myc. These

## 1.1. The c-Myc transcription factor

---

variants were shown to retain a number of c-Myc functions independent of its transactivation activity, which is lost in both cases (Anderson et al., 2016; Xiao et al., 1998). C-MycS and c-Myc-nick have received little attention and their significance is not well understood (Tansey, 2014).

### 1.1.1 c-Myc structure

The **amino-terminus** of c-Myc contains the transcriptional activation domain (TAD) (Figure 1.1). The TAD is crucial for regulating c-Myc stability and activity, serving as an interaction platform for proteins involved in chromatin and histone modifications as well as ubiquitination and subsequent degradation. This region interacts with RNA polymerase II (Pol II)-associated proteins to stimulate gene transcription.

The **carboxy terminus** of c-Myc is a basic helix-loop-helix-leucine zipper (B-HLH-LZ) region that functions as a DNA-binding domain (Figure 1.1). B-HLH-LZ proteins bind as obligate dimers and recognize a consensus sequence “CACGTG”, the “Enhancer-box” (E-box). c-Myc interacts with the small B-HLH-LZ protein MAX through the leucine zipper to form a heterodimer that constitutes a core DNA-binding module. MAX also dimerizes with other B-HLH-LZ proteins of the MAD family, which antagonize the c-Myc-MAX interaction, playing an important role in c-Myc regulation. MAD-MAX dimers bind to the same E-boxes as c-Myc-MAX dimers to repress c-Myc induced transcription.

The **central portion** of the c-Myc protein is poorly understood. This segment contains a potent nuclear localization signal (N) (Figure 1.1), which is nonetheless dispensable for c-Myc nuclear entry.

Alignment of MYC family members across species reveals conserved regions, the MYC boxes: Mbl, MbII, MbIIIa, MbIIIb and MbIV (Figure 1.1). Myc box I lies within the TAD, and it is a primary point of contact with p-TEFb, a cycling-CDK complex that phosphorylates Pol II, stimulating transcriptional elongation. Mbl also hosts phosphorylation events that create a binding site for Fbw7, a c-Myc-E3 ligase which regulates c-Myc protein stability. Myc box II functions as a center for binding multiple key interactors, including components of histone acetyltransferase (HAT) complexes. It is also a docking site for SKP2, another E3 ligase in addition to Fbw7, involved in the degradation of c-Myc. Much less is known about the other MYC boxes. Myc box IIIa participates in c-Myc destruction by the ubiquitin-proteasome system, and it also

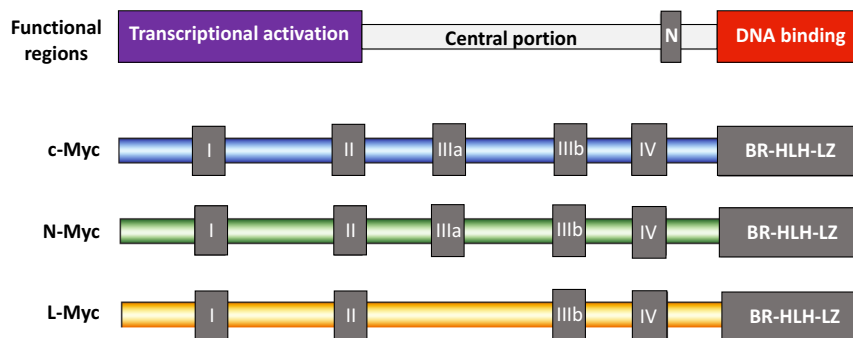


**Figure 1.1: Architecture of the MYC family.** Image at the top shows a generic representation of a mammalian MYC protein, indicating its functional regions. Below, a representation of conserved sequences present in c-, N- and L-Myc family members. Adapted from Tansey, 2014.

## 1.1. The c-Myc transcription factor

---

contributes to transcriptional repression by c-Myc via recruitment of HDAC3, a histone deacetylase. Myc box IV is required for the full proapoptotic functions of c-Myc (Conacci-Sorrell et al., 2014; Tansey, 2014).

### 1.1.2 Transcriptional properties of c-Myc

c-Myc regulates transcription in multiple scenarios:

- a) c-Myc-MAX complexes directly bind to E-boxes, which are found in the promoters of many genes, and recruit co-regulatory factors, such as GCN5, TIP60 and TRRAP (which is part of a histone acetyltransferase complex), which in turn lead to acetylation of nucleosomal histones in the vicinity of the transcriptional start site, inducing an open chromatin conformation and allowing Pol II recruitment and productive transcription (van Riggelen et al., 2010).
- b) c-Myc-MAX complexes bind also to a core promoter element, the initiator (INR), through the transcription factor MIZ1. MIZ1 by itself, acts as an activator of transcription, but its interaction with c-Myc-MAX converts it into a transrepressor complex that recruits DNA (cytosine-5)-methyltransferase 3  $\alpha$  (DNMT3 $\alpha$ ). In this way, c-Myc-MAX represses transcription of MIZ1 target genes (van Riggelen et al., 2010).
- c) c-Myc can form a MAX-independent complex with transcription factor IIIB (TFIIIB), an RNA polymerase III (Pol

III)-specific transcription factor, resulting in transcriptional activation of Pol III (van Riggelen et al., 2010).

- d) c-Myc can directly repress transcription via recruitment of histone deacetylases (HDACs). Targeted recruitment of HDACs by c-Myc is associated with loss of histones acetylation, a process leading to nucleosome compaction and establishment of a chromatin environment that is refractory to transcription (Tansey, 2014).

c-Myc was shown to have repressive as well as stimulatory roles in transcriptional regulation. However, delineating the downstream transcriptional targets of c-Myc that mediate both responses has proved elusive, with some investigators contending that c-Myc regulates the expression of all active genes (Lin et al., 2012; Nie et al., 2012), whereas others argue for the regulation of discrete genes and gene sets (Sabò et al., 2014).

The primary mechanism by which c-Myc is thought to control cellular functions is direct transcriptional regulation. However, the recent appreciation that c-Myc also regulates ribosome biogenesis, with ribosomal proteins (RPs) largely regulated at the translational level through their 5'TOPs (Gentilella and Thomas, 2012), suggests that c-Myc may regulate both transcription and translation (see below).

### **1.1.3 The control of c-Myc expression**

c-Myc mRNA and protein levels are tightly regulated under normal growing conditions. Their expression is dependent on extracellular

## 1.1. The c-Myc transcription factor

---

stimuli, such as growth factors and mitogens (Posternak and Cole, 2016). The tight control to which c-Myc expression is subjected is achieved through the rapid regulation by many different signals or at multiple levels such as transcription, translation, and stability of mRNA and protein (Figure 1.2) (Wierstra and Alves, 2008)

### **Signaling pathways impacting on the c-Myc promoter**

Activation of c-Myc transcription is an end point for a large range of signal-transduction pathways; practically every major signal transduction pathway bearing a proliferative or anti-proliferative signal, affects directly or indirectly the c-Myc promoter (Wierstra and Alves, 2008). c-Myc acts as a sensor, integrating signaling from these cellular pathways and mediating a transcriptional response that drives cell growth as well as proliferation, and impacts differentiation, survival as well as pluripotency. Transcription factors mobilized by these pathways bind to the c-Myc promoter to regulate its transcription initiation and elongation. Other factors appear to regulate c-Myc mRNA stability, export and translation. At the level of the c-Myc protein, further control is applied through posttranslational modifications and ubiquitination (Conacci-Sorrell et al., 2014).

Consistently with c-Myc being a potent stimulator of proliferation, its promoter is activated by most, if not all, major proliferation pathways (Figure 1.2), for example Wnt, Notch, interleukins (IL-2, IL-3, IL-6, IL-12), cytokines, lymphokines, growth factors (PDGF, EGF, CSF-1), hormones, PI3K/AKT, Ras/Raf, JAK/STAT and Scr (Liu and Levens, 2006; Wierstra and Alves, 2008). On the other hand, as c-Myc is central for the proliferation/differentiation switch and for the

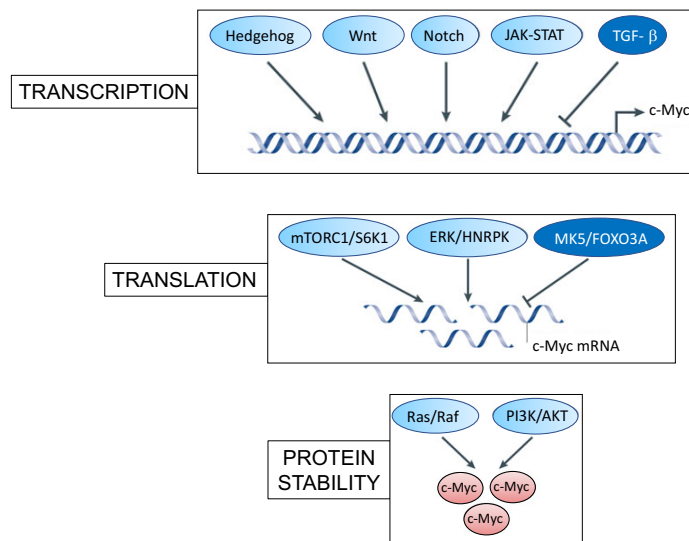


**Figure 1.2: Levels of regulation of c-Myc.** Adapted from Kress et al., 2015 .

proliferation/quiescence switch, the c-Myc promoter is repressed by many differentiation and anti-proliferation factors, such as C/EBP $\alpha$ , C/EBP $\beta$ , Blimp-1, GATA-1, KLF11, IFN- $\gamma$ , p21, p53 and TGF- $\beta$ . Downregulation of c-Myc is essential for TGF- $\beta$ -induced cell cycle arrest (Figure 1.2) (Wierstra and Alves, 2008).

### c-Myc mRNA and protein regulation

**c-Myc mRNA.** Normal c-Myc expression strictly parallels cell proliferation. In proliferating cells the amount of c-Myc mRNA is 10- to 40-fold higher than in quiescent cells, and during growth arrest and differentiation it decreases about 90%. c-Myc is largely unexpressed in quiescent cells, but it is very quickly induced by

## 1.1. The c-Myc transcription factor

---

mitogens during their reentry into the cell cycle ( $G_0/G_1$  transition) independent of *the novo* protein biosynthesis. Then c-Myc expression drops quickly, to levels that are then maintained during the cell cycle in proliferating cells. Continual expression depends on the constant presence of growth factors. Removal of these growth factors, or presence of stimuli of differentiation or other anti-proliferative signals, results in rapid downregulation of c-Myc mRNA. In terminally differentiated cells c-Myc is no longer expressed, and in adults its expression is limited to tissues with proliferating cell types or during tissue regeneration (Wierstra and Alves, 2008).

Following transcription, c-Myc mRNA is exported to the cytoplasm. Once in the cytoplasm, translation of the c-Myc mRNA is limited in time by its very short half-life, approximately 10 minutes (Dani et al., 1984).

A number of signaling cascades affect the efficiency of c-Myc translation, including mTOR complex 1 (mTORC1)/S6K1, ERK/HNRPK and MK5/FOXO3A (Figure 1.2). The mTORC1 complex represents a vital downstream node in the PI3K/AKT signal transduction pathway. mTORC1 phosphorylates and activates S6 kinase 1 (S6K1), which in turn enhances c-Myc translation efficiency by (a) stimulating the degradation of PDCD4 and therefore the release of translation initiation factors eIF4A and eIF4G, (which are part of the eIF4F complex, necessary for the cap-dependent translation of c-Myc, see section 1.2.1) (Csibi et al., 2014), and (b) by promoting the association of eIF4B with the eIF4F complex (Kuang et al., 2011). In parallel, the phosphorylation of 4E-BP1 by

mTORC1 releases eIF4E, a critical component of the eIF4F complex, which links it to mRNA (see section 1.2.1) (Wall et al., 2008). On the other hand, ERK activation increases the levels of HNRPK, a nucleocytoplasmic shuttling poly (C)-binding protein that positively regulates translation of mRNAs containing an internal ribosome entry site (IRES) with an HNRPK-binding site, among them c-Myc. Growth factors (e.g. EGF) that elicit mitogenic signals by potentiating ERK activity also enhance HNRPK expression, which in turn, increases c-Myc expression (Mandal et al., 2001; Notari et al., 2006). Another pathway regulating c-Myc translation, but this time negatively, is the MAP kinase-activated protein kinase 5 (MK5)/FOXO3A. MK5 phosphorylates and activates the transcription factor FOXO3A, which is then able to bind to and activate the promoter that controls expression of the precursor RNA of miR-34b and miR34c, two microRNAs that negatively target the 3'untranslated region (3'UTR) of c-Myc (Kress et al., 2011).

**c-Myc protein.** At the protein level c-Myc is subjected to posttranslational modifications that include phosphorylation, acetylation, glycosylation and ubiquitination, many of which interact to control particular specific states of c-Myc expression or activity (Tansey, 2014). c-Myc protein is rapidly degraded following its synthesis, having a half-life of approximately 20 min in non-transformed cells (Hann and Eisenman, 1984). The ubiquitination of c-Myc is crucial for keeping its levels low and tied to early processes that restrict its synthesis (Tansey, 2014). In the ubiquitin-proteasome system, ubiquitin is activated for conjugation by an ubiquitin-activating enzyme (E1) and then it is transferred to an E2 enzyme. An E3 ligase catalyzes transfer of the ubiquitin from the E2 to a

## 1.1. The c-Myc transcription factor

---

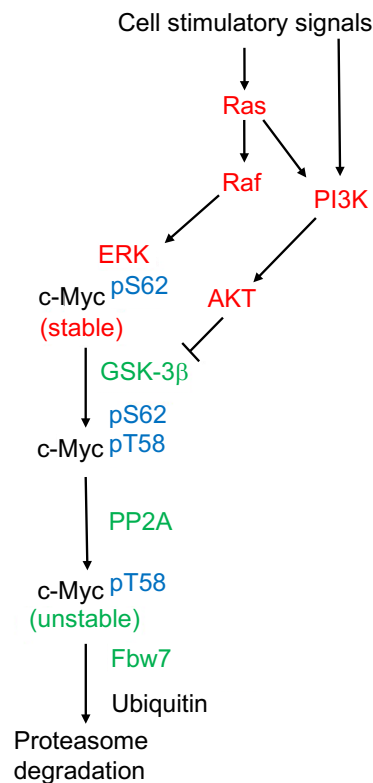


**Figure 1.3: pS62/pT58 c-Myc degradation pathway.** Proteins in red stabilize and/or activate c-Myc. Proteins in green facilitate c-Myc degradation. Adapted from Farrell and Sears, 2014.

substrate protein. Successive rounds of ubiquitination create an ubiquitin chain covalently bound to a lysine residue on the substrate protein, which tags the substrate for proteasomal degradation (Berndsen and Wolberger, 2014; Li and Kurokawa, 2015). The best-studied E3 ubiquitin ligase for c-Myc is Fbw7 (Farrell and Sears, 2014). Regulation of c-Myc stability by this ubiquitin ligase is dependent on c-Myc phosphorylation. Specific c-Myc serine and threonine residues are phosphorylated: Thr58 (T58) and Ser62 (S62). It is thought that proliferative stimuli activate specific kinases

to phosphorylate S62 and increase c-Myc activity. Phospho-S62 (pS62) can then serve as a platform for phosphorylation of T58 (pT58) by glycogen synthase kinase 3 $\beta$  (GSK-3 $\beta$ ). Protein phosphatase 2A (PP2A) subsequently dephosphorylates the stabilizing phosphate at S62 and pT58-c-Myc is recognized by the ubiquitin ligase Fbw7, which directs c-Myc ubiquitination and proteasomal degradation (Figure 1.3) (Meyer and Penn, 2008).

The activation of Ras, a protein which is a central component of mitogenic signaling events, insures transient accumulation of c-Myc following the stimulation of cell growth through the control of c-Myc phosphorylation sites T58 and S62. Ras activation initiates two signaling cascades: Raf and PI3K/AKT. The Ras/Raf cascade ends with ERK phosphorylating c-Myc's S62, while the Ras/PI3K/AKT cascade leads to increased inhibitory phosphorylation of GSK-3 $\beta$ , preventing the phosphorylation of T58. Thus, following growth stimulation, c-Myc protein would be stabilized through the ERK-mediated phosphorylation of S62 and GSK-3 $\beta$  activity would be held in check by AKT phosphorylation. Then as Ras activity decreases, this would result in a drop of AKT activity and GSK-3 $\beta$  would become active, triggering c-Myc degradation (Figure 1.3) (Sears et al., 2000).

### 1.1.4 Major cellular functions induced by c-Myc

**Cell cycle.** c-Myc is one of the early response genes induced upon exposure of quiescent cells to growth factors and it is required for mitogen-induced reentry into the cell cycle. c-Myc also accelerates

## 1.1. The c-Myc transcription factor

---

both the G<sub>1</sub> and G<sub>2</sub> phases of the cell cycle, causing cells to cycle more rapidly and allowing them to have reduced requirements for growth factors to maintain the cycling state. Forced c-Myc expression is sufficient to drive quiescent cells to re-enter the cell cycle independent of growth stimuli. c-Myc has this capacity through direct activation of cyclin/CDK expression and inhibition of specific cell cycle checkpoints (Tansey, 2014).

**Apoptosis.** c-Myc proteins induce apoptosis through a number of mechanisms. The extent of the apoptotic response is correlated with the level of c-Myc expression (Evan, 1992). c-Myc can promote apoptosis by disturbing the equilibrium between pro- and anti-apoptotic proteins; for example, during lymphomagenesis, c-Myc suppresses the expression of the anti-apoptotic Bcl-2 and Bcl-X(L) proteins, and at the same time it stimulates the expression of the pro-apoptotic BH3-only protein (and Bcl-2 antagonist) Bim, priming the mitochondria for cytochrome C release and induction of the apoptotic program (Tansey, 2014). c-Myc can also act directly on the same process by activating Bax, the mitochondrial protein responsible for inducing the events that lead to caspase activation. c-Myc is also able to promote apoptosis by inducing the expression of additional proteins, such as the E2F family of transcriptional regulators, which themselves trigger apoptotic tumor-defense mechanisms. However, it is thought that the most important process through which c-Myc induces apoptosis is via the ARF-MDM2-p53 axis (Figure 1.4A) (Tansey, 2014). c-Myc increases the expression of the ARF tumor suppressor, which binds and inactivates MDM2. MDM2 is an E3 ubiquitin ligase that targets p53 for degradation, therefore its inactivation leads to rapid induction of p53 and

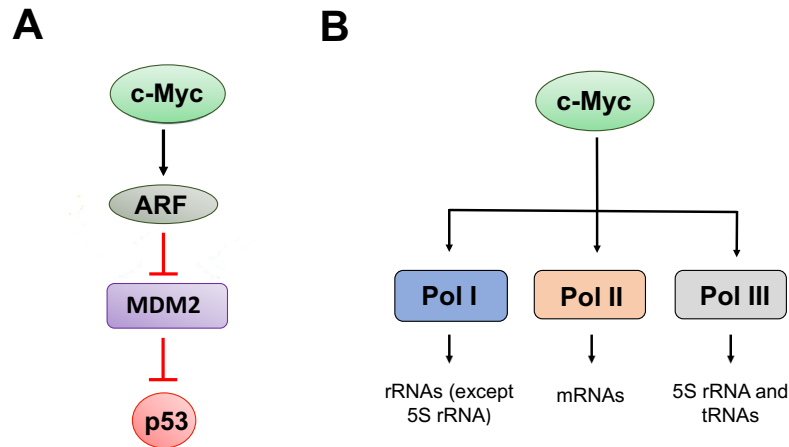


**Figure 1.4: Regulation of ARF and the three RNA polymerases by c-Myc.** (A) c-Myc-induced p53 activation through ARF. (B) c-Myc control of the three RNA polymerases.

activation of its broad tumor-suppressive apoptotic downstream responses (Shi and Gu, 2012; Tansey, 2014). Murine models have confirmed the importance of c-Myc inducing ARF (known as p19<sup>ARF</sup> in mouse) expression (Eischen et al., 1999), but the regulation of its human counterpart (namely p14<sup>ARF</sup>) is less known. It has been shown that ectopic expression of c-Myc and other oncogenes such as Ras, and E2F1 upregulate p19<sup>ARF</sup> expression, but in human cells only E2F1, but neither Ras nor c-Myc initially appeared to induce the transcription of p14<sup>ARF</sup> (Lindstrom and Wiman, 2003), though there is some disagreement on this point (Chen, 2013). It has also been shown that c-Myc abrogates ubiquitination of p14<sup>ARF</sup>, promoting ARF stabilization and ARF-dependent p53-mediated growth arrest (Chen et al., 2010a, 2013). This stabilization has been suggested to be an important mechanism through which cells discriminate between low (normal) and high (oncogenic) levels of c-Myc (Daniel et al., 2008). The role of ARF-MDM2-p53-mediated apoptosis in combatting the

## 1.1. The c-Myc transcription factor

---

tumorigenic potential of c-Myc is reflected in the frequent loss of p53 in human cancers and evidenced by data from mouse model systems showing that loss of this pathway collaborates with c-Myc to drive oncogenesis (Tansey, 2014).

**Cell growth and metabolism.** Overexpression of c-Myc has significant effects on cell proliferation, growth and size, that have been associated with marked changes in the total rate of protein synthesis (van Riggelen et al., 2010). Cells forced to express c-Myc grow to twice their size, making twice as many proteins and having twice the total RNA content of cells with normal c-Myc levels (Nie et al., 2012). A critical mechanism by which c-Myc regulates the growth response is through general increased expression of proteins involved in ribosome biogenesis and protein translation. c-Myc coordinates protein synthesis by transcriptionally regulating ribosomal RNAs and ribosomal proteins (rRNAs and RPs), and of gene products necessary for the processing of rRNA, the nuclear export of ribosomal subunits and the initiation of mRNA translation (van Riggelen et al., 2010). c-Myc activates the transcription of RNA polymerase I (Pol I) and Pol III, which increases synthesis of rRNAs and transfer RNAs (tRNAs). On the other hand, c-Myc controls the transcription of RPs and genes required for rRNA processing as well as nuclear-cytoplasmic transport of mature ribosomal subunits through Pol II (Figure 1.4B). c-Myc can also regulate translation through the transcription of translation initiation factors required for cap-dependent translation, and by promoting methylation of the mRNA-cap structure through the RNA guanosine-7-

methyltransferase, a modification essential for cap binding to eIF4E and recruitment of the 40S ribosome subunit, and therefore, for cap-dependent translation (see section 1.2.1) (Dunn and Cowling, 2015; van Riggelen et al., 2010).

c-Myc enhances protein synthesis during tumorigenesis not only through transcriptional control, but also recently it has been shown that c-Myc can activate mTOR-dependent phosphorylation of 4E-BP1. 4E-BP1 phosphorylation blocks its ability to bind and negatively regulate the translation initiation factor eIF4E, therefore promoting eIF4E's ability to recruit the 40S ribosomal subunit to the 5'cap of mRNAs and enhance translational initiation (Pourdehnad et al., 2013). The importance of enhanced protein synthesis to c-Myc function is demonstrated by the finding that reducing ribosome number, by crossing mice overexpressing c-Myc with those that are haploinsufficient for a ribosomal protein, inhibits the transition of precancerous cells to the tumorigenic state (Barna et al., 2008). However, others have shown that haploinsufficiency of the same RP leads to p53 activation (Barkić et al., 2009), which instead of reducing translation, could be responsible for suppressing tumorigenesis (see section 1.3).

### **1.1.5 c-Myc in cancer**

In normal cells, both c-Myc mRNA and protein expression are continuously dependent on mitogen signaling. However, in most human cancers (approximately 70%), c-Myc expression is deregulated and/or elevated compared to healthy tissues

## 1.1. The c-Myc transcription factor

---

(Posternak and Cole, 2016). Considerable progress has been made within the last decade in understanding that c-Myc deregulation is not confined to big genetic changes at the c-Myc locus, but instead c-Myc can be deregulated by different mechanisms that target its expression and/or activity either directly or indirectly (Meyer and Penn, 2008).

Cancer cells deregulate c-Myc in many ways, but two main categories can be distinguished: changes in the c-Myc gene that stimulate increased c-Myc mRNA production, or changes external to c-Myc that constitutively deactivate critical upstream regulatory mechanisms. Alterations in the c-Myc gene itself can include chromosomal translocation (in Burkitt's lymphomas c-Myc locus is placed under the control of the immunoglobulin  $\mu$  heavy chain enhancer, driving very high levels of mRNA synthesis), and retrovirus integration, but the most common increase in c-Myc synthesis is gene amplification. Although stability of the c-Myc message or c-Myc protein can be increased extrinsically (Tansey, 2014), in most tumors, c-Myc shows elevated and persistent activity due to the relentless induction by upstream oncoproteins, such as mutated protein kinases or Ras as well as constitutive activation of the Wnt/ $\beta$ -Catenin pathway (Daniel et al., 2008).

**Consequences of c-Myc activation.** The first evidences of c-Myc's potential to drive tumorigenesis came from in vitro studies, in which c-Myc was able to transform normal embryonic fibroblasts in cooperation with other oncogenes. In subsequent murine models, it was shown that other mutagenic events are necessary in order to induce c-Myc's tumorigenic potential (Dang, 2012). Some data

suggests that low-level deregulated c-Myc may be a more efficient initiator of oncogenesis than over-expressed c-Myc, since the latter can be tolerated only by cells that have already lost their tumor suppressor pathways. High initial levels of c-Myc potently induce cell proliferation, but may even impede onset of tumorigenesis by breaching the ARF/apoptotic triggering threshold and engaging intrinsic tumor suppression (Daniel et al., 2008). Actually, activation of the oncogenic c-Myc strongly selects for a second mutation that eliminates an apoptotic pathway (e.g., p53) or for activation of a second cooperating oncogene that inhibits apoptosis and stimulates cell survival (e.g., Ras). It seems that abrogation of c-Myc-potentiated apoptosis is crucial for cellular transformation and, once this takes place, clonal tumors can appear. If c-Myc-induced apoptosis is suppressed, c-Myc activation alone is sufficient to trigger immediate carcinogenic progression in the absence of other cooperating oncogenic lesions (Wierstra and Alves, 2008). The importance of the ARF-MDM2-p53 pathway in c-Myc-induced apoptosis is shown by the increased tumorigenesis that occurs with the loss of these tumor suppressors in mouse models of c-Myc oncogenesis (Meyer and Penn, 2008). Many c-Myc induced transgenic lymphomas lack functional ARF or p53 (Dang, 2012).

Cancer cells are often dependent on the continued expression of specific activated or overexpressed oncogenes for maintenance of their malignant phenotype, an event termed “oncogene addiction”. Accordingly, it appears that deregulated c-Myc is not only able to initiate oncogenesis, but it is also critical for tumor maintenance, as

## 1.2. Ribosome biogenesis

---

in transgenic mouse models with inducible c-Myc, established tumors regress upon withdrawal of c-Myc ectopic expression, demonstrating that once established, these tumors are addicted to c-Myc. In fact, expression of a dominant-negative inhibitor of c-Myc hetero-dimerization in vivo has resulted in tumor regression, indicating that inhibiting c-Myc function could be a potential therapeutic strategy (Dang, 2012).

## 1.2 Ribosome biogenesis

In all living organisms, translation of the genetic code is performed in the ribosomes, which convert information encoded in mRNA into functional proteins. In the majority of cells, ribosomes are relatively stable and therefore their cellular content depend largely on the rate of ribosome synthesis or biogenesis, a complex process dependent on the coordinated synthesis of RPs, rRNAs and their subsequent processing and assembly into mature ribosomes. The coordination of ribosome biogenesis is extremely complex and most of the cellular energy is used to generate ribosomes. Cells need to grow considerably in size before being able to undergo cell division, and without a robust and constant protein translation this would not be achievable. In fact, in a growing cell, ribosomes employ a large part of their time making proteins to constitute new ribosomes (Macinnes, 2016).

### 1.2.1 The process of ribosome biogenesis

#### Ribosome composition

Each ribosome is composed of a small and a large subunit, and each subunit contains rRNAs and RPs (Figure 1.5). The chief role of the small ribosomal unit (**30S** in prokaryotes and **40S** in eukaryotes) is to recognize the 5' end of mRNAs and initiate the translational process. The large ribosomal subunit (**50S** in prokaryotes and **60S** in eukaryotes) catalyzes peptide bond formation through its peptidyl transferase ribozyme activity (Gamalinda and Woolford, 2015). In eukaryotes, the 40S ribosomal subunit is loaded with a methionyl tRNA (Met-tRNA) by initiation factor eIF2, forming the 43S pre-initiation complex (43S PIC) together with eIFs 1, 1A, 2, 3 and 5 (Figure 1.6). This complex then binds to the initiation factor eIF4F complex (which comprises eIF4E bound to the 7-methylguanosine ( $m^7G$ ) cap at the 5' end of the mRNA, the scaffold protein eIF4G, the helicase eIF4A, the RNA binding protein eIF4B and the mRNA poly A binding protein (PABP), to form the 48S PIC. Once formed the 48S PIC scans the 5' untranslated region (5'UTR) until it encounters an

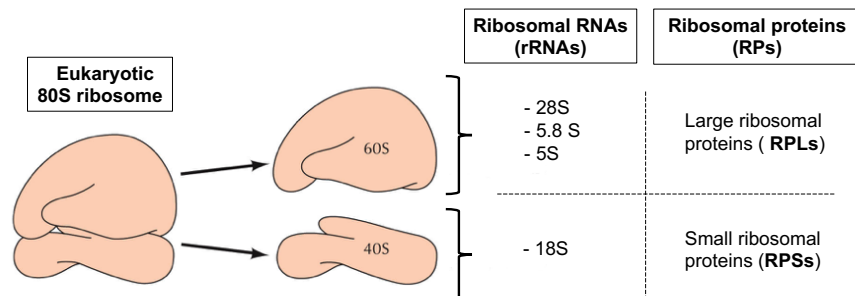


**Figure 1.5: Composition of the eukaryotic 80S ribosome.** Adapted from Cooper and Hausman, 2006,

## 1.2. Ribosome biogenesis

---

AUG translational start codon. Once the AUG start codon is found, the GTP bound to eIF2 is hydrolyzed, eIFs are released from the 48S PIC and joining of the 60S subunit is catalyzed by eIF5B-GTP. GTP hydrolysis triggers release of eIF5B-GDP and eIF1A to yield the final **80S** monosome, ready to accept the appropriate aminoacyl-tRNA and synthesize the first peptide bond. This mode of translation initiation constitutes the cap-dependent translation (Figure 1.6). A number of eukaryotic mRNAs can bypass the scanning process and recruit the 48S complex to the start codon using specialized sequences called internal ribosome entry sites (IRESs) (Sonnenberg and Hinnebusch, 2009).

Once formed, translating ribosomes have only a short-lasting existence: when production of a specific protein has finished, the two subunits separate and are either stored as subunits or reinitiate on a new mRNA. Ribosomes can function in a “free state” in the cytoplasm but they can also be bound to the endoplasmic reticulum (ER). The association between ribosome and ER facilitates the further processing and checking of newly made proteins by the ER.

### **rRNA synthesis**

In eukaryotes ribosome biogenesis involves multiple coordinated steps : the synthesis of precursor rRNA in the nucleolus and nucleus, the transcription of RP mRNAs, their translation in the cytoplasm and their import into the nucleus and nucleolus, the assembly and processing of the pre-90S ribosome, or 90S processome, into the

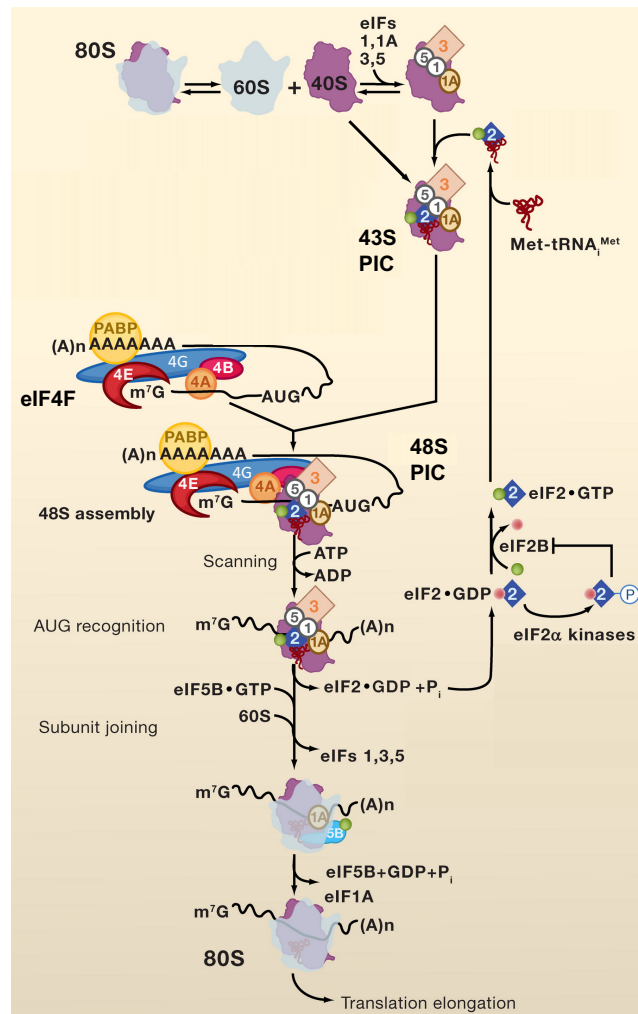


**Figure 1.6: Eukaryotic cap-dependent translation.** Adapted from Sonenberg and Hinnebusch, 2009.

40S and the 60S precursor ribosomal subunits and their transport into the cytoplasm, where processing is completed to generate the mature 40S and 60S ribosomal subunits (Figure 1.7). In eukaryotes, the small subunit includes 18S rRNA and 33 RPs; the large subunit includes 5S rRNA, 28S rRNA, 5.8 rRNA and 46 RPs (Figure 1.5).

## 1.2. Ribosome biogenesis

---

Ribosome biogenesis is a highly complex molecular biochemical event, which is orchestrated by hundreds of molecular components and assembly factors. rRNA synthesis begins with transcription of the 47S precursor rRNA by Pol I in the nucleolus, where the genes encoding rRNA (rDNA) are found in multiple copies organized in tandem repeats (Danilova, 2015). During its transcription, the 47S rRNA is assembled with RPs, ribosome biogenesis factors and small nucleolar RNAs (snoRNAs) to form a large 90S pre-ribosome. The 47S rRNA precursor is subsequently modified, processed and cleaved into the mature 5.8S, 18S and 28S rRNAs (Yelick and Trainor, 2015). Following the first step of pre-rRNA processing, the complex splits into two pre-ribosomes, called pre-40S and pre-60S, which are eventually exported to the cytoplasm where they undergo further maturation steps and then join as a 40S and 60S subunits to form the mature ribosome (Figure 1.7) (Oeffinger, 2016).

The 5S rRNA precursor, transcribed from multiple copies of the 5S gene, is not synthesized in the nucleolus, but in the nucleoplasm by Pol III. 5S rRNA is then transported to the cytoplasm where it is further processed and binds with RPL5, forming a complex which is next transported into the nucleus and then the nucleolus. Here the 5S rRNA/RPL5 complex assembles with RPL11 in a precursor ribonucleic protein particle, which is then incorporated into the 90S pre-ribosomal particle (Ciganda and Williams, 2011).

The different steps in which the pre-rRNA is modified, folded and processed are catalyzed with the aid of small nucleolar RNAs (snoRNAs), which are active as part of small ribonucleoprotein particles (snoRNPs) and mediate methylation and pseudouridylation

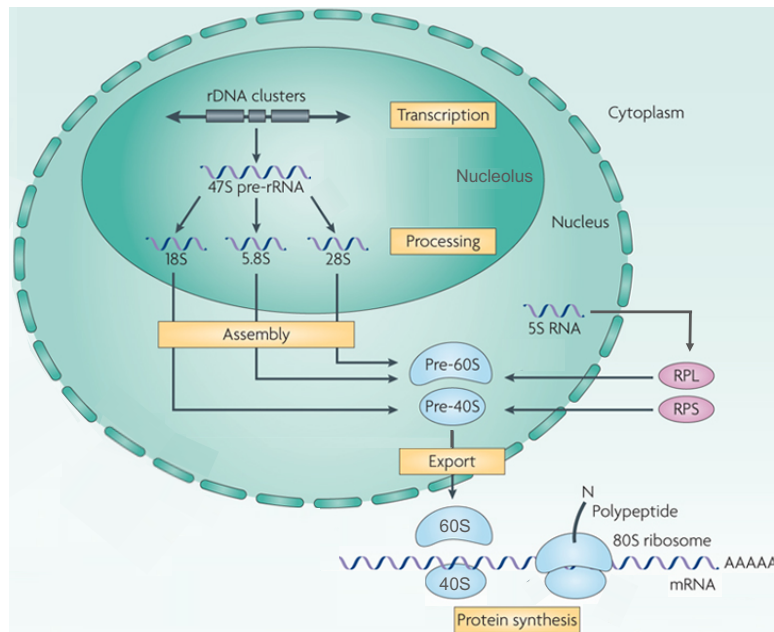


**Figure 1.7: Schematic representation of ribosome biogenesis.**  
Adapted from van Riggelen et al., 2010.

of nucleotides (Lafontaine, 2015). These snoRNP complexes are targeted to their substrate via base pairing between rRNA and snoRNA and then they guide the methyltransferase or pseudouridine synthase to the position of modification. Many of these modifications are clustered around conserved positions in the active site of the mature ribosome, and without them ribosome biogenesis and function are compromised (Strunk and Karbstein, 2009). SnoRNA-mediated rRNA modification is a major source of ribosome heterogeneity, and not all positions are always modified (Lafontaine, 2015). The combinatorial potential is immense and recent studies further argue that these modifications have led to generation of

## 1.2. Ribosome biogenesis

---

heterogeneous populations of ribosomes, which may be involved in controlling unique patterns of translation.

### **Ribosomal protein synthesis and subunit assembly**

Following transcription by Pol II, RPs are synthesized in the cytoplasm and then imported into the nucleus (Figure 1.7). Throughout the transcription and folding of the pre-rRNA, RPs are assembled into small or large pre-ribosomes as they migrate through the nucleoplasm. The final maturation steps occur after the particles are exported into the cytoplasm (Phipps et al., 2011). Unlike in lower eukaryotes, such as *Saccharomyces cerevisiae*, in higher eukaryotes the production of RPs is largely controlled at the translational level through a 5'-terminal oligopyrimidine (5'TOP) sequence (Gentilella and Thomas, 2012), independent of rRNA transcription and processing (Pierandrei-Amaldi et al., 1985; Warner, 1977). It is suggested that this is a recent evolutionary event, which developed to more rapidly provide RPs on demand in complex multicellular organisms (Lam et al., 2007).

### **1.2.2 Lesion in ribosome biogenesis and the IRBC**

As a large metabolic investment of energy is made to give rise to ribosomes, molecular mechanisms have evolved to sense the fidelity of this critical cellular process. Indeed, different studies have demonstrated that perturbation of ribosome biogenesis activates the tumor suppressor p53 through the binding of several RPs and RNA

to its negative regulator, MDM2, independent of DNA damage. However, the underlying molecular mechanisms have yet to be clearly determined for how lesions in ribosome biogenesis are sensed by this p53-dependent checkpoint mechanism.

### The p53 protein

The p53 protein is a transcription factor known as the “guardian of the genome” because of its central role in coordinating the cellular responses to a broad range of cellular stress factors (Kruse and Gu, 2009). In response to different cellular insults, p53 is relieved of its negative regulators, MDM2 and MDMX (also known as MDM4), allowing its stabilization and activation. This activation can lead to transient cell cycle arrest, DNA repair, apoptosis or senescence (Biegging et al., 2014).

The p53 protein contains (1) two amino-terminal transcriptional activation domains (TADs), a proline-rich domain (PRD), a DNA-binding domain (DBD), a tetramerization domain (TET) and a carboxy-terminal region that is rich in basic residues (Figure 1.8). The importance of p53 in tumor suppression is clear, as half of all

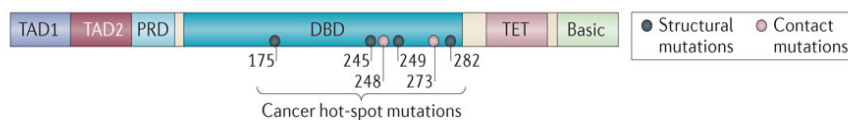


**Figure 1.8: p53 structure.** Six common p53 “hot-spot” mutations are categorized as either structural or contact p53 mutants, both of which disrupt the protein-DNA interaction and the transactivation of p53 target genes (Biegging et al., 2014).

## 1.2. Ribosome biogenesis

---

human cancers have inactivating mutations in the p53 gene. In human tumors, inactivation of p53 typically occurs through mutations in the DBD of the p53 protein (Bieging et al., 2014). Moreover, in cancers retaining wild-type p53, its functions are probably inactivated by defects upstream or downstream p53 signaling network.

p53 is thought to be mainly regulated by MDM2 and the related protein MDMX. In normal, unstressed cells, p53 activity is maintained at low levels through a combination of ubiquitin-dependent degradation in the cytoplasm and repression of p53 transcriptional activity in the nucleus. MDM2 functions as an E3 ligase to ubiquitinate p53 and it becomes active upon heterodimerization with its homolog MDMX, which does not have E3 ligase activity. This heterodimer promotes nuclear export of p53 and its proteasomal degradation via monoubiquitination or polyubiquitination, respectively, as well as inhibiting MDM2 auto-ubiquitination and degradation. Both MDM2 and MDMX also directly repress p53 transcriptional activity (Bursac et al., 2014). The MDM2 protein contains three highly conserved regions: the N-terminal domain, important for p53 binding; the C-terminal domain, containing a RING finger essential for its E3 ubiquitin ligase function; and a central acidic domain, comprising a highly conserved C4 zinc finger. ARF, RPL5, RPL11 and other small basic proteins have been shown to interact with the central acidic domain, indicating that this region could act as a place to receive and integrate MDM2-regulatory signals into the p53 pathway (Figure 1.9) (Macias et al., 2010).



**Figure 1.9: Schematic representation of MDM2 structure.** MDM2 landmarks include the N-terminal p53-binding domain, the acidic domain that binds ARF and RPs, and the C-terminal domain, containing a RING finger. MDM2 also contains a nucleolar localization signal (NSL), and a nuclear export signal (NES). Approximate binding areas for p53, ARF and ribosomal proteins are indicated. Adapted from Lindström et al., 2007.

The ability of MDM2-MDMX to inhibit p53 is critical under non-stressed cell conditions, but when the cell suffers stress, various mechanisms ensure that these two proteins are repressed from inhibiting p53. DNA damage (1), oncogenic signals (2) and ribosomal stress (3) are three of numerous types of cellular insults that elicit a p53 response (Figure 1.10). Moreover, MDM2 is a transcriptional target of p53, so when p53 is activated, an auto-regulatory feedback loop is generated ensuring that p53 will be downregulated once the insult or its consequences are alleviated.

1- DNA damage triggers the DNA damage response (DDR). This response leads to post-translational modifications of both p53 and the MDM2-MDMX heterodimer, which disrupt their interactions and increases their auto-degradation, leading to p53 stabilization and transcriptional activation (Bursac et al., 2014).

2- On the other hand, oncogenic stress can cause p53 stabilization by two ways: one is by activating the DDR signaling pathway and the second is by increasing the binding of the protein ARF to MDM2's central acidic domain. The DDR in this setting is induced

## 1.2. Ribosome biogenesis

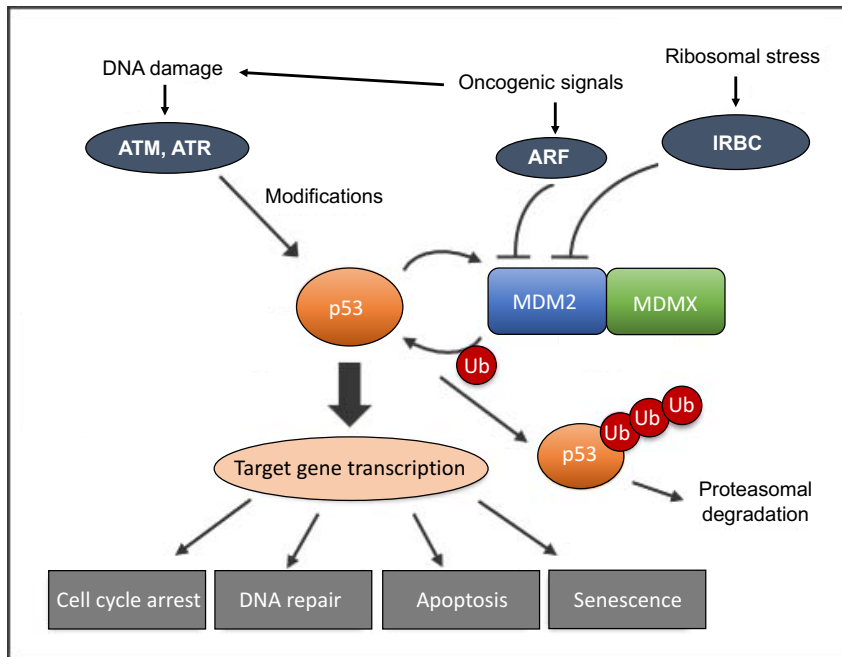


**Figure 1.10: The p53 signaling pathway.** DNA damage activates several kinases (ATM, ATR), and other checkpoint kinases, which modify p53, MDM2 and MDMX. These modifications block their interactions, resulting in p53 stabilization. Oncogenic stress activates ARF, that binds MDM2 and stabilizes p53, and it can also produce DNA damage. Ribosomal stress causes the re-direction of the IRBC complex from ribosome assembly to MDM2 inhibition, stabilizing p53. An activated p53 protein subsequently transactivates several target gene expressions. Depending on the cell type and stressor, the consequences could be either cell cycle arrest, DNA repair, apoptosis or senescence. Adapted from Chakraborty, Uechi and Kenmochi, 2011.

by acceleration of cell cycle progression guided by genes such as Ras, c-Myc, E2F, E1A,  $\beta$ -catenin and v-abl; the acceleration induces stalling and collapse of DNA replication forks, which leads to the formation of double strand breaks. ARF binding to MDM2 inhibits p53 ubiquitination and promotes MDMX ubiquitination by MDM2, therefore activating p53 (Bursac et al., 2014).

3- A growing body of evidence has demonstrated that perturbation of distinct steps in ribosome biogenesis can trigger the p53 tumor suppressor response independently of DNA damage and the ARF tumor suppressor. It has been shown that inhibition of rRNA transcription, inhibition of rRNA processing, decreased expression of proteins required for maturation of 18S and 28S rRNA and decreased expression of specific RPs of either 40S or 60S can induce a p53-mediated stress signal (see below) (Bursac et al., 2014).

### **The impaired ribosome biogenesis checkpoint (IRBC)**

The existence of a checkpoint monitoring the fidelity of ribosome biogenesis was initially described by our laboratory following the deletion of the RPS6 gene in the liver of adult mouse. The livers of mice in which the RPS6 gene had been deleted could recover their lost liver mass following a fasting/feeding paradigm. The fasting/feeding paradigm led to an ~ 50% decrease and recovery in cell mass, but no change in cell number. However, when such animals were subjected to hepatectomy, the remaining liver cells failed to de-differentiate and re-enter the cell cycle to pass through one to one and a half rounds of cell replication required to recover the lost liver mass (Volarević and Thomas, 2001). Later our laboratory demonstrated that depletion of an essential RP of either subunit results in the induction of p53 and G<sub>1</sub> cell cycle arrest; these data led us to the finding that cells monitor not total ribosome number, but the status of nascent ribosome biogenesis (Fumagalli et al., 2009).

## 1.2. Ribosome biogenesis

---

It was already known that upon ribosome biogenesis impairment p53 levels were able to rise and cause cell cycle arrest because of the ability of specific RPs to bind to MDM2. This response was first associated to disruption of the nucleolus and passive diffusion of some RPs to the nucleoplasm, in particular RPS7, RPL5, RPL11 and RPL23, which were shown to bind MDM2 (Zhang and Lu, 2009). Nevertheless, our laboratory demonstrated that impaired 40S or 60S ribosome biogenesis does not cause nucleolar disruption, and therefore the shuttling of RPs from nucleolus to nucleoplasm is not a not a passive event, but instead a regulated process (Fumagalli et al., 2009). More recently, in experiments inducing selective disruption of 40S and 60S ribosome biogenesis by depleting cells of either RPS7 or RPL23 respectively, it was shown that RPL11 and RPL5, in a mutually dependent manner, were required for p53 induction upon disruption of ribosome biogenesis, but neither RPS7 nor RPL23 depletion were able to suppresses p53 upregulation. Not only the p53 response was not abrogated by RPS6 or RPL23 depletion but also depletion alone of either of the two RPs led to a p53 induction equivalent to the one observed when depleting RPS6 and RPL7a, respectively. This response was completely reversed by co-depletion of either RPL5 or RPL11. This would indicate that only RPL5 and RPL11 are implicated in the impaired ribosome biogenesis checkpoint (IRBC), as only their depletion reversed p53 stabilization caused by impaired ribosome biogenesis (Fumagalli et al., 2012).

In yeast, it is known that orthologs of RPL11 and RPL5 form a complex with the 5S rRNA prior to their incorporation into the nascent 90S processome (Zhang et al., 2007). Based on this, a

recent study from our laboratory predicted that, in higher eukaryotes, RPL5 and RPL11 could also constitute a complex together with the 5S rRNA. Indeed, it was demonstrated that decreasing the levels of nascent 5S rRNA by depletion of transcription factor IIIA (TFIIIA), a Pol III cofactor specifically required for its transcription, completely reversed the effects of impaired ribosome biogenesis on the stabilization of p53, recapitulating the effects observed for RPL5 and RPL11 depletion. Co-depletion of either RPL5 or RPL11 did not further reverse the effects of ribosome biogenesis impairment, indicating that RPL5, RPL11 and the 5S rRNA are mutually dependent on one another for inhibition of MDM2. It was also demonstrated that the interdependence of endogenous RPL5, RPL11 and 5S rRNA in binding and suppressing MDM2 appears to be independent of the levels of the E3 ligase; thus, binding of MDM2 would not be required for their accumulation. Moreover, the fact that the depletion of nascent rRNA, but not total 5S rRNA, was associated with suppressing the induction of p53 following impaired ribosome biogenesis suggested that it is the nascent RPL5/RPL11/5S rRNA precursor complex that is redirected from 60s ribosome biogenesis to the inhibition of MDM2. Therefore, this led our laboratory to a new model: upon inhibition of ribosome biogenesis, the majority of RPs are normally synthesized but are degraded by the ubiquitin-independent proteasomal degradation (unless they are incorporated into nascent ribosomes, as previously described) (Pierandrei-Amaldi et al., 1985; Warner, 1977), but nascent RPL5, RPL11 and 5S rRNA are redirected from 60S ribosome biogenesis to MDM2 inhibition in the cytoplasm and the nucleoplasm, thus allowing p53 stabilization (Figure 1.11) (Donati et

## 1.2. Ribosome biogenesis

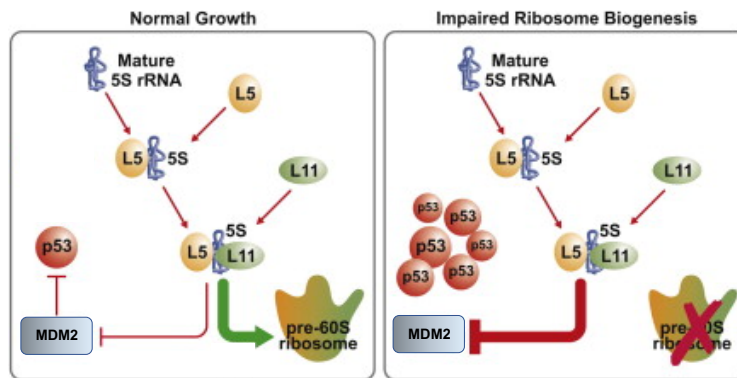


**Figure 1.11: The RPL5/RPL11/5S rRNA complex.** In normal growth conditions the nascent RPL5/RPL11/5S rRNA complex constitutes the pre-60S ribosome. However, under conditions of impaired ribosome biogenesis, this complex is re-directed from 60S ribosome biogenesis to the inhibition of MDM2, allowing p53 levels to rise. Adapted from Donati et al., 2013.

al., 2013). As it was shown that nascent RPL5, RPL11 and 5S rRNA depend on each other for MDM2 binding and p53 induction, and also that binding to MDM2 is not required for their accumulation, the formation of this RPL5/RPL11/5S rRNA complex could protect RPL5 and RPL11 from the ubiquitin-independent proteasomal degradation pathway under conditions of ribosome biogenesis impairment (Bursac et al., 2014). The stabilization of p53 by RPL5, RPL11 and 5S rRNA is not only restricted to the binding of the three components to MDM2. It has been reported that 5S rRNA binds to MDMX in normal conditions, protecting it from MDM2-dependent ubiquitination and degradation and thus contributing to p53 inhibition (Li and Gu, 2011). This suggests that 5S rRNA might behave as a positive or negative regulator of p53 depending on its association with the RPL5/RPL11 complex or MDMX, respectively (Bursac et al., 2014).

### **1.3 c-Myc, ribosome biogenesis and cancer**

The transcription factor c-Myc acts as a global controller of protein biosynthesis, however the regulation of components of the ribosome biogenesis apparatus is one of the most consistent gene expression signatures associated with c-Myc activation (Devlin et al., 2016).

c-Myc binds to sequences upstream and downstream of the coding regions of rDNA clusters and directly activates the Pol I-dependent transcription of 18S, 5.8S and 28S rRNAs by both remodeling chromatin structure and interacting with cofactors that are required for the recruitment of Pol I. In case of transcription of the 5S rRNA, c-Myc directly activates Pol III transcription by binding to TFIIIB, a Pol III-specific transcription factor. c-Myc also increases the transcription of many RPs as well as other proteins required for the processing of rRNA precursors and the nuclear-cytoplasmic transport of mature ribosomal subunits, all through Pol II-dependent transcription (van Riggelen et al., 2010).

#### **1.3.1 Ribosome biogenesis in c-Myc-driven tumorigenesis**

Recent experiments suggest that there could be a direct relationship between ribosome biogenesis and the ability of c-Myc to initiate tumorigenesis (van Riggelen et al., 2010). In E $\mu$ -Myc transgenic mice, in which c-Myc is overexpressed in the B-cell compartment, loss of one allele of RPL24 not only decreases the overall protein synthesis rates to normal levels but also decreases the incidence of

### 1.3. c-Myc, ribosome biogenesis and cancer

---

lymphoma by 20% and delays tumor onset by over 100 days, demonstrating that a modest reduction in the total expression of a single ribosomal protein gene notably hampers the ability of c-Myc to induce tumorigenesis in mice. It was proposed that c-Myc overexpression increases cap-dependent translation, impairing the switch to IRES-dependent translation required for accurate mitotic progression. This impairment would result in cytokinesis failure, an early event in cancer that facilitates the development of genomic instability (Barna et al., 2008).

Not only ribosome biogenesis has been implicated in the ability of c-Myc to initiate tumorigenesis, but also very recently, RPL5 and RPL11 were implicated in safeguarding against this c-Myc-induced tumor initiation. In a study published in 2010, *Eμ-Myc* transgenic mice, which constitutively express c-Myc in B cell lineage and develop B cell lymphoma at early age, were crossed with mice carrying a cancer-associated cysteine-to-phenylalanine substitution in the zinc finger of MDM2, which disrupts its binding to RPL5 and RPL11. Mice bearing the mutant MDM2, termed *Mdm2<sup>C305F</sup>*, retained a normal p53 response to DNA damage but lacked p53 response to perturbations in ribosome biogenesis. The *Eμ-Myc;Mdm2<sup>C305F/C305F</sup>* mice resulting from the above-mentioned cross showed a great acceleration of lymphomagenesis compared to *Eμ-Myc;Mdm2<sup>+/+</sup>* mice, indicating that the interaction of RPL5 and RPL11 with MDM2 could play an indispensable role in hampering c-Myc-mediated tumorigenesis. The RPL5/RPL11 pathway would be interfering with c-Myc tumor initiation in parallel to the ARF-MDM2 interaction, as it was also shown that p19<sup>ARF</sup> was not required for

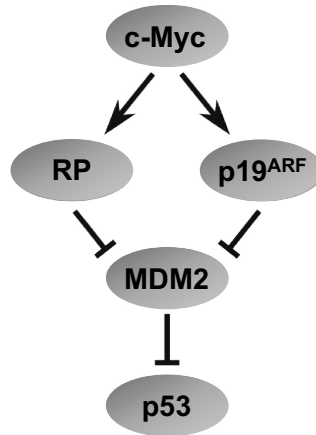


**Figure 1.12: Model for RP-MDM2-p53 signaling in response to oncogenic c-Myc.** Oncogenic c-Myc induces high expression of both p19<sup>ARF</sup> and ribosomal proteins. The RP-MDM2-p53 and p19<sup>ARF</sup>-MDM2-p53 represent two parallel signaling pathways in response to oncogenic c-Myc stimulation. Adapted from Macias et al., 2010.

p53 response to ribosomal stress by using ARF<sup>-/-</sup> mouse embryo fibroblasts (MEFS) (Figure 1.12) (Macias et al., 2010).

In line with c-Myc's importance in driving ribosome biogenesis, and knowing that c-Myc hyperactivation could be counteracted by the accumulation and binding of free RPL5 and RPL11 to MDM2, several studies have focused on how this process could be exploited as a therapeutic strategy to selectively kill c-Myc-driven malignant cells. A recent publication using E $\mu$ -Myc B cells, demonstrated how Pol I transcription, whose components are robustly upregulated in c-Myc activation conditions, can be therapeutically targeted to selectively activate p53 and kill malignant cells, while maintaining a viable population of wild-type cells of the same lineage (Bywater et al., 2012). The efficacy of this therapeutic approach was mediated through inhibition of ribosome biogenesis, leading to p53-mediated

### 1.3. c-Myc, ribosome biogenesis and cancer

---

apoptosis following binding and sequestration of the ubiquitin ligase MDM2 by RPL5 and RPL11, showing that c-Myc's control of Pol I transcription is required for its oncogenic potential, independent of its function in regulating protein translation and proliferative growth (Bywater et al., 2012; Devlin et al., 2016).

It is important to highlight that, although the above studies showed that RPL5 and RPL11 or RPL11 bind to and inhibit MDM2 in E $\mu$ -Myc B cells, in neither study by Macias et al. or Bywater et al. was demonstrated that the 5S rRNA or the IRBC complex are implicated in this response (Bywater et al., 2012; Macias et al., 2010).

#### 1.3.2 Ribosome biogenesis in colorectal cancer

Colorectal cancer (CRC) is the third most common cancer and the third leading cause of cancer-associated death worldwide. Activation of the Wnt/APC signaling pathway and inactivation of the TGF- $\beta$  signaling pathways are nearly ubiquitous events in CRC, resulting in increased activity of c-Myc (Muzny et al., 2012). Importantly, the binding of RPL5 and RPL11 to MDM2 has also been shown to play a critical role in CRC tumorigenesis. In a very recent study, *Mdm2*<sup>C305F</sup> mice were crossed with *Apc*<sup>Min/+</sup> mice, which carry a dominant mutation in APC that results in truncation of the gene product. The *Apc*<sup>Min/+</sup> mice are known to overexpress c-Myc and to be prone to intestinal tumor formation. In the study, it was shown that the animals resulting from the cross, the *Apc*<sup>Min/+</sup>; *Mdm2*<sup>C305F/C305F</sup> mice, displayed increased tumor size and incidence

compared with their *Apc*<sup>Min/+</sup>; *Mdm2*<sup>+/+</sup> counterparts, correlating with decreased p53 protein abundance and activation. This result would indicate that loss of the RPL5/RPL11-interaction with MDM2 sensitizes mice to APC-loss driven colon tumorigenesis (Liu et al., 2017).

Consistent with these findings, and reinforcing the concept of attacking the hyperactivation of ribosome biogenesis in c-Myc-driven tumors as an “Achilles’ heel” to selectively kill malignant cells, a recent publication has shown that oxaliplatin, a compound used as the front-line therapy for CRC in combination with 5-fluorouracil (5-FU), does not activate the DNA damage response, as originally thought, but instead kills tumor cells by apparently inducing IRBC. The data from this study suggests that the increased expression of the translational machinery represents a “translational addiction” in CRC, which would be responsible for the effectiveness of oxaliplatin. The authors found that APC expression was significantly correlated with translation-metagenes expression in several cancers, including breast and lung. Indeed, they further show that APC expression may serve as a molecular marker for stratification for the treatment of a number of cancer types (Bruno et al., 2017).

### **1.3.3 p53 response in c-Myc-driven tumors**

In mouse models, c-Myc expression appears to cause p53 stabilization and activation through two primary pathways: one would be by inducing ARF, which binds and inhibits MDM2, and the other, based on the above mentioned studies using the *Mdm2*<sup>C305F</sup>

### 1.3. c-Myc, ribosome biogenesis and cancer

---

mouse, may be the IRBC complex, as it appears that MDM2 inhibition by RPL5/RPL11 plays an important role in the stabilization of p53 in a c-Myc-driven setting (Liu et al., 2017; Macias et al., 2010). However, others have argued that an increased rate of ribosome biogenesis may instead promote tumorigenesis by downregulating p53 expression and activity (Derenzini et al., 2017). In these studies, different experimental models characterized by an upregulation of rRNA synthesis were first shown to have reduced p53 protein levels as a consequence of increased p53 proteasomal degradation (Donati et al., 2011). In later experiments, it was demonstrated that interleukin 6 (IL-6) treatment upregulated rRNA transcription and downregulated p53 protein levels, with these events linked to an increase in c-Myc protein levels. Considering that the onset of colon cancer in patients with inflammatory bowel disease is a representative example of chronic inflammation-related tumorigenesis, the epithelial cells of the colon mucosa of patients with ulcerative colitis were analyzed and it was shown that they were characterized by a nuclear hypertrophy, which indicates an upregulated rRNA synthesis, as well as showing reduced expression of p53 compared to cells of the normal mucosa. Together, these data led the authors to conclude that c-Myc upregulation, by promoting ribosome biogenesis and therefore by enhancing rRNA transcription, increases the recruitment of RPs to form ribosomes, reducing the amount of the IRBC complex, which normally binds and inhibits MDM2. The authors suggest that in this setting, the reduced amount of IRBC complex would cause a rise in p53 degradation and a consequent down-regulation of p53 expression and activity

## 1. INTRODUCTION

---

(Brighenti et al., 2014; Derenzini et al., 2017). These points are addressed in the Results and Discussion sections of this thesis.

### 1.3. c-Myc, ribosome biogenesis and cancer

---

# **OBJECTIVES**



## 2 Objectives

The aim of this thesis is to understand the role of the IRBC complex in the regulation of p53 in a c-Myc-driven tumor setting. Previous results from our laboratory have demonstrated that p53 levels are up-regulated upon insults to ribosome biogenesis, through the action of a pre-ribosomal complex containing the ribosomal proteins L5 (RPL5), RPL11 and the 5S ribosomal RNA (5S rRNA), termed the IRBC complex. This complex is re-directed from 60S biogenesis to the binding and inhibition of MDM2 when ribosome biogenesis is inhibited, allowing p53 stabilization and increasing its levels (Donati et al., 2013). On the other hand, prior studies have shown that when E $\mu$ -Myc transgenic mice, which constitutively express c-Myc in B-cell lineage and develop B-cell lymphoma at an early age, are crossed with mice harboring a point mutation in MDM2 which disrupts RPL5 and RPL11 binding to MDM2, lymphomagenesis is greatly accelerated (Macias et al., 2010). Taking into account the relevance of these findings, the general aim of the thesis is to decipher the molecular mechanism by which p53 is regulated in c-Myc-driven colorectal tumors. Specifically, we set out to investigate whether c-Myc regulates p53 by directly modulating the IRBC complex and whether c-Myc enhances or suppresses this response. To this end, we selected as a model colon cancer cell lines and focused on the four following objectives:

1. – Global effects of c-Myc depletion in colon cancer cells.
2. – Function of c-Myc in production of ribosomal components.
3. – Effect of c-Myc depletion on p53 levels.

## 2. OBJECTIVES

---

4. – Role of the RPL5/RPL11/5S rRNA complex in mediating p53 levels in response to c-Myc depletion.

# **RESULTS**



## **3 Results**

### **3.1 Global effects of c-Myc depletion in colon cancer cells**

#### **3.1.1 c-Myc depletion results in decreased proliferation and accumulation of cells in G<sub>0</sub>/G<sub>1</sub> phase of the cell cycle**

To better understand the underlying mechanisms by which p53 is regulated in c-Myc driven tumors, we set out to investigate the effects of c-Myc downregulation on p53 levels. We first evaluated the global effects of c-Myc depletion on a number of cellular parameters, to better characterize our experimental model.

This study was performed using colorectal cancer (CRC) cell lines, as it is known that events leading to c-Myc activation are pervasive in CRC (Muzny et al., 2012). We analyzed the poorly differentiated RKO and HCT116 human CRC cell lines. RKO cells carry mutations in (a) BRAF, a serine/threonine kinase of the Raf family that acts downstream of Ras, inducing constitutive ERK signaling, and in (b) the gene encoding the catalytic subunit of PI3K $\alpha$ , p110 $\alpha$  (PIK3CA), which results in constitutive activation of PI3K $\alpha$  (Ahmed et al., 2013). HCT116 cells carry mutations in KRAS, PIK3CA, and they are also heterozygous for  $\beta$ -catenin, harboring one wild type allele and one mutant allele with a deletion that eliminates the serine residue at codon 45.  $\beta$ -catenin mutations lead to constitutive activation of  $\beta$ -catenin/TCF-4-regulated transcription, including that of c-Myc.

### 3.1. Global effects of c-Myc depletion in colon cancer cells

Moreover, RKO and HCT116 cells have 2-fold greater c-Myc protein levels than well differentiated colon tumor cell lines (Taylor et al., 1992) and in both cell lines the ARF tumor suppressor is dysfunctional, either by methylation or mutation of the gene (Burri et al., 2001; Martin et al., 2008; Weber et al., 2002), allowing us to focus on the IRBC complex as the major MDM2 regulator in these cells.

To analyze the effects of c-Myc downregulation in the CRC cell lines, we performed RNA interference to deplete endogenous c-Myc levels. To determine the best c-Myc siRNA dose for our studies, we initially treated HCT116 cells with two different c-Myc siRNAs (siMyc 1 and siMyc 2) using increasing concentrations for up to 48 hours, as compared to a non-silencing control siRNA (siNS). As shown in

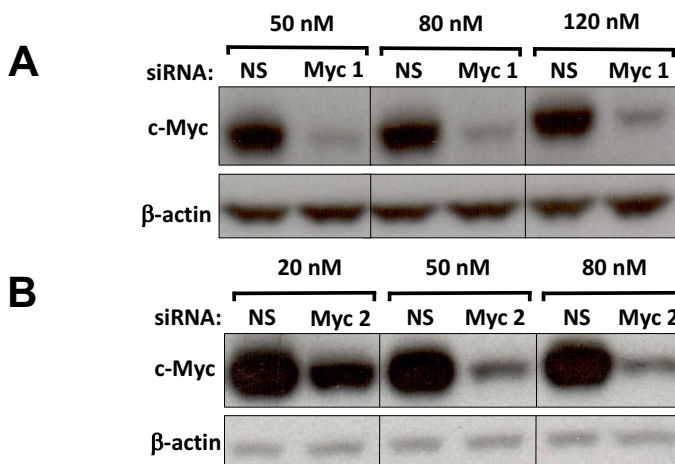


**Figure 3.1: Effects of c-Myc depletion on c-Myc protein levels in HCT116 cells.** (A) HCT116 cells were transfected at increasing concentrations with either a non-silencing siRNA (siNS) or siMyc 1. (B) HCT116 cells were transfected with siNS or siMyc 2 at increasing concentrations. Western blot of whole cell lysates was performed as described in Materials and Methods.  $\beta$ -actin serves as loading control.

### 3. RESULTS

Figure 3.1, compared to siNS, either siMyc 1 or siMyc 2 appeared to be effective in almost completely depleting c-Myc protein at a concentration of 50 nM, as measured by Western blot analysis.

We next compared the efficacy of c-Myc depletion by siMyc 1 and siMyc 2 over time in HCT116 cells. As seen in Figure 3.2, at 24, 48 and 72 hours of treatment, we observed a stronger reduction in c-Myc protein levels with siMyc 2 than with siMyc 1, and the results at 24 and 48 hours were similar in terms of the level of depletion achieved. Using the 48-hour time point as a reference, we evaluated the extent of c-Myc mRNA depletion in RKO and HCT116 cells by quantitative real-time PCR (Figure 3.3.). Although we observed an approximate equivalent reduction in c-Myc mRNA levels with both siMyc 1 and siMyc 2 (between ~45-60%), siMyc 2 appears to be better at reducing c-Myc mRNA levels in both cell lines, consistent with the effects on c-Myc protein levels in HCT116 cells (Figure 3.2).

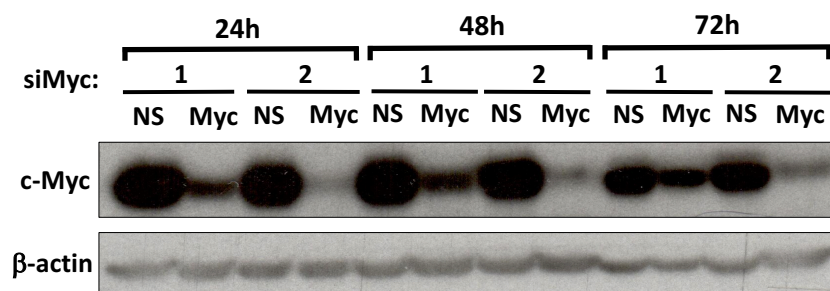


**Figure 3.2: Effects of c-Myc depletion on c-Myc protein levels in HCT116 cells at different time points.** HCT116 cells were transfected with siNS, siMyc 1 or siMyc 2 for different times, using a siRNA concentration of 50 nM. Western blot analysis of whole cell lysates was performed as described in Materials and Methods. β-actin serves as loading control.

### 3.1. Global effects of c-Myc depletion in colon cancer cells

---

Next, we evaluated the impact of c-Myc depletion on the proliferation of CRC cells. siRNA depletion of c-Myc was carried out over 24, 48 and 72 hours and proliferation was measured by crystal violet staining. As shown in Figures 3.4B and 3.4C, in both HCT116 and RKO cells treated with siMyc 2, as compared to the siNS, a clear reduction in proliferation rates was evident at 48 hours, with a more pronounced effect at 72 hours. A similar effect was obtained for siMyc 1 in HCT116 cells (Figure 3.4A). The results were largely equivalent using two different siRNAs, supporting the argument that inhibition of proliferation was an on-target effect caused by c-Myc depletion.

A large body of literature suggests that inhibition of c-Myc in primary cells or non-transformed cell lines leads to a strong proliferative arrest in the G<sub>0</sub>/G<sub>1</sub> or G<sub>1</sub>/S phases of the cell cycle, whereas c-Myc-depleted tumor cells show inhibition of cell proliferation, but have

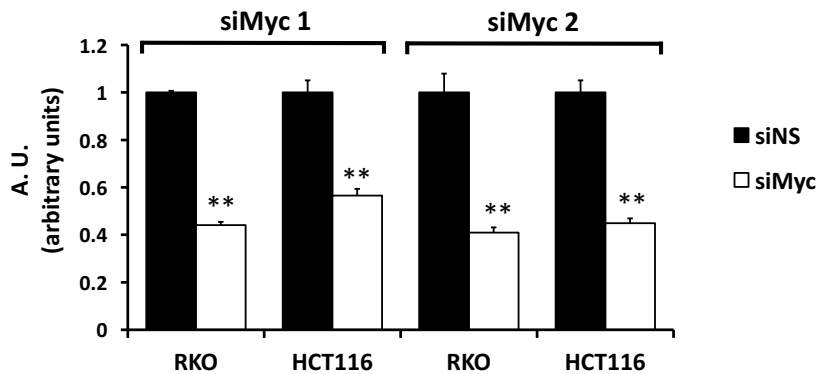


**Figure 3.3: Effects of c-Myc depletion on c-Myc mRNA levels in CRC cells.** RKO and HCT116 cells were transfected with siNS, siMyc 1 or siMyc 2 for 48 hours, using a siRNA concentration of 50 nM. Relative c-Myc mRNA levels were determined by quantitative real-time PCR as described in Materials and Methods.

been reported to present a more variable effect on the cell cycle phases affected (Wang et al., 2008). To determine the effect of c-Myc inhibition in RKO and HCT116 cells, we used propidium iodide (PI) staining and flow cytometry to evaluate the cell cycle parameters 48 hours after siMyc 2 transfection. Surprisingly, when analyzing RKO cells by light scattering, we observed two well-differentiated cell populations by forward scatter (FSC), which is known to be proportional to cell-surface area or size. One population was constituted by smaller cells, hereafter designated “small cells”, represented ~65% of the total number of cells, and the second one

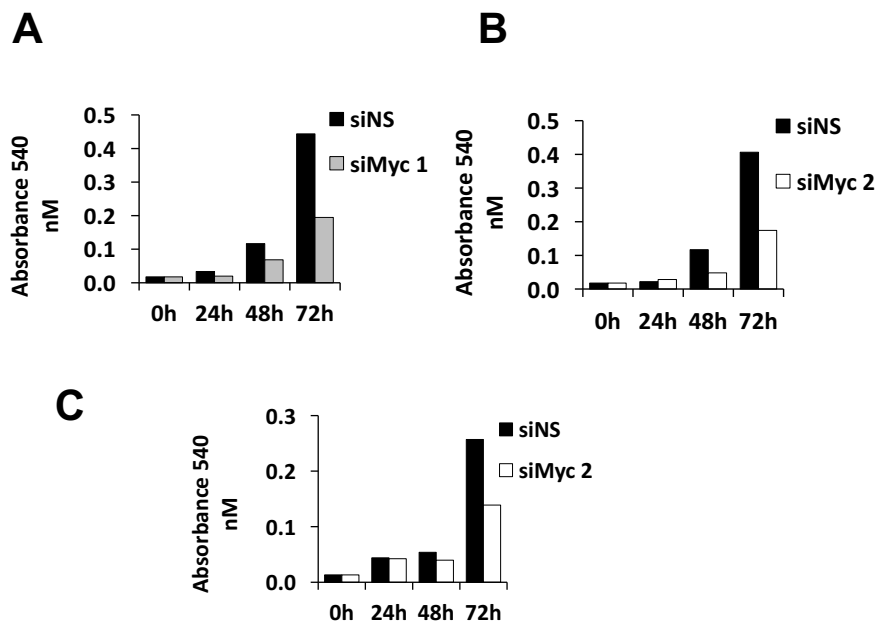


**Figure 3.4: c-Myc depletion decreases proliferation in CRC cells.** CRC cells were transfected with siNS, siMyc1 or siMyc 2 for 24, 48 and 72 hours, and proliferation was measured by crystal violet staining as described in Materials and Methods. (A) HCT116 cells were transfected with siNS or siMyc 1. (B) HCT116 cells were transfected with siNS or siMyc 2. (C) RKO cells were transfected with siNS or siMyc 2.

### 3.1. Global effects of c-Myc depletion in colon cancer cells

comprised of larger cells, designated “big cells”, represented ~35% of the cells (Figure 3.5A). Nevertheless, when analyzing the response to c-Myc depletion, we observed that both populations

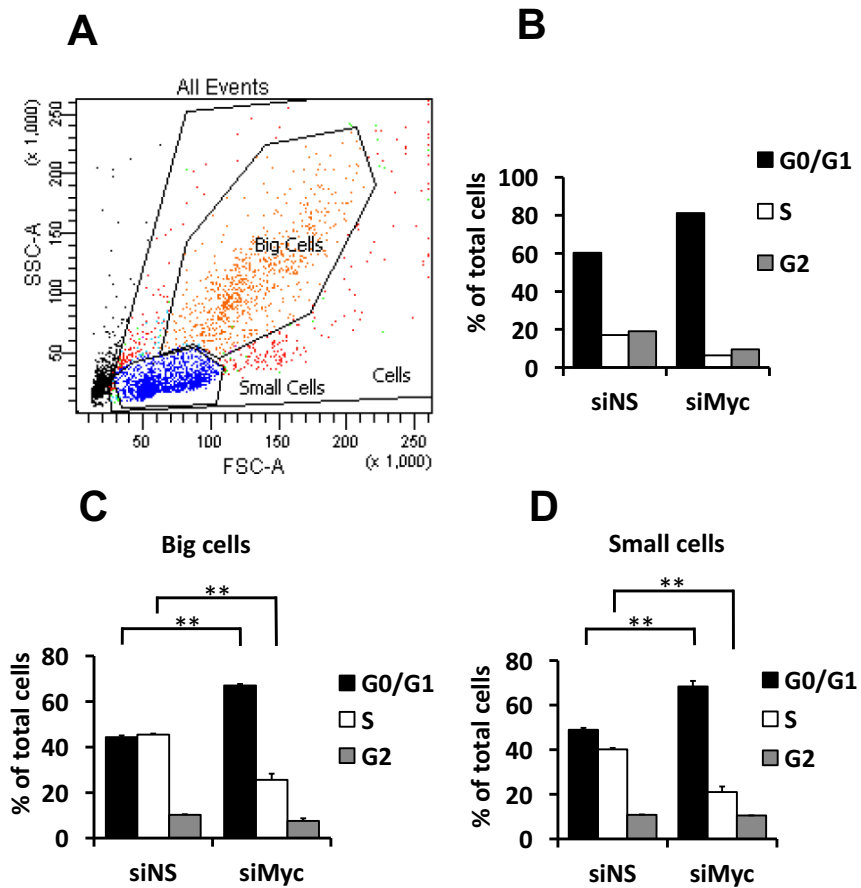


**Figure 3.5: Cell cycle analyses of CRC cells.** (A) Normal growing RKO cells were analyzed by flow cytometry. Differences in forward (FSC) and side scatter (SSC) indicated the existence of two different populations, referred to as “small cells” and “big cells”. (B) HCT116 cells were treated with siNS or depleted from c-Myc using siMyc 2 (siMyc), and analyzed by flow cytometry. (C, D) RKO cells were treated either with siNS or siMyc 2 (siMyc) and analyzed by flow cytometry. The analysis was performed separately for each of the two populations found to constitute this cell line, as referred to in (A).

responded similarly, showing an increased accumulation of cells in  $G_0/G_1$  phase of the cell cycle of approximately 20% and a comparable reduction of cells in S phase (Figures 3.5C and 3.5D). The effect of c-Myc depletion on HCT116 cells appeared equivalent to that observed in RKO cells, with an apparently similar increase in the accumulation of cells in  $G_0/G_1$ , and a decrease in cells in S phase and  $G_2$  (Figure 3.5B). The data are consistent with the requirement of c-Myc expression to drive both RKO and HCT116 cells through  $G_0/G_1$  phase of the cell cycle.

#### **3.1.2 Reduction of c-Myc levels modifies cellular size and shape and causes a decrease in the rate of global protein synthesis**

Given the findings above, that cells appear to be accumulating in  $G_0/G_1$  phase of the cell cycle, and that the overexpression of c-Myc is known to have significant effects on cell growth and cell size, which have been associated with marked changes in the total rate of protein synthesis (van Riggelen et al., 2010), we investigated the extent to which c-Myc depletion affected both parameters. Although increased cell size has been associated with augmented c-Myc expression (Lloyd, 2013), in different models systems loss of c-Myc expression has been linked to reduced cell size (Muncan et al., 2006; Zanet et al., 2005). In HCT116, c-Myc depletion caused an apparent clear decrease in cell size, whereas RKO cells exhibited a change in cell shape, becoming thinner (Figure 3.6). Consistent with the apparent slowdown in cell proliferation, cell cycle progression

### 3.1. Global effects of c-Myc depletion in colon cancer cells

---

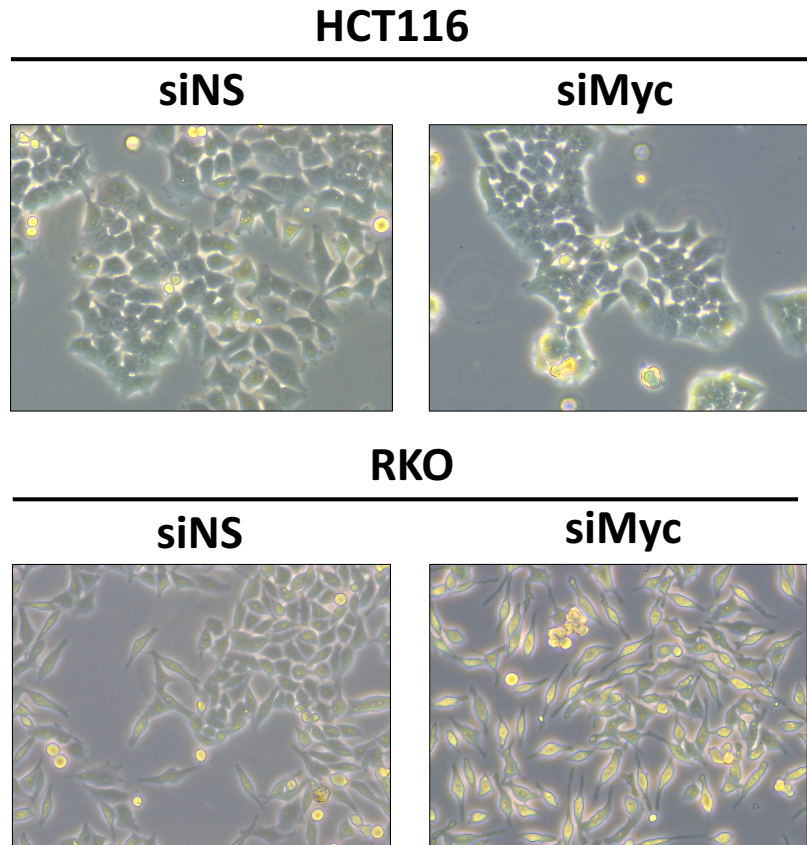


**Figure 3.6: c-Myc depletion induces changes in cell size and cell shape in CRC cells.** HCT116 and RKO cells were treated with control siNS or c-Myc siRNA (siMyc) for 48 hours using a concentration of 50 nM. (A) HCT116 cells depleted from c-Myc present reduced cell size than siNS-treated cells. (B) RKO cells treated with c-Myc siRNA appear thinner than control cells.

and reduced cell size, we found that the incorporation of  $^3\text{H}$ -leucine into nascent total protein in c-Myc depleted RKO cells is reduced by approximately 45% (Figure 3.7). Thus, the inability of RKO cells to grow and proliferate may in part be caused by reduction in translational capacity.

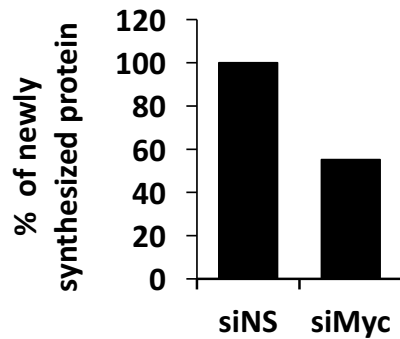


**Figure 3.7: c-Myc depletion decreases the global protein synthesis rate in RKO cells.** Quantification of the incorporation of  $^3\text{H}$ -leucine into total protein in RKO cells treated with siNS or siMyc 2 (siMyc) for 48 hours, performed as described in Materials and Methods. Values obtained from the siNS-treated sample are considered to represent 100% of newly synthesized protein.

## 3.2 Function of c-Myc in production of ribosomal components

### 3.2.1 c-Myc depletion decreases the synthesis of RPs

As presented in the Introduction (see section 1.3) one of the chief transcriptional targets of c-Myc are the components the ribosome, both the RPs and rRNA genes. Thus, the observed reduction in translational capacity (Figure 3.7) caused by c-Myc depletion may be attributed to a reduction in ribosome content.

To determine to which extent c-Myc depletion affects RPs in CRC cell lines, we performed RNA interference experiments to

### 3.2. Function of c-Myc in production of ribosomal components

knockdown endogenous c-Myc and studied the effects on the RP's mRNAs. As shown in Figure 3.8A, RP mRNA levels in RKO cells were significantly decreased upon 48 hours of c-Myc depletion, with RPL5 mRNA showing the most marked reduction (~60%). In HCT116 cells, we also observed a significant decrease in RPL5 mRNA and a tendency to diminish for other RP mRNAs tested, in this case RPL11, RPL7a and RPS19, which are two small- and one large-ribosomal subunit proteins respectively (Figure 3.8B). The findings are consistent with a reduction in c-Myc-mediated Pol II-driven RP mRNA transcription following c-Myc depletion by siRNA treatment.

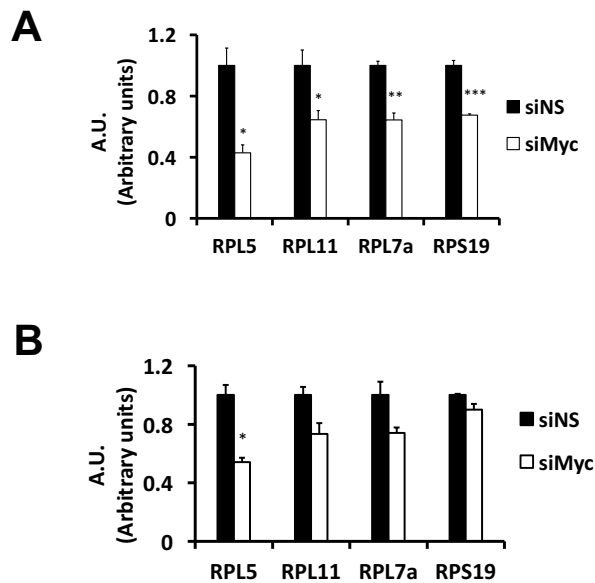


**Figure 3.8: Effect of c-Myc depletion on RP mRNAs in CRC cells.** CRC cells were treated with siNS or siMyc 2 for 48 hours and mRNA levels of different RPs were determined by quantitative real-time PCR as described in Materials and Methods. (A) RKO cells were treated with siNS or siMyc 2 (siMyc). (B) HCT116 cells were treated with siNS or siMyc 2 (siMyc).

### 3. RESULTS

Despite the reduction in RP mRNAs, ribosomes are known to have a long half-life and RPs are produced in excess, such that only 30% of newly made proteins are incorporated into nascent ribosomes, with remaining proteins being degraded by the proteasome (Lam et al., 2007). This raises the possibility that a reduction of RP mRNAs may not alter cellular ribosome content. To examine how c-Myc depletion affects RP levels, we depleted c-Myc in HCT116 and RKO cells and analyzed individual RPs by Western blot analysis. The results show that, despite the reduction in total mRNA, there is little to no effect on the levels of RPL11, RPS19 or RPL5 in HCT116 cells (Figures 3.9A and 3.9B). The same tendency was observed in RKO cells (Figures 3.9C and 3.9D). This indicates that c-Myc depletion alters the synthesis of RP mRNAs, without having an apparent effect on total RPs levels in HCT116 and RKO cells.

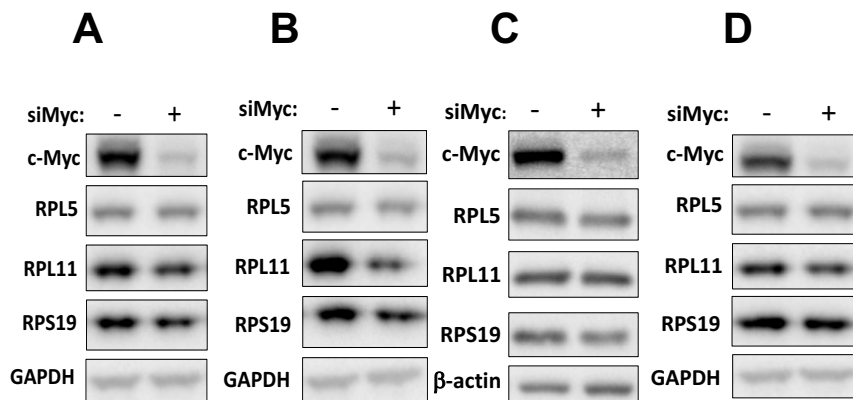


**Figure 3.9: Effect of c-Myc depletion on RPs in CRC cells.** CRC cells were treated with siNS or c-Myc siRNA for 48 hours and protein levels of different RPs were determined by Western blot analysis as described in Materials and Methods. (A) HCT116 cells were treated with siNS or siMyc 2. (B) HCT116 cells were treated with siNS or siMyc 1. (C). RKO cells were treated with siNS or siMyc 2. (D) RKO cells were treated with siNS or siMyc 1. GAPDH and  $\beta$ -actin serve as loading controls.

### 3.2. Function of c-Myc in production of ribosomal components

---

The findings above address the question of total cellular RPs, which can represent 4-5 million copies per mammalian cell (Granneman and Tollervey, 2007), but do not address the fate of nascent RP synthesis. In order to answer this question, we focused on nascent RPL5 synthesis, as its mRNA had fallen the largest extent following c-Myc depletion (Figure 3.8), whereas its total levels appeared unaffected (Figure 3.9). We analyzed the effect of c-Myc-silencing on newly synthesized cellular proteins by pulse labeling NS- or c-Myc-siRNA treated RKO cells with the methionine analogue L-azidohomoalanine (AHA). Analysis of newly synthesized biotinylated proteins by streptavidin-IRDye800 showed a general decrease of *de novo* synthesized proteins in the c-Myc-depleted condition (Figure 3.10A), consistent with the studies on total protein measured by <sup>3</sup>H-leucine incorporation (Figure 3.7). In whole cell extracts from c-Myc siRNA depleted cells, RPL5 levels were not changing, consistent with prior Western blot analyses (Figure 3.9). However, the amount of newly synthesized RPL5 pulled down by the streptavidin beads was strikingly decreased upon c-Myc depletion, whereas there was no effect on newly synthesized GAPDH (Figure 3.10B). Thus, although there is little effect observed on total RPL5 protein levels, there is a dramatic inhibition of the *de novo* synthesis of RPL5 following c-Myc depletion.

The newly synthesized RPs are rapidly transported into the nucleolus, whereas once they are incorporated into mature ribosomes they are re-exported to the cytoplasm (Lam et al., 2007). To further investigate the decrease of *de novo* synthesized RPs under c-Myc-depleted conditions, following treatment with c-Myc siRNA we separated newly synthesized RPs from whole cell lysates

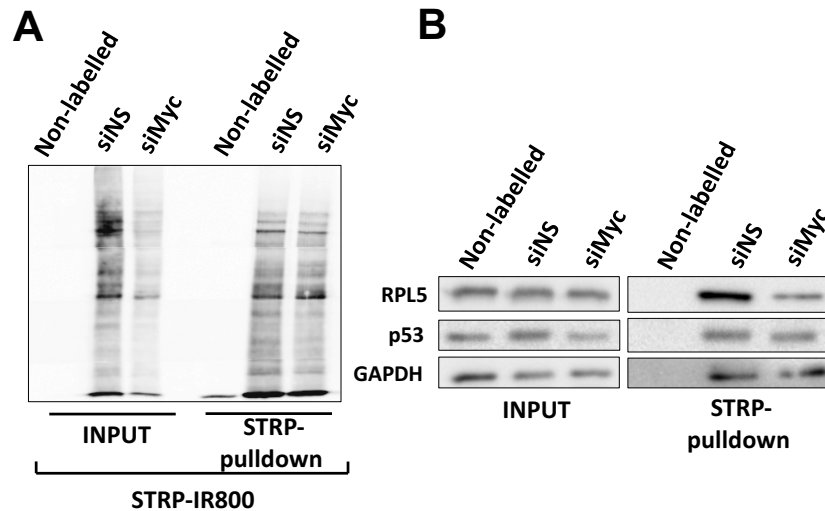


**Figure 3.10: Effect of c-Myc depletion on newly synthesized proteins.**

(A) RKO cells were treated with siNS or siMyc 2 for 48 hours and *de novo* synthesized proteins were labelled by alkyne-biotine click-it reaction (see Materials and Methods). The labelling efficiency of the experimental conditions was evaluated by Western blotting of biotinylated proteins and hybridizing the membrane with streptavidin-IRDye800. The intensity of the signals was detected using an infrared scanner. (B) Total cell extracts (INPUT) and nascent proteins from INPUTs, pulled down using streptavidin-agarose beads (STRP-pulldown), were resolved by Western blot analysis with the indicated antibodies

by high-speed ultracentrifugation (Donati et al., 2013) in HCT116 cells, RKO cells and a third CRC cell line termed LoVo. This protocol has been shown to allow the separation of mature ribosomes from whole cell extracts, obtaining a post-ribosomal lysate which contains newly synthesized RPs that have not been incorporated into ribosomes or degraded by the proteasome (Donati et al., 2013). Western blot analyses of both the total lysate and the post-ultracentrifugation fraction, referred to as “non-ribosomal” fraction, were performed for RPL5 and RPL7a (Figure 3.11). There was little

### 3.2. Function of c-Myc in production of ribosomal components

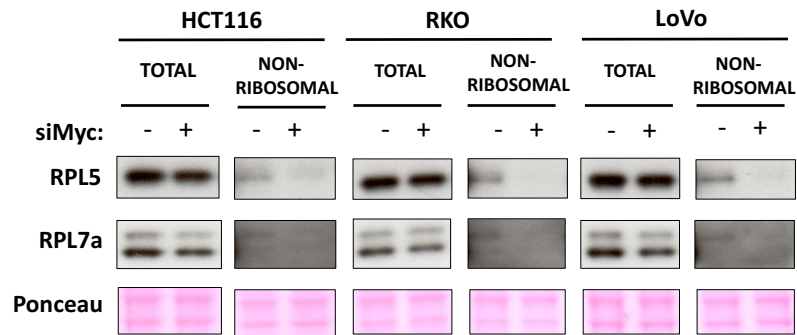


**Figure 3.11: “Non-ribosomal” RPs decrease upon c-Myc depletion in CRC cells.** HCT116, RKO and LoVo cells were treated with siNS or siMyc 2 for 48 hours and protein samples were subjected to high-speed ultracentrifugation to remove ribosomes, as described in Materials and Methods. Western blot analysis was performed for both whole cell lysates (TOTAL) and for lysates obtained after the ultracentrifugation (NON-RIBOSOMAL), and levels of different RPs were determined with the corresponding antibodies. Ponceau staining serves as a loading control.

effect on the levels of either RPL5 or RPL7a in the total lysates, consistent with the findings above (Figure 3.9). However, when we examined the “non-ribosomal” fraction, the levels of RPL5 and RPL7a were strongly reduced after the high-speed ultracentrifugation in c-Myc-depleted samples (Figure 3.11), consistent with the reduction in newly synthesized AHA-labeled RPL5 pulled down by the streptavidin beads (Figure 3.10).

#### 3.2.2 c-Myc depletion decreases the synthesis of rRNA

The rate-limiting step in ribosome biogenesis is argued to be the production of rRNA (Poortinga et al., 2015), such that if RPs do not bind to rRNA in the nucleolus they are rapidly degraded in the

nucleus, where they shuttle in the absence of rRNA (Bursać et al., 2012; Lam et al., 2007). Given that c-Myc drives Pol I and Pol III transcription of rRNA, and that newly synthesized levels of nascent RPL5 fall following c-Myc depletion, this maybe a reflection not only of RP mRNA levels but also of rRNA synthesis. To measure the extent to which c-Myc depletion affects rRNA synthesis in CRC cells, we measured steady-state levels of rRNA species by ethidium bromide (EB) staining and nascent rRNA levels by pulse labeling with  $^3\text{H}$ -uridine in c-Myc-depleted HCT116 cells. An EB-agarose gel

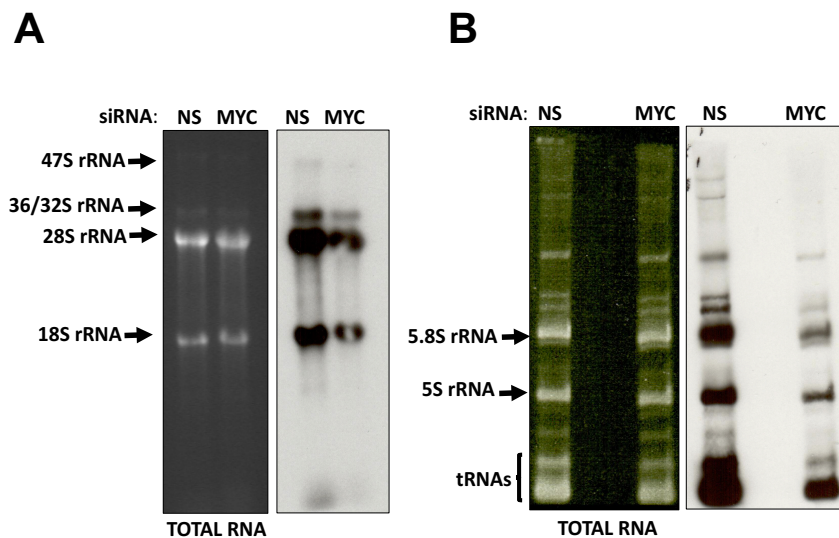


**Figure 3.12: Effect of c-Myc depletion on newly synthesized rRNAs.** (A) EB-stained agarose gel (left) and autoradiogram of a Northern blot (right) of total cellular RNA from HCT116 cells treated with siNS (NS) or siMyc 2 (MYC) and labeled with  $^3\text{H}$ -uridine for 1 h and then chased for 4 h in non-labeled uridine-containing medium. The autoradiogram shows a reduction of all rRNA species, indicating a general decrease of ribosome biogenesis. (B) EB-stained TBE-urea polyacrylamide gel (left) and autoradiogram of a Northern blot (right) of newly synthesized  $^3\text{H}$ -uridine-labeled 5S rRNA in HCT116 cells transfected with siNS (NS) or siMyc 2 (MYC).

### 3.2. Function of c-Myc in production of ribosomal components

---

showed that c-Myc siRNA depletion, as compared to NS siRNA treatment, had no impact on the steady-state levels of rRNA, whereas depletion of c-Myc led to an equivalent reduction in all rRNA species synthesized by Pol I (47S and 36/32S rRNA precursors, 28S rRNA and 18S rRNA) (Figure 3.12A). We also examined *de novo* synthesized 5S rRNA by performing Northern blot analysis with the same <sup>3</sup>H-uridine-labeled samples in a polyacrylamide gel (Figure 3.12B). As in the case of Pol I-dependent transcripts, we observed that Pol III-dependent transcription of 5S rRNA and tRNAs was diminished in c-Myc siRNA-treated cells as compared to control cells. These results indicate that c-Myc depletion in HCT116 cells leads to a general decrease in all Pol I and Pol III-dependent transcripts, in contrast to the accumulation of 36/32S rRNA precursors occurring in conditions of ribosome biogenesis impairment upon depletion of RPL5, RPL11 or TFIIIA (Donati et al., 2013).

The results described in this section demonstrate that c-Myc depletion decreases newly synthesized RPs by either reducing their transcription and/or translation, resulting in a diminished presence of newly synthesized RPs in the “non-ribosomal” fraction. In parallel, decreased c-Myc levels causes a general reduction in the synthesis of all rRNA species. Thus, c-Myc depletion profoundly affects ribosome biogenesis in CRC cell lines.

### 3.3 Effect of c-Myc depletion on p53 levels

#### 3.3.1 Reduction of c-Myc levels causes a drop in p53 protein

When E $\mu$ -Myc transgenic mice are crossed with mice harboring the C305F point mutation in MDM2, which disrupts RPL5 and RPL11 binding to MDM2, lymphomagenesis is greatly accelerated. Spleens of E $\mu$ -Myc mice with wild-type MDM2 present evident p53 induction, which is attenuated in spleens of E $\mu$ -Myc mice carrying the mutant MDM2 (E $\mu$ -Myc;*Mdm2*<sup>C305F/C305F</sup>) (Macias et al., 2010). This decreased p53 induction has been correlated to the increased mortality of E $\mu$ -Myc;*Mdm2*<sup>C305F/C305F</sup> mice and thus, to the notion that binding of RPL5 and RPL11 to MDM2 constitutes an important tumor barrier against oncogenic c-Myc, through the induction of p53. These results would appear consistent with earlier findings described in c-Myc overexpressing cells of E $\mu$ -Myc transgenic mice and in studies linking c-Myc overexpression with increased p53 protein levels (Eischen et al., 1999; Hermeking and Eick, 1994; Zindy et al., 1998). However, the role of RPL11 and RPL5 in mediating p53 levels is controversial, as others have claimed that c-Myc upregulation, by promoting ribosome biogenesis, increases the recruitment of RPs to form ribosomes, thus reducing the amount of RPs available to bind MDM2 and leading to decreased p53 protein levels (Brighenti et al., 2014; Derenzini et al., 2017). Moreover, although different studies have implicated RPL5 and RPL11 in regulating p53 in response to c-Myc, the pre-ribosomal complex

### 3.3. Effect of c-Myc depletion on p53 levels

---

RPL5/RPL11/5S rRNA has not been directly implicated in this response. Given these findings, we set out to investigate the status of p53 either in RKO or HCT116 cells following c-Myc depletion, as compared to treatment with the siNS control. We found that, in both cell lines, p53 levels decreased following c-Myc-depletion, though the effects were more pronounced for siMyc 2 (Figure 3.13A) than for siMyc 1 (Figure 3.13B). These effects were accompanied by a clear reduction in its target gene MDM2 (Figure 3.13), which is largely responsible for degrading both p53 and also ubiquitinates itself (Shadfan et al., 2012). As others have described that c-Myc depletion leads to increased p53 levels in hepatocellular carcinoma cells (Brighenti et al., 2014), we performed siRNA interference against c-Myc in the hepatocellular carcinoma cell line HepG2 using siMyc 2. Contrary to what has been published, we saw a decrease in p53 levels in HepG2 cells upon c-Myc depletion independent of

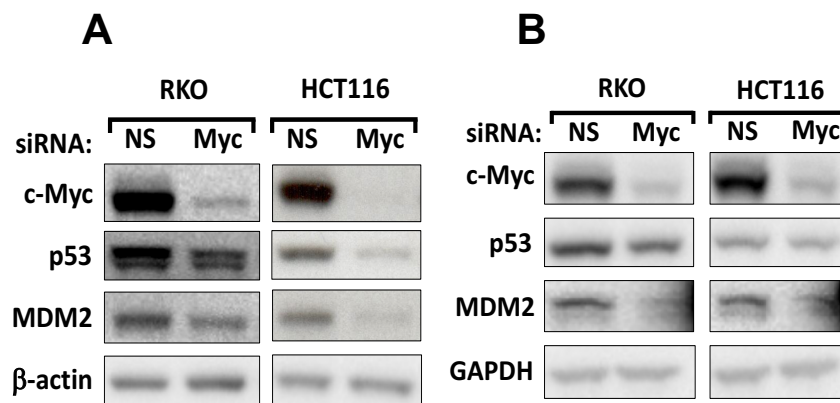


**Figure 3.13: Effect of c-Myc depletion on p53 and MDM2 protein levels in CRC cells.** (A) RKO and HCT116 cells were treated with siNS (NS) or siMyc 2 (Myc). (B) RKO and HCT116 cells were treated with siNS (NS) or siMyc 1 (Myc). Whole cell lysates were analyzed by Western blot analysis for the indicated proteins with the corresponding antibodies.  $\beta$ - actin and GAPDH serve as loading controls.

### 3. RESULTS

time (Figure 3.14). Thus, diminished c-Myc expression causes a decrease in p53 levels that is not specific to CRC cell lines, potentially arguing that the RPL5/RPL11/5S rRNA complex, which when redirected to MDM2, has been recently termed the impaired ribosome biogenesis checkpoint (IRBC) complex (Gentilella, in press) is acting as an intrinsic tumor suppressor or tumor barrier, when c-Myc levels become oncogenic, as first described by Lowe et al. (Lowe et al., 2004).

If the IRBC complex is acting to suppress MDM2, then upon c-Myc depletion this inhibition would be potentially relieved, leading to a reduction in p53 levels. Such a model would be consistent with earlier studies showing that under c-Myc-overexpression conditions, p53 levels rise mainly due to an increased protein stability (Zindy et al., 1998), although others have reported that p53 mRNA levels also increase in c-Myc-overexpressing cells (Hermeking and Eick, 1994). To investigate whether c-Myc depletion decreases p53 mRNA levels

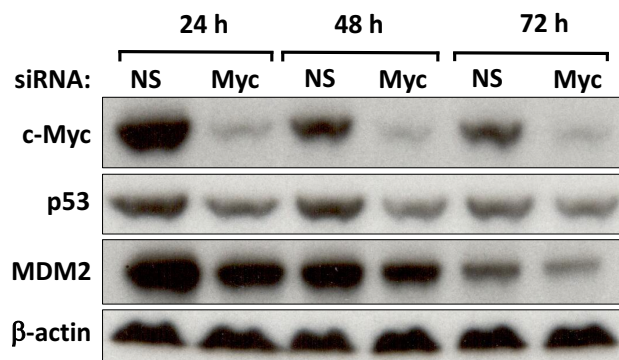


**Figure 3.14: Effect of c-Myc depletion on p53 and MDM2 protein levels in HepG2 cells.** HepG2 cells were treated with siNS (NS) or siMyc 2 (Myc) for the times indicated. Whole cell lysates were analyzed by Western blot analysis for the indicated proteins with the corresponding antibodies.  $\beta$ -actin serves as loading control.

### 3.3. Effect of c-Myc depletion on p53 levels

---

in CRC cells, we measured by quantitative real-time PCR the levels of the p53 transcript in these conditions as compared to cells treated with siNS control. Surprisingly, and at odds with earlier studies showing that both c-Myc and N-Myc depletion reduce p53 mRNA levels (Chen et al., 2010b; Roy et al., 1994), we did not observe a decrease in the p53 transcript levels, but instead we found that p53 messenger RNA levels were significantly increased upon c-Myc siRNA treatment in HCT116 cells as well as a similar trend in RKO cells (Figure 3.15). Moreover, increased p53 mRNA levels were observed when depleting c-Myc levels using either siMyc 1 and siMyc 2, supporting our contention that these effects were specific for c-Myc depletion. Thus, neither inhibition of transcription nor mRNA half-life appear to be responsible for the drop in p53 protein levels in c-Myc-silenced cells.

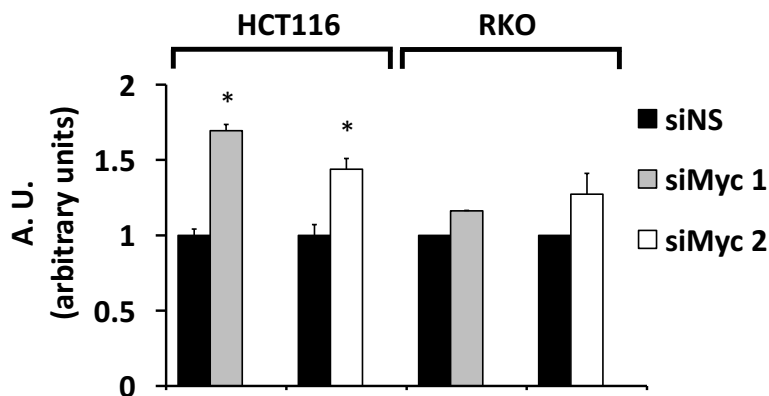


**Figure 3.15: Effect of c-Myc depletion on p53 mRNA levels.** HCT116 and RKO cells were treated for 48 hours with siNS, siMyc 1 or siMyc 2. Relative p53 mRNA levels were determined by quantitative real-time PCR as described in Materials and Methods.

As we previously showed that general protein synthesis was diminished in c-Myc-depleted conditions (Figure 3.7), this raised the possibility that even though p53 mRNA levels are rising its nascent protein levels are declining, as those of RPL5 (Figure 3.10). To test this possibility, we employed methionine analogue AHA-pulse-labeled extracts of newly synthesized proteins from NS- or c-Myc-siRNA-treated RKO cells and pulled down *de novo* synthesized proteins with streptavidin beads, examining the newly synthesized biotinylated p53 protein by Western blot analysis, as described above (see Figure 3.10). We observed that although in whole cell extracts from c-Myc siRNA depleted cells p53 protein levels were decreasing, the amount of newly synthesized p53 pulled down by the streptavidin beads was not significantly changed in c-Myc-versus NS-siRNA-treated cells (Figure 3.10). This result indicates that the decreased p53 levels in c-Myc depleted conditions are not due to a diminished *de novo* synthesis, but to a post-translational event.

Given that in c-Myc-depleted cells we found that neither reduced p53 mRNA levels nor decreased p53 synthesis accounted for reduced p53 levels, we set out to examine whether the decreased p53 levels could be explained by a decrease in the stability of p53 protein. Additionally, and in parallel to p53, we also see a decrease in MDM2 protein levels (Figure 3.13). As pointed out earlier, MDM2 is the major p53 target gene, however, MDM2 is also the major E3 ligase not only for p53, but as well as for itself, and its ability to mediate p53 degradation, and potentially that of MDM2, is inhibited by the IRBC complex (Donati et al., 2013). Given the potential reduction in nascent RPs and 5S rRNA following c-Myc depletion, this could lead

### 3.3. Effect of c-Myc depletion on p53 levels

to the loss in stability of both p53 and MDM2, which would be mediated by a reduction in the IRBC complex and thus in the inhibition of MDM2. To examine this possibility, we evaluated the half-life of p53 and MDM2 in a time-course experiment on Western blots in c-Myc-silenced RKO cells or siNS control cells after treatment with cycloheximide at a dose which blocks protein

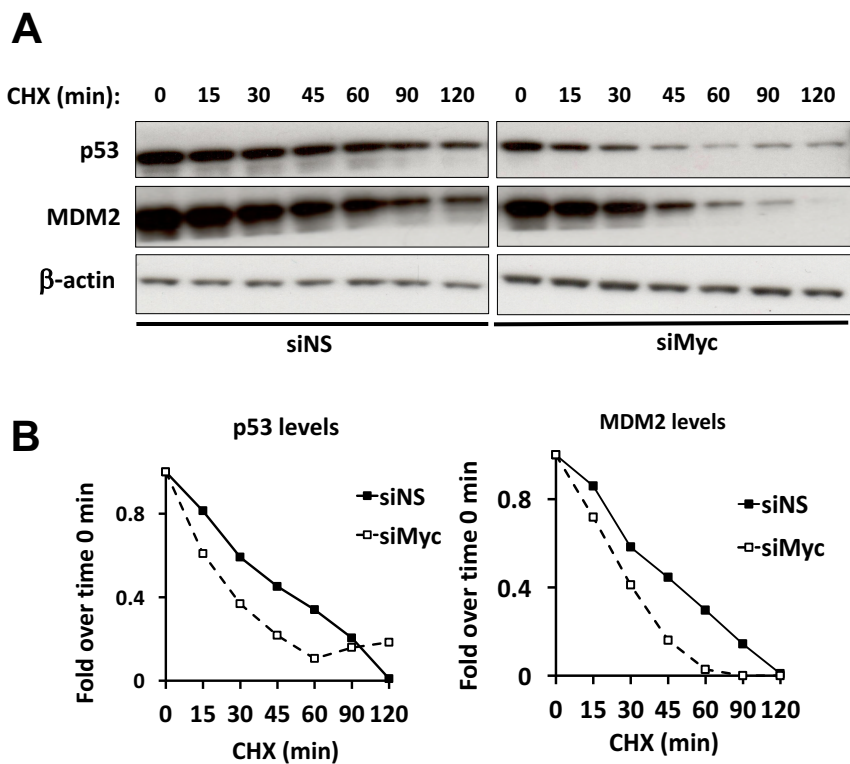


**Figure 3.16: Decreased half-life of p53 and MDM2 proteins under c-Myc depleted conditions.** Time course analysis of p53 and MDM2 protein expression in control (siNS) and siMyc 2-silenced (siMyc) RKO cells, 48 hours after the end of the silencing procedure, exposed to cycloheximide (CHX) at a concentration of 20  $\mu$ g/ml for the times indicated. Western blot analyses were performed (A) and relative amounts of p53 and MDM2 were quantified by densitometry and normalized to  $\beta$ -actin (B), as described in Materials and Methods.

### 3. RESULTS

synthesis. We found that the half-life of p53 and MDM2 in c-Myc depleted cells was reduced to almost half of that of control cells (Figure 3.16). Additionally, when analyzing MDM2 mRNA levels in siMyc 2-treated RKO cells by quantitative real-time PCR, we found little change in cognate transcript as compared to siNS-treated cells. (Figure 3.17). Thus, the decreases we observe in MDM2 protein levels in siMyc 2- treated RKO cells are probably not due to a reduction in its total mRNA levels, though we cannot rule out changes in mRNA half-life or a decrease in newly transcribed MDM2 mRNA. However, taken together, these results support a model in which reduced p53 and MDM2 protein stability are potentially mediated by the activation of MDM2.

If there is no change in the synthesis of p53 following c-Myc depletion but the half-life of p53 decreases this argues for an enhancement in its degradation rate. Hence, we performed an experiment in which we blocked proteasome activity with the small

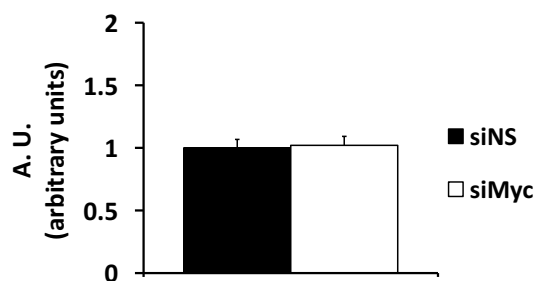
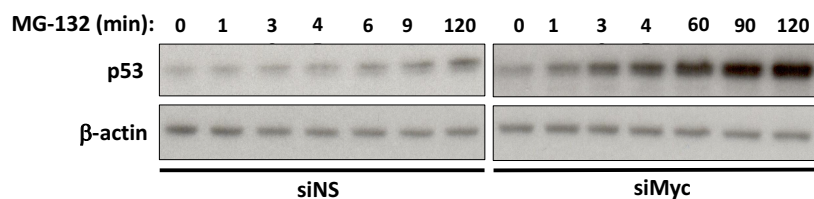


**Figure 3.17: Effect of c-Myc depletion on MDM2 mRNA levels.** RKO cells were treated for 48 hours with siNS or siMyc 2 (siMyc). Relative MDM2 mRNA levels were determined by quantitative real-time qPCR as described in Materials and Methods.

### 3.3. Effect of c-Myc depletion on p53 levels

inhibitor molecule MG-132. We measured the levels of p53 in c-Myc-depleted cells for the times indicated and observed that they increased almost twice as fast as compared to the siNS-treated cells, as evaluated by Western blot analysis (Figure 3.18), consistent with the extent to which p53 half-life was observed to be reduced under c-Myc-depleted conditions (Figure 3.16). This increased accumulation in c-Myc depleted cells versus control cells treated

**A**



**B**

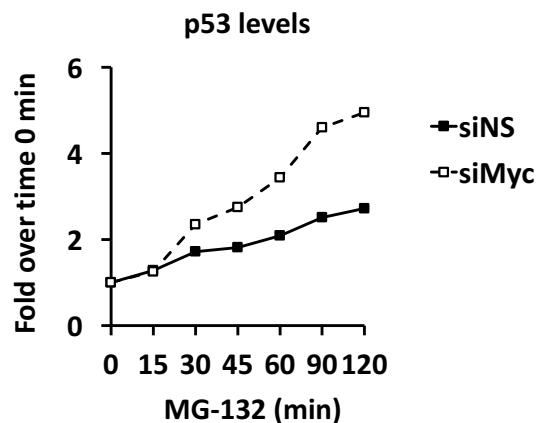


**Figure 3.18: Increased degradation of the p53 protein under c-Myc-depleted conditions.** Time course analysis of p53 protein expression in control (siNS) and siMyc 2-silenced (siMyc) RKO cells, 48h after the end of the silencing procedure, exposed to the proteasomal inhibitor MG-132 at a concentration of  $10\mu\text{M}$ , for the times indicated. Western blot analyses were performed (A) and relative amounts of p53 were quantified by densitometry and normalized to  $\beta$ -actin (B), as described in Materials and Methods.

with MG-132 supports an increased proteasome-mediated degradation of p53 under conditions where c-Myc protein levels are diminished.

Taken together, these data demonstrate that c-Myc depletion in CRC cells causes a drop in p53 protein levels through a reduction in the stability of the p53 protein, mediated by an increase in degradation by the proteasome.

#### **3.4 Role of the RPL5/RPL11/5S rRNA complex in mediating p53 levels in response to c-Myc depletion**

##### **3.4.1 c-Myc depletion decreases the availability of the IRBC complex**

The binding of RPL5 and RPL11 to MDM2 has been shown to play a critical role in APC-driven tumorigenesis in mice, as described in section 1.3.2. However, although it is known that APC loss leads to increased c-Myc protein levels, there is no study relating c-Myc and RPL5 and RPL11 extra-ribosomal functions in colon. Moreover, despite the fact that different studies using Mdm2<sup>C305F</sup> mutant mice have implicated RPL5- and RPL11-binding to MDM2 in c-Myc-driven malignancies, none have analyzed whether RPL5 and RPL11 are acting together with the 5S rRNA in the nascent IRBC complex, as has been described under conditions of impaired ribosome biogenesis (Donati et al., 2013).

### 3.4. Role of the RPL5/RPL11/5S rRNA complex in mediating p53 levels in response to c-Myc depletion

We have shown that c-Myc depletion in CRC cell lines causes a decrease in p53 levels due to increased proteasomal degradation (Figures 3.13, 3.16 and 3.18). As we also demonstrated that “non-ribosomal” RPs and all nascent rRNAs species were decreased under conditions where c-Myc is depleted, we hypothesized that the diminished p53 stability could be mediated by a reduction in the IRBC complex, and thus reduced inhibition of MDM2. To test this possibility, we immunoprecipitated RPL5 from RKO cells treated either with c-Myc siRNA alone or c-Myc siRNA followed with Actinomycin D, an inhibitor of Pol I which acutely induces the IRBC, and scored for the association of MDM2, RPL11 and 5S rRNA in the immunoprecipitates. Prior to immunoprecipitation, cell lysates were subjected to high-speed ultracentrifugation to clear mature

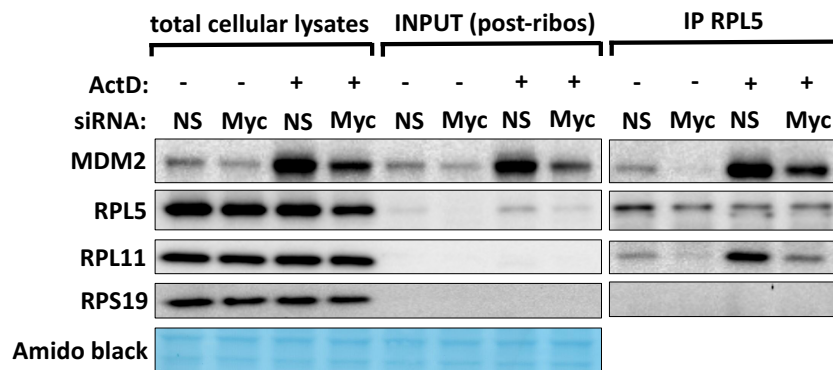


**Figure 3.19: Effects of depleting c-Myc on the IRBC complex under impaired ribosomal stress conditions.** RKO cells were transfected for 48h with siNS (NS) or siMyc 2 (Myc) and treated with or without Actinomycin D (ActD) after the end of the silencing procedure, at a concentration of 5nM, for 6 hours. Western blot analyses show the expression levels of MDM2, RPL5 and RPL11 in the post-ribosomal lysates (INPUT) and immunoprecipitated from post-ribosomal lysates with anti-RPL5 rabbit antibody (IP RPL5). Expression of RPS19, an RP which does not constitute the IRBC complex, was only detectable in total cellular lysates. Amido black served as loading control.

ribosomes. This step does not alter the levels of MDM2 compared to those of the total lysates, employing amido black as a control, whereas the majority of RPs are cleared from the lysate (Figure 3.19), as described earlier (Figure 3.11). The RPL5 immunoprecipitates from the postribosomal lysates were then used for protein analysis. In those samples treated with siMyc 2 alone, we observed an evident decrease in MDM2 and RPL11 binding to RPL5 as compared to the control siNS-treated cells (Figure 3.19). Under Actinomycin D-treated conditions, we were able to detect enhanced binding of both MDM2 and RPL11 to RPL5 in siNS-treated control cells, as compared to the same cells not treated with the Pol I inhibitor (Figure 3.19). Moreover, the enhanced binding of MDM2 and RPL11 to RPL5 in the presence of Actinomycin D was significantly reduced in c-Myc depleted cells (Figure 3.19). To

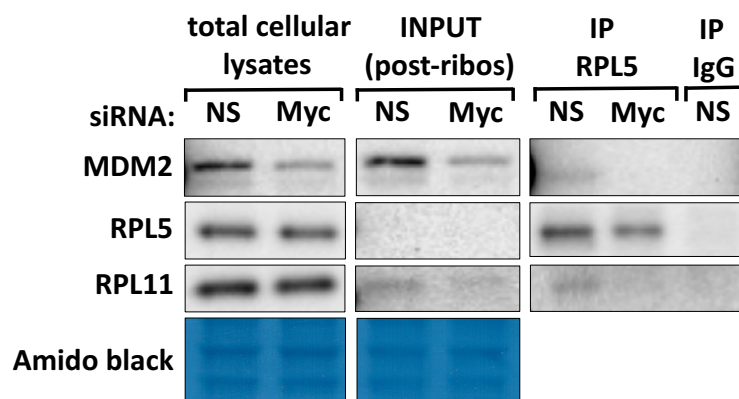


**Figure 3.20: Effects of depleting c-Myc on the IRBC complex under non-stressed conditions.** RKO cells were transfected with siNS (NS) or siMyc 2 (Myc) for 48h. Western blot analyses show the expression levels of MDM2, RPL5 and RPL11 in the post-ribosomal lysates (INPUT) and immunoprecipitated from cell lysates with anti-RPL5 rabbit antibody (IP RPL5) or rabbit immunoglobulin G control (IP IgG). Amido black served as loading control.

### 3.4. Role of the RPL5/RPL11/5S rRNA complex in mediating p53 levels in response to c-Myc depletion

---

ensure that the differences observed were significant in the c-Myc-depleted cells versus the siNS-treated cells, we repeated the experiment without the Actinomycin D-treated samples, and employed a control immunoglobulin G (IgG) (Figure 3.20). The results show that MDM2 and RPL11 co-immunoprecipitated with RPL5 in the immunoprecipitates from siNS control postribosomal lysates, whereas they were largely undetectable in the RPL5 immunoprecipitates from c-Myc depleted postribosomal lysates. In contrast to the RPL5 immunoprecipitates, RPL5 as well as RPL11

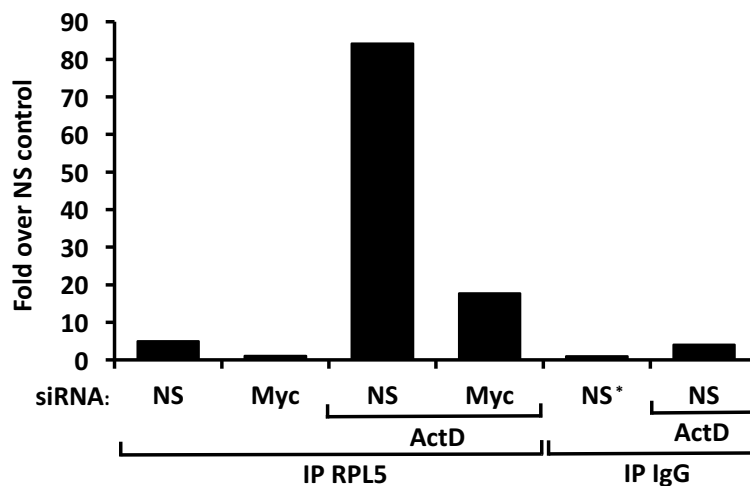


**Figure 3.21: Effects of depleting c-Myc on the levels of the 5S rRNA-component of the IRBC complex.** RKO cells were transfected with siNS (NS) or siMyc 2 (Myc) for 48h, and treated with or without Actinomycin D (ActD) after the end of the silencing procedure, at a concentration of 5nM, for 6 hours. Samples were collected and subjected to ultra-centrifugation, and lysates were then immunoprecipitated with anti-RPL5 rabbit antibody (IP RPL5) or rabbit immunoglobulin G control (IP IgG). Levels of immunoprecipitated 5S were determined by quantitative real-time PCR as described in Materials and Methods. Values represent fold change over the control siNS-treated sample (\*) immunoprecipitated with the IgG antibody.

and MDM2 were undetectable in the IgG control immunoprecipitates from siNS control postribosomal lysates (Figure 3.20). When analyzing by real-time PCR the presence of 5S rRNA in the RPL5 immunoprecipitates treated with and without Actinomycin D, we were able to detect the non-coding rRNA in the postribosomal lysates of siNS control-treated cells, with its levels severely reduced in c-Myc depleted cells (Figure 3.21). The amount of 5S rRNA immunoprecipitated with RPL5 antibody could be enhanced by Actinomycin D treatment, but again the amount of 5S rRNA was reduced in the postribosomal lysates of c-Myc depleted cells as compared to the siNS control treated cells (Figure 3. 21). In contrast, the amount of 5S rRNA immunoprecipitated by the IgG antibody from the postribosomal lysates of siNS-treated cells, subsequently treated without or with Actinomycin D, was hardly detectable (Figure 3.21). The results show that in c-Myc depleted cells the formation of the RPL5/RPL11/5S rRNA complex is strongly decreased, but the induction of the IRBC complex can still be enhanced by Actinomycin D treatment, though at reduced levels to those of control cells. Taken together, the findings argue that upon c-Myc depletion the synthesis of the IRBC is reduced, freeing MDM2 and allowing the degradation of p53.

### 3.4. Role of the RPL5/RPL11/5S rRNA complex in mediating p53 levels in response to c-Myc depletion

---

# **DISCUSSION**



## 4 Discussion

c-Myc is known to be activated in almost all CRC tumors. For this type of cancer, chemotherapy remains the mainstay of palliative treatments, but their efficacy is limited and the outcomes are mixed, with no clear validated or available response predictors, despite multiple efforts to identify such markers (Jensen et al., 2012). Thus, defining more precisely the mechanism by which cells respond to high levels of c-Myc could be crucial to either find new treatments or refine the currently available ones for CRC. Importantly, different studies previously linked either APC-driven tumors or increased c-Myc activity with elevated sensitivity to impaired ribosome biogenesis (Bruno et al., 2017; Bywater et al., 2012). One of these studies revealed that oxaliplatin, a drug used in first-line therapy along with the antimetabolite 5-fluorouracil (5-FU) to treat CRC and other gastrointestinal cancers, kills cells not by causing DNA damage, but by inhibiting ribosome biogenesis (Bruno et al., 2017). The authors demonstrate that depletion of RPL11 relieves this effect, suggesting that this response is dependent on the impaired ribosome biogenesis checkpoint (IRBC) (Bruno et al., 2017). These findings not only highlight the importance of understanding the mechanism of action of each available drug used in front-line cancer therapy, making evident the necessity of first delineating the mechanism by which cancer cells respond to oncogenic stress, but they also provide evidences arguing for the importance of attacking the hyperactivation of ribosome biogenesis in c-Myc-driven tumors as an “Achilles” heel” to selectively kill malignant cells.

#### 4. DISCUSSION

---

In line with these observations, the aim of this thesis is to understand the molecular mechanism by which p53 is regulated in c-Myc-driven CRC. Based on previous data showing that when E $\mu$ -Myc mice harbor a mutated MDM2 protein which is not able to bind RPL5 and RPL11, lymphomagenesis is greatly accelerated (Macias et al., 2010), we set out to investigate whether c-Myc regulates p53 by directly regulating the RPL5/RPL11/5S rRNA complex (also termed the IRBC complex) in colon. We demonstrated that c-Myc depletion causes a reduction in p53 levels in CRC cells due to enhanced degradation by the proteasome and, in parallel, produces a reduction in the levels of the IRBC complex, consistent with c-Myc depletion leading to reduced p53 levels as a consequence of reduced availability of the nascent IRBC complex. Our work examines for the first time the correlation between c-Myc levels, p53 levels and the levels of all the different components of the IRBC complex, including the 5S rRNA, in CRC cells, thus helping to better characterize the mechanisms underlying c-Myc-driven tumorigenesis in CRC.

**c-Myc depletion produces a decrease in proliferation, causes accumulation of cells in G<sub>0</sub>/G<sub>1</sub> phase, modifies cellular size and shape and reduces the global rate of protein synthesis in CRC cells**

The proliferation of all somatic cells relies on mitotic division, which is determined by progression through the cell cycle. We showed that c-Myc depletion in CRC cells causes a reduction in proliferation,

accompanied by an accumulation of cells in  $G_0/G_1$  phase of the cell cycle. Critically, the accumulation of cells in the  $G_0/G_1$  phase occurred in parallel with diminished levels of the p53 protein, whose function promotes cell cycle arrest. The decrease in p53 levels does not appear to be sufficient to rescue the proliferative insufficiencies originated by c-Myc depletion, as has been suggested in studies of melanoma cells (Wang et al., 2008). One of the possible actors that could be playing a role in the accumulation of cells in  $G_0/G_1$  is the cyclin-dependent kinase inhibitor p21, known to be transcriptionally repressed by c-Myc and to act as modulator of  $G_1/S$  transition (Abbas and Dutta, 2009; Besson et al., 2008). However, in melanoma cells p21 depletion was unable to release the c-Myc depletion-induced cell cycle arrest (Wang et al., 2008). It seems more likely that p53 levels drop because of a reduction in oncogenic stress and that cells are not progressing through the  $G_1 \rightarrow S$  barrier because of the requirement of c-Myc for passing through early  $G_1$  phase of the cell cycle.

It is widely known that c-Myc upregulation is linked to an increase in the rates of protein biosynthesis, paralleled by an increase in the total amount of cellular protein (Iritani and Eisenman, 1999; Schuhmacher et al., 1999). Conversely, c-Myc null fibroblasts display a reduced rate of protein synthesis and have been also described to show morphological changes : they appear thin and spread out, losing their fibroblastic shape and displaying a circular outline with occasional long processes (Mateyak et al., 1997). Likewise, we observe that the global rates of protein synthesis were reduced upon c-Myc depletion in the RKO CRC cells. These cells also exhibit a distinct phenotype, appearing “thinner” and elongated

#### 4. DISCUSSION

---

as compared to control cells. In contrast, c-Myc-depleted HCT116 cells displayed a clear decrease in cell size, in agreement with findings in intestinal cells lacking c-Myc, which are observed to be smaller than wild-type cells (Muncan et al., 2006). Together, these data are consistent with the requirement of c-Myc as an essential player in regulating cell growth and proliferation in colon cancer cells, as it has been shown for other cell types (Wang et al., 2008).

#### **Reduced levels of c-Myc in CRC cells leads to decreased synthesis of RPs and rRNA**

A number of reports have implicated c-Myc in directly regulating the expression of RP genes. Some models have described changes in RP mRNA levels following c-Myc upregulation (Coller et al., 2000; Kim et al., 2000), whereas an earlier study suggested that c-Myc inactivation can result in different outcomes with respect to RP expression, depending on the type of cancer (Wu et al., 2008). We find that in CRC cells, RP mRNA levels tend to decrease upon c-Myc depletion, with the decrease being more significant for RPL5 mRNA. In accordance with the small changes observed in some of the RP mRNAs following c-Myc depletion, previous studies based on mRNA expression levels have shown that a large fraction of c-Myc target genes respond weakly, or even fail to respond, depending on the cell type (Fernandez et al., 2003). Our results suggest that RP mRNAs tend to follow c-Myc levels in colorectal tumors, though not as profoundly as has been shown for

osteosarcoma and lymphoma in conditional transgenic models in which c-Myc was inactivated (Wu et al., 2008).

Despite the tendency in the reduction of RP mRNA levels, we found in CRC cells that total RP levels did not significantly change under conditions where c-Myc was depleted. However, we showed that the *de novo* synthesis of RPL5 was markedly diminished upon c-Myc depletion. Moreover, even though *de novo* synthesis of cellular proteins in general was diminished as a function of total cellular protein analyzed, the effect on RPL5 appears to be specific and not a general consequence of reduced c-Myc levels, as the *de novo* synthesis of GAPDH and p53 were not affected by c-Myc depletion. In addition, we demonstrated that protein levels of RPL5 and RPL7a not incorporated into the ribosome dramatically decreased under conditions of reduced levels of c-Myc, consistent with reduction of newly synthesized RPs. It was recently demonstrated that translation efficiency for RP genes increases upon c-Myc induction in osteosarcoma cells (Elkon et al., 2015). Accordingly, we speculate that, in CRC cells, RPs respond to c-Myc depletion at both the mRNA and the protein translation level by coordinately decreasing mRNA production, and to a much larger extent their translation efficiency. Indeed, consistent with our finding above, in the study by Elkon et al. they show that the major effects on RP expression are not regulated at the transcriptional level, but at the translational level (Elkon et al., 2015). Additional experiments checking the effect of c-Myc depletion on the *de novo* synthesis of other RPs would be needed to ascertain whether the decrease in translation is a general event occurring for all RPs in CRC cells. It would be also of interest to determine the effects of c-Myc depletion on the ribosome content

#### 4. DISCUSSION

---

and translational machinery by polysome profiling, a technique which provides a “photograph” of the cellular translational machinery at a determined moment. Given the apparent reduction in *de novo* synthesized cellular proteins, we would expect to observe a decrease in polysomes and an increase in the number of free 40S and 60S subunits. This technique would also allow us to analyze the distribution of RP mRNAs along different fractions of the polysome profile: thus, we could determine whether these mRNAs are shifting towards association with smaller polysomes or non-polysomes, which would again indicate reduced translation efficiency, as suggested by *de novo* synthesis experiments.

In the studies by Elkon et al. described above, they also report that translational induction of RP genes upon c-Myc activation was significantly abolished by treating cells with an inhibitor of mTOR, while having no marked effect on other branches of the c-Myc response-network (Elkon et al., 2015). It was recently shown, using mTOR inhibitors, that mTOR complex 1 (mTORC1), through the phosphorylation and inhibition of 4E-BP1, selectively upregulates the translation of a set of mRNAs characterized by an oligopyrimidine tract at their transcriptional start site, which invariably begins with a cytosine base. This family of mRNAs, termed 5'TOP mRNAs, is largely made of RP mRNAs (reviewed in Gentilella and Thomas, 2012). Therefore, we would speculate that c-Myc depletion would affect RP mRNAs through downregulation of the mTORC1 network. In support of this hypothesis, a subsequent study uncovered a functional link between c-Myc and mTOR, in

which c-Myc activation led to mTOR-dependent phosphorylation and inhibition of 4E-BP1 in sites of early hyperplasia of B-cell lymphomas (Pourdehnad et al., 2013). However, it is known that the role of mTOR-mediated regulation of the 5'TOPs is also exerted through LARP1, an mRNA binding protein that was found to be target of mTORC1. LARP1 was first demonstrated to bind to the Poly(A) tails of mRNAs, and selectively control the levels of 5'TOP mRNAs (Aoki et al., 2013). This role is apparently controversial, with one group arguing it is an activator (Tcherkezian et al., 2014) and the other a repressor (Fonseca et al., 2015) of 5'TOP translation under conditions of mTORC1 inhibition. In a recent publication from our group, we show that LARP1 does not affect the translation of 5'TOP mRNAs (Gentilella et al., in press). Instead, we find that 40S ribosomes, in a complex with LARP1, selectively stabilize 5'TOP mRNAs, a response which is enhanced by mTOR inhibition and dependent on the 5'TOP sequence (Gentilella et al., in press). In normal growing conditions, RP mRNAs are distributed equally among the non-polysome and polysome fractions; however, treatment of cells with the mTOR inhibitor rapamycin leads to their sequestration in the 40S-LARP1 complex and redistribution to the non-polysomal fraction (Gentilella et al., in press). Thus, the 40S-LARP1 complex could come into play under conditions of nutrient or growth factor deprivation, allowing the preservation of 5'TOPs until proliferative conditions are improved (Gentilella et al., in press). Given these data, it could be possible that regulation of mTORC1 by c-Myc could not only affect mTORC1-dependent 4E-BP1 phosphorylation (Pourdehnad et al., 2013), but also LARP1. We would hypothesize that, if under conditions of c-Myc depletion there

#### 4. DISCUSSION

---

is a strong decrease in RP translation as compared to their cognate RP mRNA levels, as we describe here, this could be due to the sequestration of RP mRNAs by the 40S-LARP1 complex in small polysomes or non-polysomes. This would explain the relatively small changes in 5'TOP mRNA levels versus the apparent decrease of *de novo* synthesized RPs. This question would be addressed by fractionating polysome profiles, subjecting the free 40S fraction to LARP1-immunoprecipitation and analyzing the bound mRNAs by RNA-Seq, as our laboratory recently described (Gentilella et al., in press).

Ribosomes are constituted not only by RPs but also by rRNA. c-Myc has been described to regulate rRNA genes by both Pol I and Pol III. We demonstrated that in HCT116 cells c-Myc depletion leads to a general decrease in all Pol I and Pol III-dependent transcripts. Consistent with this finding, previous studies in HeLa cells showed a dose-dependent decrease in pre-rRNA upon c-Myc depletion, as well as a reduction in 5S rRNA (Grandori et al., 2005). Conversely, c-Myc overexpression in different cell lines was correlated with augmented synthesis of rRNAs and their precursors, as well as with increased levels of Pol III-dependent transcripts (Gomez-Roman et al., 2003; Grandori et al., 2005). It has been shown both in *Xenopus* embryos (Amaldi et al., 1989; Pierandrei-Amaldi et al., 1985) and in HeLa cells (Warner, 1977) that if rRNA is limiting in ribosome biogenesis, RPs in excess are rapidly degraded. Thus, the reduction in RP levels may not only be attributed to a decrease in *de novo* synthesis of RPs, but as well to their increased degradation. To

determine if degradation is involved, one should carry out a pulse-chase experiment with either the methionine analogue AHA or radioactive  $^{35}\text{S}$ -methionine to label and follow the dynamics of *de novo* synthesized RPs.

### **c-Myc depletion decreases p53 protein levels in CRC cells**

We observe that in CRC cells, where c-Myc activation is prevalent, c-Myc depletion causes a reduction of p53 protein levels. These results are in contrast to other studies reporting increased p53 protein levels upon c-Myc depletion (Brighenti et al., 2014; Wang et al., 2008). We initially reasoned that the effect of c-Myc depletion on p53 levels could be tissue-dependent; however, when we performed c-Myc depletion in the hepatocellular carcinoma cell line HepG2 there was also a significant drop in p53 protein levels, in accordance with the data obtained in CRC cells and contrary to the findings of Brighenti et al. (Brighenti et al., 2014). These controversial results about the effects of decreased c-Myc levels on p53 in HepG2 cells might depend on the siRNAs used, as we did not employ the same siRNA described to be used by Brighenti et al.. Nonetheless, our data set, obtained with two different siRNAs, indicates that in poorly differentiated CRC lines c-Myc depletion results in a decrease in p53 levels. However, we do not discard results arguing that p53 levels are differently regulated in c-Myc depleted conditions in other tumor cell types (Wang et al., 2008).

#### 4. DISCUSSION

---

The same laboratory which observed reduced p53 levels under c-Myc depleted conditions also argued in an early publication that increased rRNA synthesis, which we can find under conditions of c-Myc overactivation, would lead to the consumption of the newly synthesized RPs into nascent 60S ribosomes in cells stimulated to proliferate, leading to p53 downregulation (Donati et al., 2011). However, in the case of c-Myc depletion, our studies demonstrate that reduction of c-Myc levels contemporaneously downregulates Pol I- and Pol II-dependent transcripts as well as the production of RPs. Moreover, it is known that when c-Myc upregulates ribosome biogenesis, in addition to increasing rRNA transcription, it also stimulates the production of RPs, as already reported (van Riggelen et al., 2010). Hence, we propose that upon c-Myc overactivation, all ribosomal components are induced to the same extent and therefore there is no unbalance between rRNA synthesis and RP production. Therefore, in c-Myc-overexpressing cells, the IRBC complex would not be consumed in making 60S ribosomes, but instead it would be used to both form ribosomes and bind and inhibit MDM2, allowing p53 levels to rise, as seen in  $E\mu$ -Myc mice (Macias et al., 2010).

As described above, we have demonstrated that “non-ribosomal” RPs and p53 protein levels drop upon c-Myc depletion in CRC cells. Additionally, we found that the decrease in p53 protein levels results from an enhanced degradation by the proteasome. These findings would appear consistent with results obtained in the  $E\mu$ -Myc mouse model, where the authors showed that both p53 and total RP levels were increased in c-Myc-overexpressing cells (Macias et al., 2010),

leading them to predict that oncogenic c-Myc regulates p53 stability by increasing the levels of RPs, which bind to MDM2, inhibiting p53 degradation (Macias et al., 2010). However, recent studies from our laboratory demonstrated that the nascent 5S rRNA, together with RPL5 and RPL11, constitutes the inhibitory complex that binds and inhibits MDM2 (Donati et al., 2013). Moreover, rRNA synthesis is argued to be the rate-limiting step in ribosome biogenesis (Amaldi et al., 1989; Pierandrei-Amaldi et al., 1985; Warner, 1977). Thus, we speculate that the 5S rRNA may be the rate-limiting step in generating a stable RPL5/RPL11/5S rRNA complex. Taking this into account, and based on our data showing that c-Myc depletion in CRC cells leads to reduced levels of RPs, rRNA and p53, we established that reductions in the production of all ribosomal components also lead to a decrease in the formation of ribosomes and of the RPL5/RPL11/5S rRNA complex. This would mean that less complex is available to bind and inhibit MDM2, and consequently, MDM2 is liberated to degrade p53.

In our studies, in addition to establishing a decrease in p53 protein levels upon c-Myc depletion, we also noticed diminished MDM2 protein levels. MDM2 is widely accepted to be the major negative regulator of p53, which in turn, positively regulates MDM2 by acting as a transcription factor of the *Mdm2* gene (Barak et al., 1993). We demonstrated that the drop in MDM2 protein levels upon c-Myc depletion was not related to decreased transcription of the *Mdm2* gene, but instead appeared to be due to decreased stability of the MDM2 protein. The ubiquitin-proteasome system is known to be

#### 4. DISCUSSION

---

responsible for regulating MDM2 protein levels. MDM2 is an E3 ligase known to not only ubiquitinate p53 but also itself (Shadfan et al., 2012). Importantly, a recent study showed that auto-ubiquitination of MDM2 results in enhanced substrate ubiquitin ligase activity and in a strong recruitment of E2-conjugating enzymes, the enzymes that offer the ubiquitin molecules to the E3 ligases to be transferred to a target protein, suggesting a model in which polyubiquitin chains on MDM2 increase the local concentration of E2 enzymes and permit processivity of substrate ubiquitination (Ranaweera and Yang, 2013). They further proposed that auto-ubiquitination acts as a mechanism to eliminate excessive E3s when their concentration reach a threshold as substrates diminish, thus allowing a homeostatic control of E3s' levels. Although it remains to be determined whether other E3 ligases could also contribute to both MDM2 and p53 decreased levels upon c-Myc depletion (Lee et al., 2012; Li and Kurokawa, 2015), we propose from our results that in c-Myc-depleted CRC cells, MDM2 inhibition by the IRBC complex is reduced, allowing MDM2 to auto-ubiquitinate itself, resulting first in enhanced substrate ubiquitin ligase activity towards p53, and when p53 levels are significantly decreased, polyubiquitinated MDM2 is degraded by the proteasome.

##### **The formation of the IRBC complex is reduced under c-Myc-depleted conditions**

As stated above, based on our data showing that c-Myc depletion in CRC cells leads to reduced levels of RPs, rRNA and p53, we established that reductions in the production of all ribosomal components also lead to a decrease in the formation of ribosomes and of the RPL5/RPL11/5S rRNA complex. We further confirmed this by treating c-Myc depleted RKO cells with Actinomycin D, which induces the IRBC by blocking Pol I transcription: under c-Myc depleted conditions, we observed that the formation of the RPL5/RPL11/5S rRNA complex is reduced as compared to siNS-treated control cells, but can still be enhanced upon Actinomycin D treatment. These results support that c-Myc depletion in CRC cells leads to decreased p53 levels as a consequence of diminished availability of the nascent pre-ribosomal RPL5/RPL11/5S rRNA complex. Conversely, they further underscore that c-Myc overexpression drives the formation of the RPL5/RPL11/5S rRNA complex, which would be used to make new ribosomes but also to inhibit MDM2, resulting in p53 stabilization. Importantly, if we consider that cells do not generate excess RPs, including RPL5 and RPL11, or that matter the RPL5/RPL11/5S rRNA complex, without generating more ribosomes, this raises the possibility that, in the case c-Myc overexpression, it may be that the cell “senses” c-Myc dysregulation by an as yet undescribed mechanism, and redirects the RPL5/RPL11/5S rRNA complex to the binding an inhibition of MDM2, executing the IRBC. This model would be consistent with the results from Fumagalli et al., who demonstrated that depletion of a

#### 4. DISCUSSION

---

RP from the 40S ribosomal subunit, disrupting 40S ribosome biogenesis, does not affect the rate of 60S ribosome biogenesis but, however, the IRBC complex is redirected to the binding of MDM2 (Fumagalli et al., 2009, 2012). It will be important in the future to determine whether the transition of the RPL5/RPL115S rRNA-precursor complex into a tumor suppressor is a passive, or instead a regulated event.

Taken together, our observations shed light on important questions. First, we demonstrate that, in CRC cells, c-Myc depletion downregulates p53 and in parallel reduces the amount of newly synthesized ribosomal components. These results reinforce the argument that, in a scenario in which we have c-Myc upregulation, we will find sufficient IRBC complex available to induce p53, contrary to what others have suggested (Brighenti et al., 2014; Derenzini et al., 2017). Second, despite the fact that different studies using MDM2<sup>C305F</sup> mutant mice have proven a role for RPL5 and RPL11 binding to MDM2 in c-Myc-driven malignancies (Liu et al., 2017; Macias et al., 2010), none analyzed whether RPL5 and RPL11 are acting together with 5S rRNA in the IRBC complex, as it has been described under conditions of impaired ribosome biogenesis (Donati et al., 2013). Our work examines for the first time the correlation between c-Myc levels, p53 levels and the levels of all the different components of the IRBC complex, including the 5S rRNA. Third, although others previously identified the RP-MDM2-p53 pathway as a critical mediator of colorectal tumorigenesis following APC-loss and suggested a role for c-Myc in this setting (Liu et al., 2017), here

we show a direct correlation between c-Myc levels, the levels of the IRBC complex and those of the p53 protein in CRC cells.

Remarkably, RPL11 was shown to be responsible for down-regulating both c-Myc levels and activity under conditions of ribosomal stress (Challagundla et al., 2011; Dai et al., 2010), and RPL11 and RPL5 were recently described to cooperatively and negatively regulate c-Myc mRNA levels (Liao et al., 2014). These findings were confirmed *in vivo*, when it was observed that fibroblasts and hematopoietic tissues from mice heterozygous for the *Rpl11* gene, which are predisposed to develop lymphomagenesis, presented higher basal c-Myc levels. Moreover, in the same study, it was shown that complete or partial deletion of *Rpl11* in mouse embryo fibroblasts impaired the activation of p53 by ribosomal stress and by DNA damage (Morgado-Palacin et al., 2015). This would indicate that both impaired activation of p53 by ribosomal stress and increased c-Myc levels could contribute to the observed tumor-prone phenotype of heterozygous *Rpl11* mice. Given these data, it would be of great interest to investigate whether RPL5 and RPL11 are acting together with the 5S rRNA in the IRBC complex, controlling both c-Myc levels and activity. However, other experiments should also be performed to determine whether RPL11 and RPL5 are accountable for reducing c-Myc levels in all tumor types, as preliminary studies from our laboratory were able to reproduce c-Myc increased levels upon RPL11 depletion in the U2OS osteosarcoma cell line, but not in HCT116 cells. If the IRBC complex would be found to exert such regulation of c-Myc action, it

#### 4. DISCUSSION

---

would mean a dual role in hampering tumorigenesis: on one side, it would be accountable for activating the p53 pathway, and on the other, it would restrain the action of c-Myc, as suggested by the results from Morgado-Palacin and coworkers. This would imply that inducing ribosomal impairment in c-Myc-overexpressing tumors could be a very potent strategy for those cancers retaining wild-type p53. Additionally, c-Myc-overexpressing cancers bearing p53 mutations could also be hit by treatments inducing ribosomal stress, as in such cancers, the IRBC complex would still be able to decrease c-Myc levels and c-Myc-dependent transcriptional signaling, thus attacking this c-Myc-hyperactivation, to which tumors seem to be addicted.

# **CONCLUSIONS**



## 5 Conclusions

1. c-Myc is necessary for CRC cells to pass through G<sub>1</sub> phase of the cell cycle, with reduced c-Myc levels leading to accumulation in G<sub>0</sub>/G<sub>1</sub> phase, and consequently to reduced proliferation.
2. c-Myc levels affect cellular shape, size and global protein synthesis rates of CRC cells.
3. Ribosomal protein (RP) mRNAs, but not RPs, tend to follow c-Myc levels in CRC cells.
4. The *de novo* synthesis of RPs appears to be reduced in c-Myc depleted cells, as measured by pulse labeling of RPL5 with AHA and by the levels of “non-ribosomal” RPL5 and RL7a in the supernatant of the ultracentrifuged fraction of whole cell lysates.
5. Levels of newly synthesized ribosomal RNA (rRNA) are equally decreased for both Pol I- and Pol III-dependent transcripts under c-Myc-depleted conditions in RKO cells.
6. c-Myc depletion causes a reduction in p53 levels in CRC cells, due to enhanced degradation by the proteasome.
7. The levels of the IRBC complex are decreased upon c-Myc depletion in CRC cells, but can be enhanced by Actinomycin D treatment, consistent with c-Myc depletion leading to reduced p53 levels as a consequence of reduced availability of the nascent IRBC complex.

## 5. CONCLUSIONS

---

**MATERIALS**  
**AND**  
**METHODS**



## **6 Materials and Methods**

### **6.1 Cell culture and drug treatment**

HCT116, RKO and LoVo human colorectal carcinoma cell lines were obtained from the American Type Culture Collection and maintained in DMEM (ThermoFisher Scientific) supplemented with 10% heat-inactivated fetal bovine serum (Sigma-Aldrich). For all studies, cells were incubated at 37°C, 5% CO<sub>2</sub> and 90-95% of relative humidity.

Actinomycin D (BioVision Technologies) was used at a final concentration of 5ng/ml for 6 hours. MG-132 (Sigma-Aldrich) and cycloheximide (Sigma-Aldrich) were used at a final concentration of 10 µM and 20 µg/ml respectively, for the times indicated.

### **6.2 Transfection procedures**

siRNA transfections were performed following manufacturer's instructions in Opti-MEM medium (Life Technologies) using Lipofectamine RNA-iMAX (Life Technologies). Unless otherwise indicated, transfections were performed during 48 hours at a final concentration of 50 nM. The following siRNAs were used: non-silencing (NS) control (GCAUCAGUGUCACGUAAUA) was purchased from Sigma Aldrich, siMyc 1 was purchased from QIAGEN (SI02662611) and siMyc 2 was purchased from Santa Cruz Biotechnology (sc-44248).

### 6.3 Total cellular proteins extraction

Cells grown in either 6 or 10-cm dishes were washed twice with ice-cold PBS, scraped and lysed on ice in extraction buffer (50mM Tris-HCl [pH 8], 250mM NaCl, 1% Triton X-100, 0.25% sodium deoxycholate, 0.05% SDS, 1 mM dithiothreitol [DTT], and protease inhibitors cocktail [Sigma-Aldrich]). Lysates were harvested in Eppendorf tubes, incubated for 10 min at 4°C in a rotatory shaker and finally centrifuged at 16,200 x g for 10 min at 4°C to recover the supernatant. Quantification of protein concentrations was performed by Bradford protein assay (Bio-Rad) following the instructions recommended by the manufacturer.

### 6.4 Western blot analysis

Equal amounts of protein lysate obtained from treated cells grown in 6, 10 or 15-cm dishes were resuspended in Laemmli SDS-sample buffer and, after treatment at 95°C for 5 min, proteins were separated on 10% or 12% sodium dodecylsulphate (SDS)-polyacrylamide gels or 4-12% NuPAGE Bis-Tris Midi Gels (ThermoFisher) by electrophoresis, and transferred to PVDF membranes (Millipore) previously activated with methanol (PanReac AppliChem) with a semi-dry transfer apparatus (LTF-Labortechnik). Blots or gels after transfer were stained with either amido black or Ponceau S solution (Sigma-Aldrich) respectively to confirm equal loading and transfer of proteins. Membranes were then de-stained and blocked for 1 hour at room temperature with Tris-buffered saline

(TBS) containing 0.1% Tween (referred to as TBS-T) and 5% non-fat dry milk (Bio-Rad). Incubations with primary antibodies were performed in TBS-T and 5% BSA (Sigma-Aldrich) overnight, and primary antibodies used were as follows: anti-c-Myc (Y69; Abcam) (used in Figures 3.9, 3.13) , anti-c-Myc (9E10; Santa Cruz Biotechnology) (used in Figures 3.1, 3.2, 3.14), anti-MDM2 (SMP14; Santa Cruz Biotechnology), anti-p53 (DO-1; Santa Cruz Biotechnology), anti-RPL11 (3A4A7; Invitrogen), anti-RPL5 (A303-933A; Bethyl Laboratories), anti RPL7a (PMID:2403926), anti- $\beta$ -actin (A2228; Sigma-Aldrich), anti-GAPDH (2118; Cell Signaling). The following day, membranes were washed three times (10 min each) with TBS-T and incubated for 1 hour at RT with TBS-T containing 5% non-fat dry milk (Bio-Rad) and a secondary horseradish-coupled antibody. Upon incubation with secondary antibody, membranes were washed three times (10 min each) with TBS-T and protein detection was performed by using an enhanced chemiluminescence kit (GE Healthcare). Quantification of band intensities by densitometry was carried out using the Image J software.

### 6.5 Quantitative real-time PCR

Total RNA was extracted from treated cells in culture (grown in 6-cm dishes), using TRIzol (Invitrogen) as recommended by manufacturer. RNA was resuspended in DEPC-treated water and quantified using NanoDrop 1000 spectrophotometer (Thermo Scientific). Aliquots of RNA (2-5 ug) were treated to remove DNA

## 6. MATERIALS AND METHODS

---

using DNase I (Sigma-Aldrich) following manufacturer's instructions. 1 ug of total DNase I-treated RNA was reverse-transcribed using the M-MLV enzyme (Invitrogen) following the protocol recommended by manufacturer. The resulting cDNA samples were diluted 1:10 and used in PCR reactions containing LightCycler 480 SYBR Green I Master (Roche Molecular Systems). Reactions were performed as follows: 95° for 5 min followed by 45 cycles of 95°C for 15 secs, 60°C for 15 secs and 72°C for 15 secs. The reactions were analyzed in a LightCycler 480 II apparatus (Roche Molecular Systems). Gene expression was normalized to the endogenous control  $\beta$ -actin. The sequences of the PCR primers used are reported in the table below. Relative mRNA expression was calculated using the LightCycler 480 software.

<b>Gene</b>	<b>Primer sequences</b>
5S rRNA	Forward: 5'-GGCCATACCACCCTGAACGC-3' Reverse: 5'- CAGCACCCGGTATTCCCAGG-3'
$\beta$ -actin	Forward: 5'- AATGTGGCCGAGGACTTTGATTGC-3' Reverse: 5'-AGGATGGCAAGGGACTTCCTGTAA-3'
c-Myc	Forward: 5'-ATTCTGCCCATTTGGGGCAC-3' Reverse: 5'- GTTCTCCTCCTCGTCGCAGT-3'
Firefly luciferase	Forward: 5'- ACAGATGCACATATCGAGGTG-3' Reverse: 5'- GATTTGTATTTCAGCCCATATTCG-3'
MDM2	Forward: 5'-TGTTGGTGCACAAAAGACACT-3' Reverse: 5'-CAATATGTTGTTGCTTCTCATCA-3'
p53	Forward: 5'- CTATGAGCCGCCTGAGGTTG-3'

## 6. MATERIALS AND METHODS

---

	Reverse: 5'-CTGGAGTCTTCCAGTGTGATG-3'
RPL5	Forward: 5'-GGTGTGAAGGTTGGCCTGAC-3' Reverse: 5'-GGCACCTGGCTGACCATCAAG-3'
RPL11	Forward: 5'-TCCACTGCACAGTTCGAGGG-3' Reverse: 5'-AAACCTGGCCTACCCAGCAC-3'
RPL7a	Forward: 5'-GCTGAAAGTGCCTCCTGCGA-3' Reverse: 5'-CACCAAGGTGGTGAGGTGT-3'
RPS19	Forward: 5'-ACTGGTTCTACACGCGAGCTG-3' Reverse: 5'-GCATGACGCCGTTTCTCTGAC-3'

### 6.6 Immunoprecipitation

Cells grown in 15-cm dishes were washed twice with ice-cold phosphate-buffered saline (PBS), scraped on ice using ice-cold PBS and transferred into Eppendorf tubes. Each tube was centrifuged for 3 min at 4°C at 1,000 x g. Supernatants were discarded and immunoprecipitation lysis buffer (50 mM Tris HCl [pH 7.5], 150 mM KCl, 5 mM MgCl<sub>2</sub>, 1mM EGTA, 1mM DTT, 10% glycerol, 0.8% NP40, PMSF 1mM, 100 U/ml RNaseout inhibitor [Invitrogen] and cOmplete, EDTA-free Protease Inhibitor cocktail [Roche]) was added to each cell pellet by pipetting up and down. Samples were incubated for 5 min at 4°C in a rotatory shaker, then mechanically sheared by passing through a 1-ml-syringe with a 25G x 0.0625 needle (BD Plastipak) 5 times and finally centrifuged at 16,000 x g

## 6. MATERIALS AND METHODS

---

for 15 min at 4°C to recover the supernatant. Quantification of protein concentrations was performed by Bradford protein assay (Bio-Rad) following the instructions recommended by the manufacturer. Ribosomes were pelleted by ultracentrifugation in polyallomer microtubes (Thermo Scientific) at 200,000 x g for 2 hours at 4°C using a Fiberlite F50-24 x 1,5 rotor (Thermo Scientific) to obtain postribosomal supernatants. Equivalent amounts of protein were incubated at 4°C with rotation overnight in immunoprecipitation buffer with either rabbit polyclonal anti-RPL5 (A303-933A; Bethyl Laboratories) or normal rabbit IgG (sc-2027; Santa Cruz Biotechnology) added to a final concentration of 4µg of antibody per 1 µg of sample. 20 µl of PureProteome™ Protein A/G Mix Magnetic Beads (Merck) were washed twice in immunoprecipitation lysis buffer, resuspended in 100 µl of the same buffer and added to each sample. Extracts were then mixed by rotation for an additional 2 hours at 4°C. The beads were washed following manufacturer's instructions, the supernatant was discarded and the beads were resuspended in either protein loading buffer for Western blot analysis or TRIzol reagent (Invitrogen) to recover immunoprecipitated RNA for 5S rRNA quantitative real-time PCR analysis. To normalize the samples, 1 ng of firefly luciferase mRNA was added to samples resuspended in TRIzol for 5S rRNA analysis, and these samples were processed for quantitative real-time qPCR as described above with the following modifications: a) the extracted RNA was directly resuspended in a mix containing DNase I recombinant (Sigma-Aldrich) and used directly for DNase I-treatment,; b) all the DNase I-treated RNA from each sample was reverse-transcribed using the M-MLV enzyme (Invitrogen) following

manufacturer's instructions, and c) gene expression was normalized to the exogenous control firefly luciferase.

### **6.6 Cell cycle analysis**

Treated and control cells in culture (10-cm dishes), were trypsinized, harvested, placed on ice and counted. For each experimental condition, 500,000 cells were transferred into a Falcon tube and centrifuged at 1,188 x g at 4°C for 5 min. Supernatant was discarded and the remaining cellular pellet was washed once with ice-cold PBS, fixed with 70% ethanol and placed at -20°C for at least 4 hours. Cells were then washed with ice-cold "FACS" buffer (BSA 0.1% and EDTA 5mM in PBS) and centrifuged for 5 min at 428 x g ,4°C. Supernatant was discarded and the cellular pellet was resuspended in propidium iodide (PI) staining solution (PBS, 0.1% NP40, 20 µg/ml RNase A [Invitrogen], 40 µg/ml PI [Invitrogen]). The cellular suspension was transferred to a new 5 ml-Falcon tube with cell strainer cap (Corning) and maintained at RT protected from light for at least 15 min. Samples were analyzed using FACS Canto System.

### **6.7 De novo protein analysis**

Before lysis, cells grown in 6-cm dishes were washed twice with PBS at room temperature and incubated for 15 min in 3 ml of supplemented medium, made of methionine-and cysteine-free DMEM (ThermoFisher Scientific) supplemented with 10% dialyzed

## 6. MATERIALS AND METHODS

---

serum (Sigma-Aldrich), pyruvate 1mM (ThermoFisher Scientific), GlutaMAX (ThermoFisher Scientific), L-cystin (Sigma-Aldrich), HEPES 25 mM (ThermoFisher Scientific) and equilibrated to pH 7.4 with NaOH. After this incubation, 3 ml of the supplemented medium containing in addition 50  $\mu$ M Azyde-Homoalanine (AHA) (Invitrogen), was added for 2 hours. AHA-labeled proteins were chemically processed using the Click-iT Protein Reaction Buffer kit (Invitrogen) according to manufacturer's protocol and 200  $\mu$ g of biotin-alkalyne-conjugated proteins were resuspended in 500  $\mu$ l of PBS, NaCl 150 mM, SDS 0.1% and protease inhibitors (Roche) and incubated 4 hours at 4°C with Pierce streptavidin-agarose bead (ThermoFisher Scientific). Streptavidin-biotin conjugates were washed three times with 500  $\mu$ l of wash solution (Tris-HCl [pH 7.4] 50 mM, NaCl 150 mM, SDS 0.1%), resuspended in Laemmli buffer, resolved on 10% SDS-PAGE gels and probed with the indicated antibodies. Following antibody-based-protein detection, detection of biotinylated proteins was performed by incubating the membrane with Streptavidin-IRDye 800CW (Li-Cor Biosciences) according to manufacturer's instructions and subsequent scan of the blots with an Odyssey detection system (Li-Cor Biosciences).

### 6.8 Labelling of cells with $^3\text{H}$ -leucine

Before lysis, cells grown in 6-well plates were labelled for 30 min with 10  $\mu$ Ci of L-[4,5- $^3\text{H}$ ]-leucine (PerkinElmer) per ml of medium. After the incubation, cells were washed twice with ice-cold-PBS and lysed in 100  $\mu$ l of RIPA buffer (Tris [pH 7.5] 50 mM, NaCl 150 mM,

## 6. MATERIALS AND METHODS

---

Na deoxycholate 0.5%, EDTA [pH 8.0] 1 mM, NaF 10mM, SDS 0.1%, PMSF 1mM, Triton 1% and protease inhibitor cocktails [Sigma]) on ice. Lysates were harvested in Eppendorf tubes and centrifuged at 16,200 x g for 10 min at 4°C to recover the supernatant. 1 ml of ice-cold 20% trichloroacetic acid (TCA) was added to each sample and they were incubated for 10 min on ice. Samples were centrifuged for 15 min at 16,200 x g at 4°C. Supernatants were discarded and cellular pellets were washed twice with 1 ml 5% TCA. Pellets were dried and resuspended in NaOH 0.1 M, 1% SDS. Protein concentration was determined by the BCA assay (Pierce) following manufacturer's protocol. Equal amounts of samples were used to quantify incorporated radioactivity by liquid scintillation counting.

### **6.9 Autoradiographic analysis of rRNA synthesis**

Newly synthesized RNA was labelled by incubating cells grown in 6-cm dishes for 1 hour in medium containing 1.2  $\mu$ Ci of [5,6-<sup>3</sup>H]-uridine (PerkinElmer) per ml. Labelled cells were then washed into medium containing 1 mM non-radioactive uridine (Sigma) and incubated for 4 hours at 37% in 5% CO<sub>2</sub>. RNA was extracted using TRIzol (Invitrogen) as recommended by manufacturer. To measure RNA concentration, samples aliquots of 2  $\mu$ l were diluted 1:400 in milliQ water and UV absorbance was measured at 260 nm with a spectrophotometer. An absorbance of 1 unit at 260 nm corresponds to 40  $\mu$ g of RNA per ml, therefore RNA concentration for each sample was calculated by using the following formula:

## 6. MATERIALS AND METHODS

---

$\mu\text{g}/\mu\text{l} = \text{Absorbance } 260 \text{ nm} \times \text{dilution factor} \times 40$ . Following extraction, 2  $\mu\text{g}$  of total RNA was size-separated by electrophoresis on a 1% agarose-formaldehyde gel (MOPS buffer 1x, 1% agarose, 7% formaldehyde, DEPC-treated water). Briefly, 2  $\mu\text{l}$  of each sample were resuspended on Northern blot sample buffer 2x (50% deionized formamide, 7% formaldehyde, MOPS 2x, ethidium bromide 0.0025  $\mu\text{g}/\text{ml}$ , 0.01% bromophenol blue/xylene cyanol, DEPC-treated water), denatured for 10 min at 65 °C, incubated on ice 2-3 min and loaded. The gel was ran at 80V in MOPS 1x. To evaluate 5S rRNA synthesis, 20  $\mu\text{g}$  of each RNA sample was electrophoresed on a TBE-urea 10% polyacrylamide gel (10% acrylamide/bisacrylamide, urea 7M, TBE buffer 0.5x, DEPC-treated water, ammonium persulfate solution [APS], TEMED). Briefly, the gel was first pre-ran for 30 min at 200V, and samples were resuspended in formamide-containing loading buffer 1.5x (formamide 80%, EDTA 25mM [pH 8], bromophenol blue/xylene cyanol 0.01%, DEPC-treated water), loaded on the gel and ran at 200V in TBE 0.5x. Following electrophoresis, the RNA in both cases was transferred to Hybond N+ membrane (GE Healthcare) and crosslinked by ultraviolet irradiation. The blots were then sprayed with En3Hance (PerkinElmer) and exposed to autoradiography films (Amersham Hyperfilm ECL, GE Healthcare) at -80°C.

### 6.10 Crystal violet staining

Cells were plated in 6-well plates and allowed to adhere overnight. After the indicated treatment, cells were washed twice with PBS warmed at least to RT, and 750  $\mu$ l of crystal violet solution (Sigma-Aldrich) were added to each well and incubated for 10 min at RT. The crystal violet solution was then removed and cells were washed once with water. Subsequent washes of 10-15 min with water were performed until all the residual staining was eliminated. Stained cells were lysed adding 1.5 ml 2% SDS per well and agitating the plates on an orbital shaker until the color of each well was uniform, with no areas of dense coloration at the bottom. Absorbance at 540 nm was measured in a microplate reader. Each experimental condition was performed in triplicate.

### 6.11 Statistics

Data were analyzed by Excel program. Results are presented as Mean  $\pm$ SEM, for n=2-3. Experimental data sets were compared by a two-sampled, two tailed Student's test. Values of \*P<0.05, \*\*P<0.005 and \*\*\*P<0.0005 were considered statistically significant.



# **ACKNOWLEDGEMENTS**



## 7 Acknowledgements

First of all, I would like to thank my thesis supervisor, **George Thomas**. Thank you for giving me the opportunity to be part of your lab, as it has been one of the best experiences I could have had both at the scientific and personal level.

I would also like to thank **Sara Kozma**, who has been always there to help.

Gracias también a **Albert**, por recibirme con una sonrisa y un abrazo desde el primer día, por ese cariño con el que me has tratado, y ofrecerte siempre para ayudar.

Me gustaría dar las gracias a todas las personas que forman o han formado parte del laboratorio, porque todos y cada uno de ellos me han ayudado a crecer.

**Antonio**, me recibiste con un café y me “engañaste”, como dices. Gracias por esa faceta de “profesor”, explicando siempre en detalle a los alumnos que te miramos con cara extrañada y te volvemos a preguntar (¿eh? ¿cómo?), y por tus charlas filosóficas y tus consejos.

**Giulio**, gracias porque junto con Antonio, durante mi primer año en el laboratorio me descubriste el mundo científico, aunque a veces fuera complicado seguir tus explicaciones

**Ferran**, contigo he llegado a llorar de la risa más de una vez. Gracias esos momentos.

## 7. AKNOWLEDGEMENTS

---

**Nathalie**, Nat. Siempre me acordaré de ese primer día en que fuimos juntas en el metro de vuelta a casa y ninguna sabía muy bien qué decir. Y luego mira, tantas horas de charlas. Muchas gracias por tu cariño y tu forma tan dulce de ser.

**Constanza**, Const. Gracias por hacerme reír con esa forma tuya tan natural de sacar cuestiones que te resultan curiosas.

**Eugenia**, muchas gracias por aparecer siempre con una sonrisa por la mañana en el laboratorio, saludando con tu característico “Holaa”, y contagiando tu alegría. Contigo he aprendido que al final, todos somos humanos, y que siempre podemos aprender de nosotros mismos.

**Sònia**, gracias por tu carácter tranquilo y práctico, del que también he aprendido.

**Mariona**, muchas gracias por querer siempre ayudar a solucionar las cosas, a todos los niveles.

**Sandra**, de ti he aprendido muchas cosas. Gracias por ser mi gran consejera durante mucho tiempo, y estar siempre ahí para escucharme, apoyarme y ayudarme, para un “café”.

**Cris**, muchas gracias por ser siempre tan comprensiva y tan dulce, por tu apoyo cada vez que he hablado contigo.

**Gui**, gracias por tu carácter siempre tranquilo y sonriente, que consigue que el resto nos tranquilicemos.

**Joffrey**, thank you being always there when one asks for help, and for being always making people laugh with your characteristic jokes.

## 7. ACKNOWLEDGEMENTS

---

**Fran**, gracias por estar siempre disponible cuando te he preguntado algo. Y por ser tan buen “vecino” de mesa.

**Marta**, gracias por escucharme tanto, y por hacernos a toda la vida una poquito más fácil con esa forma tan eficiente de organizarlo todo.

**Caroline**, muchas gracias por darme ánimos cada vez que he hablado contigo, han sido siempre los momentos en los que más necesitaba ese tipo de palabras.

Gracias al resto de gente del laboratorio, y de personas del COM, como Raffa y Clara.

Fuera del laboratorio, tengo que dar primero las gracias a mis padres, por su apoyo siempre incondicional y continuo; y a mi hermana, por estar siempre ahí, en cualquier momento cuando he necesitado hablar con ella.

Y por supuesto, a mis queridos **César** y **Teresa**. Gracias a los dos por todo vuestro cariño, que me ha ayudado muchísimo durante todos estos años.

Y, por último, quiero agradecer a una persona que también me ha enseñado mucho. Gracias, **Manu**, por ayudarme tanto en todos los sentidos. Por tranquilizarme cuando me he preocupado por cada cosa y cada detalle, por ser una de las personas que me han enseñado a normalizar situaciones a las que tiendo a dar más importancia de la que debería. Por cuidarme tanto. Por hacerme reír cada día en cada momento y conseguir que los últimos meses del doctorado hayan sido los que me he encontrado más tranquila y

## 7. ACKNOWLEDGEMENTS

---

más a gusto, aunque me haya tenido que ir a vivir “con los dragones”.

# **BIBLIOGRAPHY**



## 8 Bibliography

Abbas, T., and Dutta, A. (2009). p21 in cancer: intricate networks and multiple activities. *Nat Rev Cancer* 9, 400–414.

Ahmed, D., Eide, P.W., Eilertsen, I.A., Danielsen, S.A., Eknas, M., Hektoen, M., Lind, G.E., and Lothe, R.A. (2013). Epigenetic and genetic features of 24 colon cancer cell lines. *Oncogenesis* 2, e71.

Amaldi, F., Bozzoni, I., Beccari, E., and Pierandrei-Amaldi, P. (1989). Expression of ribosomal protein genes and regulation of ribosome biosynthesis in *Xenopus* development. *Trends Biochem. Sci.* 14, 175–178.

Anderson, S., Poudel, K.R., Roh-Johnson, M., Brabletz, T., Yu, M., Borenstein-Auerbach, N., Grady, W.N., Bai, J., Moens, C.B., Eisenman, R.N., et al. (2016). MYC-nick promotes cell migration by inducing fascin expression and Cdc42 activation. *Proc. Natl. Acad. Sci.* 113, E5481–E5490.

Aoki, K., Adachi, S., Homoto, M., Kusano, H., Koike, K., and Natsume, T. (2013). LARP1 specifically recognizes the 3' terminus of poly(A) mRNA. *FEBS Lett.* 587, 2173–2178.

Barak, Y., Juven, T., Haffner, R., and Oren, M. (1993). mdm2 expression is induced by wild type p53 activity. *EMBO J.* 12, 461–468.

Barkić, M., Crnomarković, S., Grabusić, K., Bogetić, I., Panić, L., Tamarut, S., Cokarić, M., Jerić, I., Vidak, S., and Volarević, S. (2009). The p53 tumor suppressor causes congenital malformations

## 8. BIBLIOGRAPHY

---

in Rpl24-deficient mice and promotes their survival. *Mol. Cell. Biol.* 29, 2489–2504.

Barna, M., Pusic, A., Zollo, O., Costa, M., Kondrashov, N., Rego, E., Rao, P.H., and Ruggero, D. (2008). Suppression of Myc oncogenic activity by ribosomal protein haploinsufficiency. *Nature* 456, 971–975.

Berndsen, C.E., and Wolberger, C. (2014). New insights into ubiquitin E3 ligase mechanism. *Nat. Struct. Mol. Biol.* 21, 301–307.

Besson, A., Dowdy, S.F., and Roberts, J.M. (2008). CDK Inhibitors: Cell Cycle Regulators and Beyond. *Dev. Cell* 14, 159–169.

Biegging, K.T., Mello, S.S., and Attardi, L.D. (2014). Unravelling mechanisms of p53-mediated tumour suppression. *Nat. Rev. Cancer* 14, 359–370.

Blackwood, E.M., Lugo, G., Kretzner, L., King, M.W., Street, A.J., Witte, O.N., and Eisenman, R.N. (1994). Functional Analysis of the AUG- and CUG-Initiated Forms of the c-Myc Protein. *5*, 597–609.

Brighenti, E., Calabrese, C., Liguori, G., Giannone, F.A., Trere, D., Montanaro, L., and Derenzini, M. (2014). Interleukin 6 downregulates p53 expression and activity by stimulating ribosome biogenesis: a new pathway connecting inflammation to cancer. *Oncogene* 33, 4396–4406.

Bruno, P.M., Liu, Y., Park, G.Y., Murai, J., Koch, C.E., Eisen, T.J., Pritchard, J.R., Pommier, Y., Lippard, S.J., and Hemann, M.T. (2017). A subset of platinum-containing chemotherapeutic agents kills cells by inducing ribosome biogenesis stress. *Nat. Med.* 23, 1–

13.

Burri, N., Shaw, P., Bouzourene, H., Sordat, I., Sordat, B., Gillet, M., Schorderet, D., Bosman, F.T., and Chaubert, P. (2001). Methylation Silencing and Mutations of the p14 ARF and p16 INK4a Genes in Colon Cancer. *81*, 217–229.

Bursac, S., Brdovcak, M.C., Donati, G., and Volarevic, S. (2014). Activation of the tumor suppressor p53 upon impairment of ribosome biogenesis. *Biochim. Biophys. Acta - Mol. Basis Dis.* *1842*, 817–830.

Bursać, S., Brdovčak, M.C., Pfannkuchen, M., Orsolčić, I., Golomb, L., Zhu, Y., Katz, C., Daftuar, L., Grabušić, K., Vukelić, I., et al. (2012). Mutual protection of ribosomal proteins L5 and L11 from degradation is essential for p53 activation upon ribosomal biogenesis stress. *Proc. Natl. Acad. Sci. U. S. A.* *109*, 20467–20472.

Bywater, M.J., Poortinga, G., Sanij, E., Hein, N., Peck, A., Cullinane, C., Wall, M., Cluse, L., Drygin, D., Anderes, K., et al. (2012). Inhibition of RNA Polymerase I as a Therapeutic Strategy to Promote Cancer-Specific Activation of p53. *Cancer Cell* *22*, 51–65.

Chakraborty, A., Uechi, T., and Kenmochi, N. (2011). Guarding the “translation apparatus”: Defective ribosome biogenesis and the p53 signaling pathway. *Wiley Interdiscip. Rev. RNA* *2*, 507–522.

Challagundla, K.B., Sun, X.-X., Zhang, X., DeVine, T., Zhang, Q., Sears, R.C., and Dai, M.-S. (2011). Ribosomal protein L11 recruits miR-24/miRISC to repress c-Myc expression in response to ribosomal stress. *Mol. Cell. Biol.* *31*, 4007–4021.

Chen, D., Shan, J., Zhu, W.-G., Qin, J., Gu, W., Badalà, F., Nouri-

## 8. BIBLIOGRAPHY

---

mahdavi, K., and Raouf, D.A. (2010a). Transcription-independent ARF regulation in oncogenic stress-mediated p53 responses. *Nature* 464, 624–627.

Chen, D., Kon, N., Zhong, J., Zhang, P., Yu, L., and Gu, W. (2013). Differential effects on ARF stability by normal versus oncogenic levels of c-Myc expression. *Mol. Cell* 51, 46–56.

Chen, L., Iraci, N., Gherardi, S., Gamble, L.D., Wood, K.M., Perini, G., Lunec, J., and Tweddle, D.A. (2010b). p53 is a direct transcriptional target of MYCN in neuroblastoma. *Cancer Res.* 70, 1377–1388.

Ciganda, M., and Williams, N. (2011). Eukaryotic 5S rRNA biogenesis. *Wiley Interdiscip. Rev. RNA* 4, 523–533.

Coller, H.A., Grandori, C., Tamayo, P., Colbert, T., Lander, E.S., Eisenman, R.N., and Golub, T.R. (2000). Expression analysis with oligonucleotide microarrays reveals that MYC regulates genes involved in growth, cell cycle, signaling, and adhesion. *Proc. Natl. Acad. Sci. U. S. A.* 97, 3260–3265.

Cooper, G. M., and Hausman, R. E. (2006). *The cell: A molecular approach*. Washington, D.C: ASM Press

Conacci-Sorrell, M., McFerrin, L., and Eisenman, R.N. (2014). An overview of MYC and its interactome. *Cold Spring Harb. Perspect. Med.* 4, a014357.

Csibi, A., Lee, G., Yoon, S.O., Tong, H., Ilter, D., Elia, I., Fendt, S.M., Roberts, T.M., and Blenis, J. (2014). The mTORC1/S6K1 pathway

## 8. BIBLIOGRAPHY

---

regulates glutamine metabolism through the eif4b-dependent control of c-Myc translation. *Curr. Biol.* *24*, 2274–2280.

Dai, M.-S.S., Arnold, H., Sun, X.-X.X., Sears, R., and Lu, H. (2007). Inhibition of c-Myc activity by ribosomal protein L11. *EMBO J.* *26*, 3332–3345.

Dai, M.S., Sun, X.X., and Lu, H. (2010). Ribosomal protein L11 associates with c-Myc at 5 S rRNA and tRNA genes and regulates their expression. *J. Biol. Chem.* *285*, 12587–12594.

Dang, C. V. (2012). MYC on the path to cancer. *Cell* *149*, 22–35.

Dani, C., Blanchard, J.M., Piechaczyk, M., El Sabouty, S., Marty, L., and Jeanteur, P. (1984). Extreme instability of myc mRNA in normal and transformed human cells. *Proc. Natl. Acad. Sci. U. S. A.* *81*, 7046–7050.

Daniel, J.M., Junttila, M.R., Pouyet, L., Karnezis, A., Bui, D.A., Brown-swigart, L., Johnson, L., Gerard, I., Shchors, K., Bui, D.A., et al. (2008). Distinct thresholds govern Myc's biological output in vivo. *Cancer Cell* *14*, 447–457.

Derenzini, M., Montanaro, L., and Trerè, D. (2017). Ribosome biogenesis and cancer. *Acta Histochem.* *119*, 190–197.

Devlin, J.R., Hannan, K.M., Hein, N., Cullinane, C., Kusnadi, E., Ng, P.Y., George, A.J., Shortt, J., Bywater, M.J., Poortinga, G., et al. (2016). Combination therapy targeting ribosome biogenesis and mRNA translation synergistically extends survival in MYC-driven lymphoma. *Cancer Discov.* *6*, 59–70.

Donati, G., Bertoni, S., Brighenti, E., Vici, M., Treré, D., Volarevic,

## 8. BIBLIOGRAPHY

---

S., Montanaro, L., and Derenzini, M. (2011). The balance between rRNA and ribosomal protein synthesis up- and downregulates the tumour suppressor p53 in mammalian cells. *Oncogene* 30, 3274–3288.

Donati, G., Peddigari, S., Mercer, C.A., and Thomas, G. (2013). 5S ribosomal RNA is an essential component of a nascent ribosomal precursor complex that regulates the Hdm2-p53 checkpoint. *Cell Rep.* 4, 87–98.

Dunn, S., and Cowling, V.H. (2015). Myc and mRNA capping. *Biochim. Biophys. Acta* 1849, 501–505.

Eischen, C.M., Weber, J.D., Roussel, M.F., Sherr, C.J., and Cleveland, J.L. (1999). Disruption of the ARF – Mdm2 – p53 tumor suppressor pathway in Myc-induced lymphomagenesis. *Genes Dev.* 2658–2669.

Elkon, R., Loayza-Puch, F., Korkmaz, G., Lopes, R., van Breugel, P.C., Bleijerveld, O.B., Altelaar, A.F.M., Wolf, E., Lorenzin, F., Eilers, M., et al. (2015). Myc coordinates transcription and translation to enhance transformation and suppress invasiveness. *EMBO Rep.* 16, 1723–1736.

Farrell, A.S., and Sears, R.C. (2014). MYC degradation. *Cold Spring Harb. Perspect. Med.* 4, 1–15.

Fernandez, P.C., Frank, S.R., Wang, L., Schroeder, M., Liu, S., Greene, J., Cocito, A., and Amati, B. (2003). Genomic targets of the human c-Myc protein. *Genes Dev.* 17, 1115–1129.

Fonseca, B.D., Zakaria, C., Jia, J.J., Graber, T.E., Svitkin, Y.,

## 8. BIBLIOGRAPHY

---

Tahmasebi, S., Healy, D., Hoang, H.D., Jensen, J.M., Diao, I.T., et al. (2015). La-related protein 1 (LARP1) represses terminal oligopyrimidine (TOP) mRNA translation downstream of mTOR complex 1 (mTORC1). *J. Biol. Chem.* 290, 15996–16020.

Fumagalli, S., Di Cara, A., Neb-Gulati, A., Natt, F., Schwemberger, S., Hall, J., Babcock, G.F., Bernardi, R., Pandolfi, P.P., and Thomas, G. (2009). Absence of nucleolar disruption after impairment of 40S ribosome biogenesis reveals an rpL11-translation-dependent mechanism of p53 induction. *Nat. Cell Biol.* 11, 501–508.

Fumagalli, S., Ivanenkov, V. V., Teng, T., and Thomas, G. (2012). Suprainduction of p53 by disruption of 40S and 60S ribosome biogenesis leads to the activation of a novel G2/M checkpoint. *Genes Dev.* 26, 1028–1040.

Gamalinda, M., and Woolford, J.L. (2015). Paradigms of ribosome synthesis: Lessons learned from ribosomal proteins. *Translation* 3, e975018.

Gentilella, A., Morón-Duran, F., Fuentes, P., Zweig-Rocha, G., Riaño-Canalias, F., Pelletier, J., Ruiz, M., Turón, G., Tauler, A., Castaño, J., Bueno, C., Menéndez, P., Kozma, S. C., and Thomas, G. (in press). Autogenous control of 5'TOP mRNA stability by 40S ribosomes. *Mol. Cell.*

Gentilella, A., and Thomas, G. (2012). Cancer biology: The director's cut. *Nature* 485, 50–51.

Gomez-Roman, N., Grandori, C., Eisenman, R.N., and White, R.J. (2003). Direct activation of RNA polymerase III transcription by c-

## 8. BIBLIOGRAPHY

---

Myc. *Nature* 421, 290–294.

Grandori, C., Gomez-Roman, N., Felton-Edkins, Z.A., Ngouenet, C., Galloway, D.A., Eisenman, R.N., and White, R.J. (2005). c-Myc binds to human ribosomal DNA and stimulates transcription of rRNA genes by RNA polymerase I. *Nat. Cell Biol.* 7, 311–318.

Granneman, S., and Tollervey, D. (2007). Building Ribosomes: Even More Expensive Than Expected? *Curr. Biol.* 17, 415–417.

Hann, S.R., and Eisenman, R.N. (1984). Proteins encoded by the human c-myc oncogene: differential expression in neoplastic cells. *Mol. Cell. Biol.* 4, 2486–2497.

Hermeking, H., and Eick, D. (1994). Mediation of c-Myc-induced apoptosis by p53. *Science* 265, 2091–2093.

Iritani, B.M., and Eisenman, R.N. (1999). c-Myc enhances protein synthesis and cell size during B lymphocyte development. *Proc. Natl. Acad. Sci. U. S. A.* 96, 13180–13185.

Jensen, N.F., Smith, D.H., Nygård, S.B., Rømer, M.U., Nielsen, K.V., and Brünner, N. (2012). Predictive biomarkers with potential of converting conventional chemotherapy to targeted therapy in patients with metastatic colorectal cancer. *Scand. J. Gastroenterol.* 47, 340–355.

Kim, S., Li, Q., Dang, C. V, and Lee, L.A. (2000). Induction of ribosomal genes and hepatocyte hypertrophy by adenovirus-mediated expression of c-Myc in vivo. *Proc. Natl. Acad. Sci. U. S. A.* 97, 11198–11202.

Kress, T.R., Cannell, I.G., Brenkman, A.B., Samans, B., Gaestel, M.,

## 8. BIBLIOGRAPHY

---

Roepman, P., Burgering, B.M., Bushell, M., Rosenwald, A., and Eilers, M. (2011). The MK5/PRAK kinase and Myc form a negative feedback loop that is disrupted during colorectal tumorigenesis. *Mol. Cell* 41, 445–457.

Kress, T.R., Sabò, A., and Amati, B. (2015). MYC: connecting selective transcriptional control to global RNA production. *Nat. Rev. Cancer* 15, 593–607.

Kruse, J.P., and Gu, W. (2009). Modes of p53 regulation. *Cell* 137, 609–622.

Kuang, E., Fu, B., Liang, Q., Myoung, J., and Zhu, F. (2011). Phosphorylation of eukaryotic translation initiation factor, 4B (EIF4B) by open reading frame 45/p90 ribosomal S6 kinase (ORF45/RSK) signaling axis facilitates protein translation during Kaposi sarcoma-associated herpesvirus (KSHV) lytic replication. *J. Biol. Chem.* 286, 41171–41182.

Lafontaine, D.L.J. (2015). Noncoding RNAs in eukaryotic ribosome biogenesis and function. *Nat Struct Mol Biol* 22, 11–19.

Lam, Y.W., Lamond, A.I., Mann, M., and Andersen, J.S. (2007). Analysis of nucleolar protein dynamics reveals the nuclear degradation of ribosomal proteins. *Curr. Biol.* 17, 749–760.

Lee, S.W., Seong, M.W., Jeon, Y.J., and Chung, C.H. (2012). Ubiquitin E3 ligases controlling p53 stability. *Animal Cells Syst. (Seoul)*. 16, 173–182.

Li, J., and Kurokawa, M. (2015). Regulation of MDM2 stability after DNA damage. *J. Cell. Physiol.* 230, 2318–2327.

## 8. BIBLIOGRAPHY

---

- Li, M., and Gu, W. (2011). A critical role for noncoding 5S rRNA in regulating Mdmx stability. *Mol. Cell* 43, 1023–1032.
- Liao, J.-M., Zhou, X., Gaignol, A., and Lu, H. (2014). Ribosomal proteins L5 and L11 co-operatively inactivate c-Myc via RNA-induced silencing complex. *Oncogene* 33, 4916–4923.
- Lin, C.Y., Lovén, J., Rahl, P.B., Paranal, R.M., Burge, C.B., Bradner, J.E., Lee, T.I., and Young, R.A. (2012). Transcriptional amplification in tumor cells with elevated c-Myc. *Cell* 151, 56–67.
- Lindstrom, M.S., and Wiman, K.G. (2003). Myc and E2F1 induce p53 through p14ARF-independent mechanisms in human fibroblasts. *Oncogene* 22, 4993–5005.
- Lindström, M.S., Jin, A., Deisenroth, C., White Wolf, G., and Zhang, Y. (2007). Cancer-associated mutations in the MDM2 zinc finger domain disrupt ribosomal protein interaction and attenuate MDM2-induced p53 degradation. *Mol. Cell. Biol.* 27, 1056–1068.
- Liu, J., and Levens, D. (2006). Making Myc. *Curr. Top. Microbiol. Immunol.* 302, 1–32.
- Liu, S., Tackmann, N.R., Yang, J., and Zhang, Y. (2017). Disruption of the RP-MDM2-p53 pathway accelerates APC loss-induced colorectal tumorigenesis. *Oncogene* 36, 1374–1383.
- Lloyd, A.C. (2013). The regulation of cell size. *Cell* 154, 1194–1205.
- Lowe, S.W., Cepero, E., and Evan, G. (2004). Intrinsic tumour suppression. *Nature* 432, 307–315.
- Macias, E., Jin, A., Deisenroth, C., Bhat, K., Mao, H., Lindström,

## 8. BIBLIOGRAPHY

---

M.S., and Zhang, Y. (2010). An ARF-Independent c-MYC-activated tumor suppression pathway mediated by ribosomal protein-Mdm2 interaction. *Cancer Cell* 18, 231–243.

Macinnes, A.W. (2016). The role of the ribosome in the regulation of longevity and lifespan extension. *Wiley Interdiscip. Rev. RNA* 7, 198–212.

Mandal, M., Vadlamudi, R., Nguyen, D., Wang, R.A., Costa, L., Bagheri-Yarmand, R., Mendelsohn, J., and Kumar, R. (2001). Growth factors regulate heterogeneous nuclear ribonucleoprotein K expression and function. *J Biol Chem* 276, 9699–704.

Martin, V., Jørgensen, H.F., Baur Chaubert, A.S., Berger, J., Barr, H., Shaw, P., Bird, A., and Chaubert, P. (2008). MBD2-mediated transcriptional repression of the p14ARF tumor suppressor gene in human colon cancer cells. *Pathobiology* 75, 281–287.

Mateyak, M.K., Obaya, a J., Adachi, S., and Sedivy, J.M. (1997). Phenotypes of c-Myc-deficient rat fibroblasts isolated by targeted homologous recombination. *Cell Growth Differ.* 8, 1039–1048.

Meyer, N., and Penn, L.Z. (2008). Reflecting on 25 years with MYC. *Nat. Rev. Cancer* 8, 976–990.

Morgado-Palacin, L., Varetto, G., Llanos, S., Gómez-López, G., Martinez, D., and Serrano, M. (2015). Partial loss of Rpl11 in adult mice recapitulates Diamond-Blackfan anemia and promotes lymphomagenesis. *Cell Rep.* 13, 712–722.

Muncan, V., Sansom, O.J., Tertoolen, L., Phesse, T.J., Begthel, H., Sancho, E., Cole, A.M., Gregorieff, A., de Alboran, I.M., Clevers, H.,

## 8. BIBLIOGRAPHY

---

et al. (2006). Rapid loss of intestinal crypts upon conditional deletion of the Wnt/Tcf-4 target gene c-Myc. *Mol. Cell. Biol.* 26, 8418–8426.

Muzny, D.M., Bainbridge, M.N., Chang, K., Dinh, H.H., Drummond, J. a., Fowler, G., Kovar, C.L., Lewis, L.R., Morgan, M.B., Newsham, I.F., et al. (2012). Comprehensive molecular characterization of human colon and rectal cancer. *Nature* 487, 330–337.

Nie, Z., Hu, G., Wei, G., Cui, K., Yamane, A., Resch, W., Wang, R., Green, D.R., Tessarollo, L., Casellas, R., et al. (2012). c-Myc is a universal amplifier of expressed genes in lymphocytes and embryonic stem cells. *Cell* 151, 68–79.

Notari, M., Neviani, P., Santhanam, R., Blaser, B.W., Chang, J.-S., Galiotta, A., Willis, A.E., Roy, D.C., Caligiuri, M.A., Marcucci, G., et al. (2006). A MAPK/HNRPK pathway controls BCR/ABL oncogenic potential by regulating MYC mRNA translation. *Blood* 107, 2507 LP-2516.

Oeffinger, M. (2016). Structural biology: Moulding the ribosome. *Nature* 537, 38–40.

Phipps, K.R., Charette, J.M., and Baserga, S.J. (2011). The SSU processome in ribosome biogenesis—progress and prospects. *Wiley Interdiscip. Rev. RNA* 2, 1–21.

Pierandrei-Amaldi, P., Campioni, N., Gallinari, P., Beccari, E., Bozzoni, I., and Amaldi, F. (1985). Ribosomal-protein synthesis is not autogenously regulated at the translational level in *Xenopus laevis*. *Dev. Biol.* 107, 281–289.

Poortinga, G., Quinn, L.M., and Hannan, R.D. (2015). Targeting

RNA polymerase I to treat MYC-driven cancer. *Oncogene* *34*, 403–412.

Posternak, V., and Cole, M.D. (2016). Strategically targeting MYC in cancer. *F1000Research* *5*, 1–7.

Pourdehnad, M., Truitt, M.L., Siddiqi, I.N., Ducker, G.S., Shokat, K.M., and Ruggero, D. (2013). Myc and mTOR converge on a common node in protein synthesis control that confers synthetic lethality in Myc-driven cancers. *Proc. Natl. Acad. Sci. U. S. A.* *110*, 11988–11993.

Ranaweera, R.S., and Yang, X. (2013). Auto-ubiquitination of Mdm2 enhances its substrate ubiquitin ligase activity. *J. Biol. Chem.* *288*, 18939–18946.

van Riggelen, J., Yetil, A., and Felsher, D.W. (2010). MYC as a regulator of ribosome biogenesis and protein synthesis. *Nat. Rev. Cancer* *10*, 301–309.

Roy, B., Beamon, J., Balint, E., and Reisman, D. (1994). Transactivation of the human p53 tumor suppressor gene by c-Myc/Max contributes to elevated mutant p53 expression in some tumors. *Mol. Cell. Biol.* *14*, 7805–7815.

Sabò, A., Kress, T.R., Pelizzola, M., de Pretis, S., Gorski, M.M., Tesi, A., Morelli, M.J., Bora, P., Doni, M., Verrecchia, A., et al. (2014). Selective transcriptional regulation by Myc in cellular growth control and lymphomagenesis. *Nature* *511*, 488–492.

Schuhmacher, M., Staeger, M.S., Pajic, a, Polack, a, Weidle, U.H., Bornkamm, G.W., Eick, D., and Kohlhuber, F. (1999). Control of cell

## 8. BIBLIOGRAPHY

---

growth by c-Myc in the absence of cell division. *Curr. Biol.* 9, 1255–1258.

Sears, R., Nuckolls, F., Haura, E., Taya, Y., Tamai, K., and Nevins, J.R. (2000). Multiple Ras-dependent phosphorylation pathways regulate Myc protein stability. *Genes Dev.* 14, 2501–2514.

Shadfan, M., Lopez-Pajares, V., and Yuan, Z.-M. (2012). MDM2 and MDMX: Alone and together in regulation of p53. *Transl. Cancer Res.* 1, 88–89.

Shi, D., and Gu, W. (2012). Dual Roles of MDM2 in the Regulation of p53: Ubiquitination Dependent and Ubiquitination Independent Mechanisms of MDM2 Repression of p53 Activity. *Genes Cancer* 3, 240–248.

Sonenberg, N., and Hinnebusch, A.G. (2009). Regulation of translation initiation in eukaryotes: mechanisms and biological targets. *Cell* 136, 731–745.

Strunk, B.S., and Karbstein, K. (2009). Powering through ribosome assembly. *RNA* 15, 2083–2104.

Tansey, W.P. (2014). Mammalian MYC proteins and cancer. *New J. Sci.* 2014, 1–27.

Taylor, C.W., Kim, Y.S., Childress-Fields, K.E., and Yeoman, L.C. (1992). Sensitivity of nuclear c-myc levels and induction to differentiation-inducing agents in human colon tumor cell lines. *Cancer Lett.* 62, 95–105.

Tcherkezian, J., Cargnello, M., Romeo, Y., Huttlin, E.L., Lavoie, G., Gygi, S.P., and Roux, P.P. (2014). Proteomic analysis of cap-

## 8. BIBLIOGRAPHY

---

dependent translation identifies LARP1 as a key regulator of 5' TOP mRNA translation. *Genes Dev.* 28, 357–371.

Volarević, S., and Thomas, G. (2001). Role of S6 phosphorylation and S6 kinase in cell growth. *Prog. Nucleic Acid Res. Mol. Biol.* 65, 101–127.

Wall, M., Poortinga, G., Hannan, K.M., Pearson, R.B., Hannan, R.D., and McArthur, G.A. (2008). Translational control of c-MYC by rapamycin promotes terminal myeloid differentiation. *Blood* 112, 2305–2317.

Wang, H., Mannava, S., and Grachtchouk, V. (2008). c-Myc depletion inhibits proliferation of human tumor cells at various stages of the cell cycle. *Oncogene* 27, 1905–1915.

Warner, J.R. (1977). In the absence of ribosomal RNA synthesis, the ribosomal proteins of HeLa Cells are synthesized normally and degraded rapidly. *J. Mol. Biol.* 115, 315–333.

Weber, H.O., Samuel, T., Rauch, P., and Funk, J.O. (2002). Human p14 ARF -mediated cell cycle arrest strictly depends on intact p53 signaling pathways. *Oncogene* 21, 3207–3212.

Wierstra, I., and Alves, J. (2008). The c-myc promoter: still Mystery and Challenge. *Adv. Cancer Res.* 99, 113–333.

Wu, C.H., Sahoo, D., Arvanitis, C., Bradon, N., Dill, D.L., and Felsher, D.W. (2008). Combined analysis of murine and human microarrays and ChIP analysis reveals genes associated with the ability of MYC to maintain tumorigenesis. *PLoS Genet.* 4, 21–26.

Xiao, Q., Claassen, G., Shi, J., Adachi, S., Sedivy, J., and Hann,

## 8. BIBLIOGRAPHY

---

S.R. (1998). Transactivation-defective c-MycS retains the ability to regulate proliferation and apoptosis. *Genes Dev.* *12*, 3803–3808.

Yelick, P.C., and Trainor, P.A. (2015). Ribosomopathies: Global process, tissue specific defects. *Rare Dis. (Austin, Tex.)* *3*, e1025185.

Zanet, J., Pibre, S., Jacquet, C., Ramirez, A., de Alborán, I.M., and Gandarillas, A. (2005). Endogenous Myc controls mammalian epidermal cell size, hyperproliferation, endoreplication and stem cell amplification. *J. Cell Sci.* *118*, 1693–1704.

Zhang, Y., and Lu, H. (2009). Signaling to p53: ribosomal proteins find their way. *Cancer Cell* *16*, 369–377.

Zhang, J., Harnpicharnchai, P., Jakovljevic, J., Tang, L., Guo, Y., Oeffinger, M., Rout, M.P., Hiley, S.L., Hughes, T., and Woolford, J.L. (2007). Assembly factors Rpf2 and Rrs1 recruit 5S rRNA and ribosomal proteins rpL5 and rpL11 into nascent ribosomes. *Genes Dev.* *21*, 2580–2592.

Zindy, F., Eischen, C.M., Randle, D.H., Kamijo, T., Cleveland, J.L., Sherr, C.J., and Roussel, M.F. (1998). Myc signaling via the ARF tumor suppressor regulates p53-dependent apoptosis and immortalization. *Genes Dev.* *12*, 2424–2433.



